DISSERTATIONES PHYSICAE UNIVERSITATIS TARTUENSIS
49

DISSERTATIONES PHYSICAE UNIVERSITATIS TARTUENSIS
49

ATOMIC LAYER DEPOSITION OF TITANIUM, ZIRCONIUM AND HAFNIUM DIOXIDES: GROWTH MECHANISMS AND PROPERTIES OF THIN FILMS

JAAN AARIK

TARTU UNIVERSITY
PRESS

The study was carried out at the Institute of Experimental Physics and Technology, Institute of Material Science and Institute of Physics, University of Tartu, Estonia

The dissertation was admitted on January 24, 2007, in partial fulfilment of the requirements for the degree of Doctor of Philosophy in physics (applied physics), and allowed for defence by the Council of the Department of Physics, University of Tartu.

Supervisor: Prof. Lembit Pung, D.Sc., Institute of Experimental Physics and Technology, University of Tartu, Tartu, Estonia

Opponents: Prof. Enn Mellikov, D.Sc., Department of Materials Science, Tallinn University of Technology, Tallinn, Estonia

Dr. Mária Hartmanová, D.Sc., Institute of Physics, Slovak Academy of Sciences, Bratislava, Slovakia

Defence: March 30, 2007, at the University of Tartu, Tartu, Estonia

ISSN 1406–0647
ISBN 978–9949–11–542–6 (trükis)
ISBN 978–9949–11–543–3 (PDF)

Tartu Ülikooli Kirjastus
www.tyk.ee
Tellimus nr. 37

CONTENTS

LIST OF ORIGINAL PUBLICATIONS

This thesis is based on the following publications that are referred to in the text by their corresponding Roman numerals.

I. J. Aarik, A. Aidla, A.-A. Kiisler, T. Uustare, V. Sammelselg, Influence of substrate temperature on atomic layer growth and properties of HfO_2 thin films, Thin Solid Films 340 (1999) 110–116.

II. J. Aarik, A. Aidla, H. Mändar, V. Sammelselg, T. Uustare, Texture development in nanocrystalline hafnium dioxide thin films grown by atomic layer deposition, J. Cryst. Growth 220 (2000) 105–113.

III. J. Aarik, A. Aidla, H. Mändar, T. Uustare, Atomic layer deposition of titanium dioxide from $TiCl_4$ and H_2O: investigation of growth mechanism, Appl. Surf. Sci. 172 (2001) 148–158.

IV. J. Aarik, A. Aidla, T. Uustare, K. Kukli, V. Sammelselg, M. Ritala, M. Leskelä, Atomic layer deposition of TiO_2 thin films from TiI_4 and H_2O, Appl. Surf. Sci. 193 (2002) 277–286.

V. J. Aarik, A. Aidla, V. Sammelselg, T. Uustare, M. Ritala, M. Leskelä, Characterization of titanium dioxide atomic layer growth from titanium ethoxide and water, Thin Solid Films 370 (2000) 163–172.

VI. J. Aarik, A. Aidla, T. Uustare, M. Ritala, M. Leskelä, Titanium isopropoxide as a precursor for atomic layer deposition: Characterization of titanium dioxide growth process, Appl. Surf. Sci. 161 (2000) 385–395.

VII. J. Aarik, A. Aidla, H. Mändar, V. Sammelselg, Anomalous effect of temperature on atomic layer deposition of titanium dioxide, J. Cryst. Growth 220 (2000) 531–537.

VIII. J. Aarik, J. Karlis, H. Mändar, T. Uustare, V. Sammelselg, Influence of structure development on atomic layer deposition of TiO_2 thin films, Appl. Surf. Sci. 181 (2001) 339–348.

IX. J. Aarik, A. Aidla, H. Mändar, T. Uustare, M. Schuisky, A. Hårsta, Atomic layer growth of epitaxial TiO_2 thin films from $TiCl_4$ and H_2O on α-Al_2O_3 substrates, J. Cryst. Growth 242 (2002) 189–198.

X. J. Aarik, A. Aidla, H. Mändar, T. Uustare, V. Sammelselg, Growth kinetics and structure formation of ZrO_2 thin films in chloride-based atomic layer deposition process, Thin Solid Films 408 (2002) 97–103.

XI. J. Aarik, J. Sundqvist, A. Aidla, J. Lu, T. Sajavaara, K. Kukli, A. Hårsta, Hafnium tetraiodide and oxygen as precursors for atomic layer deposition of hafnium oxide thin films, Thin Solid Films 418 (2002) 69–72.

XII. J. Aarik, H. Mändar, M. Kirm, L. Pung, Optical characterization of HfO_2 thin films grown by atomic layer deposition, Thin Solid Films 466 (2004) 41–47.

Author's contribution to original publications

The author of the thesis has designed and upgraded the ALD reactor used in growth experiments, planned the experiments, performed real-time measurements, selected methods for post-growth studies and collected the data obtained. He has also taken part in the analysis of results and written all original papers that the thesis is based on.

LIST OF ABBREVIATIONS AND SYMBOLS

AES	Auger electron spectroscopy
AFM	Atomic force microscopy
ALD	Atomic layer deposition
Cp	cyclopentadienyl, C_5H_5
dmae	diethylaminoethoxide, $(OC_2H_5)N(CH_3)_2$
Et	ethyl, $–C_2H_5$
EL	Electroluminescence
EMPA	Electron probe microanalysis
FET	Field-effect transistor
HRTEM	High-resolution transmission electron microscopy
^{i}Pr	isopropyl, $–CH(CH_3)_2$
Me	methyl, $–CH_3$
MIM	Metal–insulator–metal
MOS	Metal–oxide–metal
QCM	Quartz crystal microbalance
QMS	Quadrupole mass spectrometer
RHEED	Reflection high-energy electron diffraction
^{t}Bu	*tert*-butyl, $–CH(CH_3)_3$
TOF ERDA	Time of flight elastic recoil detection analysis
XRD	X-ray diffraction
XRF	X-ray fluorescence
α	Absorption coefficient
$h\nu$	Photon energy
k	Dielectric constant (permittivity)
λ	Wavelength
T_G	Growth temperature, i.e. substrate temperature during film growth

1. INTRODUCTION

A large variety of electronic and optoelectronic components and devices, such as capacitors, transistors, integrated circuits, dynamic memories, electroluminescence (EL) devices, photodiodes, light emitting diodes, laser diodes, solar cells, chemical sensors, etc. contain metal oxide thin films as constitutional parts of them. These films are used as insulating layers but they may also form reflective and antireflective dielectric coatings, tunnel barriers etc. In chemical sensors and optoelectronic devices, some oxides are applied as semiconductive and conductive materials.

Need in smaller dimensions and higher reliability of electronic and optical devices sets additional requirements on the materials used. Minimization of the device sizes frequently depends on the possibilities to diminish the thickness of thin films used in the device structure. Simultaneously other parameters of the films have to be maintained or even improved in order to achieve expected performance of the device. Large-scale integration of electronic devices as well as the minimization of production costs requires an increase of substrates sizes used in the device processing. Correspondingly, thin film deposition methods applied in the processing must enable one to grow uniform layers on large-area substrates whereas the thickness and other film parameters should be precisely and reliably controlled.

During three last decades significant efforts have been directed to investigation of multilayer structures where quantum effects appear due to the limited thickness of layers. The thin film thickness at which the quantum effects appear is typically below 10–20 nm. In addition, extensive studies have been concentrated on polycrystalline materials where crystallite sizes range from few nanometers to few tens of nanometers. Because of small crystallite sizes, quantum effects appear in this kind of nanocrystalline materials as well. As a result, parameters of such materials may remarkably differ from those of single crystals and amorphous materials. Frequently the nanocrystalline materials are applied in the form of thin films. In these cases the crystallite sizes and, correspondingly, the material properties may depend on the film thickness. Consequently, a precise control of the deposition process is important in those applications too.

A number of methods have been applied for deposition of thin solid films. Vacuum evaporation, ion sputtering, laser ablation and molecular beam epitaxy are physical methods that have most frequently been used for thin film growth. Vacuum evaporation in a reactive atmosphere, reactive ion sputtering, chemical vapor deposition, ion-assisted chemical vapor deposition, photo-assisted chemical vapor deposition, chemical beam epitaxy, in turn, are some examples of chemical methods for thin film deposition. In the case of all these methods, a substrate is simultaneously exposed to all starting materials (precursors) needed for film formation while the film thickness depends directly on the deposition

time and precursor fluxes. Dependently on growth conditions and substrates used, thin films can be grown non-epitaxially or epitaxially whereas in the latter case the thin film structure and its crystallographic orientation are determined by the crystal structure of the substrate.

In addition to the methods mentioned above, there are techniques, which give an opportunity to deposit thin films in a self-controlled layer-by-layer mode. The terms like chemical buildup (see the paper by Aleskovskii and Drozd [1] and references therein), molecular layering [1,2], atomic layer epitaxy [1,3–9], molecular layer epitaxy [10–13] and atomic layer deposition (ALD) [14–23] have most frequently been used to denote these methods. Various terms are introduced to indicate application of new precursors, for instance molecular precursors [10–13] instead of elemental ones, or to stress the epitaxial [5] or non-epitaxial [24] character of the thin film growth. In all cases, however, the films are formed in successive self-saturated adsorption processes. Such processes stop by themselves after formation of an adsorbate layer of a certain thickness and composition. Usually the thickness is below or about one monolayer of surface intermediate species formed in the adsorption process. In order to continue the growth, the surface should be re-activated. Therefore the deposition process consists of cycles whereas each cycle must contain at least one exposure to a precursor, and one surface re-activation step. As one or less than one atomic layer of the thin film material is deposited in each adsorption step, application of the term “atomic layer deposition”, which has become the most popular one in the last years [14–23], is well justified. Application of this term, differently from those containing the word “epitaxy”, is entirely approved in the case of non-epitaxial deposition modes too.

If the conditions for ALD are properly chosen, then one adsorption step results in deposition of a material amount, which is almost independent of modest variations of precursor doses and cycle length. As a very thin layer of the film material is deposited during a single growth cycle, the cycle must usually be repeated many times to grow films of required thickness. For these reasons, the film thickness is very uniform and precisely controlled by the number of reaction cycles even on large-area substrates and surfaces of very complex shapes.

Although the layer-by-layer methods of thin film deposition have been studied for a rather long period, there are still problems, which need more detail investigation. Those are related, for instance, to mechanisms of surface reactions, especially in case of molecular precursors used for deposition from the gas phase in low-pressure flow-type reactors. Similarly, initial stages of the thin film growth, formation of interfacial layers, dependence of crystallization processes on process parameters, effect of structure development on the growth rate, possible influence of the carrier gas on the thin film growth, etc. are not completely understood yet. For this reason, some of the problems are discussed in the present thesis.

The work described in this thesis was performed to investigate ALD processes of some technologically important oxides, such as titanium dioxide (TiO_2), zirconium dioxide (ZrO_2) and hafnium dioxide (HfO_2), and to study the influence of process parameters on properties of thin films of these materials. Real-time measurements were used to better understand the reaction mechanisms. Particular attention was concentrated on the effects of crystallization on the ALD growth and properties of thin films obtained. The thesis is based on results published since 1999.

2. RESEARCH BACKGROUND AND OBJECTIVES

2.1. History of development and principles of atomic layer deposition

Recently Ritala and Leskelä [20] and Puurunen [23] have written extensive reviews on atomic layer deposition. In addition, reviews by Goodman and Pessa [6], Suntola [7,8], Niinistö and Leskelä [9], Leskelä and Ritala [18,19], Nishizawa and Kurobayashi [13], Yong and Jeong [25] and Niinistö et al. [21] describe different aspects of the ALD method. The papers published by Goodman and Pessa [6], Suntola [7,8] and Ritala and Leskelä [23] in detail concentrate on the principles and advancements of the ALD method as well as on the reactors used for ALD. Therefore those issues do not need detailed discussions in this work. Nevertheless, some important facts from the history of ALD and some specific problems related to the present thesis will be mentioned in this section.

The first systematical studies on the layer-by-layer synthesis of solids in successive surface reactions were performed in 1960-s while the priority of these studies belonged to the Prof. Aleskovskii's group [26–30]. The first papers published by this group were concentrated on modification of high-surface-area supports and characterization of adsorption reactions of chlorides and water vapor with silica gel [26]. However, they also demonstrated that successive reactions of metal chlorides and H_2O with silicon powder resulted in formation of an oxide layer on the silicon surface [27]. During the exposure of a hydroxylated surface to a metal chloride metal atoms together with some amount of chlorine were bound to the surface while during the following exposure to H_2O the chlorine was replaced with hydroxyl (OH) groups. In this way, both metal and oxygen as constituent elements of the oxide were added onto the surface and a hydroxylated surface similar to the initial one was obtained. Later similar reactions were used for deposition of thin films of TiO_2 [28] and SiO_2 [29] on planar silicon substrates too. To denote the deposition method, its developers introduced the terms "chemical build-up" and "molecular layering" [1].

A method, in which self-saturated adsorption of elemental precursors was applied for deposition of thin films, was developed in the middle of 1970-s. The method was given the name "atomic layer epitaxy" and patented by Finnish researchers Suntola and Antson [3]. Although the method was more frequently used for non-epitaxial than for epitaxial growing of thin films, the term "atomic layer epitaxy" dominated during the following 20 years. Suntola and his coworkers also performed a significant development of the deposition equipment [3,31,32]. As a result, deposition of films with reasonable rate became possible and the method was considered as one of the most promising techniques for processing EL displays [7,33,34]. However, the elemental

precursors could found successful application only in processing of II–VI compounds [5,24,35–38]. In order to deposit metal oxides [1,2,7–9,11,12,15–21,28–32,39–87] and III–V compounds [10,13,88–108], complex precursors were needed because the vapor pressures of many elemental metals were too low to avoid their unlimited condensation on the solid surface. The simplest and most reliable complex precursors were chlorides combined with hydrides for deposition of oxides [1,5,7,8,11,12,18–21,25–32,41–43,46–55,59–62,67,68,73–84] as well as III–V [101–106] and II–VI [4,7–9,31,32] compounds while metalorganic complexes combined with hydrides were widely employed for deposition of III–V compounds [10,13,88–100,107,108].

In all ALD processes mentioned above, adsorption of precursors from the gas phase or molecular beams was utilized to deposit thin films in the layer-by-layer mode. In addition to this approach, solid films have been grown in the self-saturated layer-by-layer processes from liquid precursors. These methods are known as successive ionic-layer adsorption and reaction [109–111] and electrochemical atomic layer epitaxy [112]. This thesis is concentrated, however, only on the methods, where the precursors are adsorbed from the gas phase.

In the simplest ALD processes, two precursors are usually exploited and the deposition process consists of exposure of the solid surface to the first precursor, purge period, exposure of the surface to the second precursor and another purge period. This processing cycle, called an ALD cycle, is repeated to obtain a film of required thickness. In each exposure to a precursor, a surface reaction takes place and, as a result, the surface becomes passivated towards this precursor. In the case of elemental precursors, approximately a monolayer of precursor atoms should be adsorbed to passivate the surface. In the case of complex precursors, adsorption usually stops, when the precursor ligands form a sufficiently dense layer on the surface. The surface concentration of ligands needed to passivate the surface together with the composition of the adsorbate layer determine the amount of the film material deposited in this reaction step. The dependence of these parameters on the processing conditions is one of the main issues to be discussed in this thesis. The purge period following the reaction step is necessary to remove the gaseous reaction products and unused precursor from the reaction zone. However, if the precursor stability is insufficient, then some changes can also take place in the composition of the adsorbed species during the purge period, especially when the growth temperature, T_G, i.e. the substrate temperature during the film growth, is high and the purge period is long. The stability of a surface layer formed in the adsorption reactions is another significant factor influencing the thin film growth. During the next reaction step, when the other precursor is adsorbed on the surface, some amount of the film material is formed, the surface is passivated towards this precursor and reactivity of the surface towards the first precursor is recovered. In the following purge period, as in the first one, the

gaseous reaction products as well as unused precursor are removed from the reactor and the surface layer is stabilized.

Instead of the second precursor one can also apply a gas that forms volatile compounds with the adsorption-limiting ligands [113–118], thermal pulse [119], laser pulse [119] or synchrotron radiation pulse [120,121] in order to recover the reactivity of the surface to the precursor used in the first reaction step. In this way, thin films of elemental materials have been grown [113–121]. On the other hand, for deposition of compound materials, successive exposures of the surface to more than two precursors are sometimes needed [122] in order to complete an ALD cycle.

The first applications of ALD were directed to the development of EL devices [7,33,34], field effect transistors (FET) [92] and diode lasers [93]. Correspondingly, ALD of II–V and III–V compounds needed for these devices was extensively studied in this period. In the production of EL devices, the advantages of ALD were mainly due to the uniform thickness of films on large-area substrates, high EL yield and low degradation rate of devices [7]. In the case of FET-s and diode lasers, a significant benefit was expected from improved reproducibility of the deposition process and higher quality of semiconductor quantum wells and superlattices prepared by ALD [92,93].

Since 1990-s a continuously increasing interest in ALD of oxides has been observed. Initially corresponding studies were aimed at modification of catalysts [123,124]. Very soon the main interest was concentrated, however, on the microelectronic technology. It was realized that, due to downscaling of component sizes in integrated circuits, the thicknesses of the dielectrics, which were based on silicon dioxide (SiO_2) and silicon nitride (SiN_x), had been reduced close to their minimum acceptable values. Further thickness decrease that was required to develop a technology for the node size of 70 nm or lower would have resulted in unreasonably high values of tunnel current through the dielectric [125,126]. In order to find a way for further development, a search for suitable high-permittivity (high-*k*) dielectrics was started in 1990-s [127–136]. These dielectrics were expected to enable achieving sufficiently high capacitance values of capacitors and gate stacks of FET-s at greater dielectric thickness and lower tunnel current values. Correspondingly, the further down-scaling the sizes of microelectronic devices was also expected to become possible. Together with application of new materials in the microelectronic technology, a need in advanced deposition methods arose. Among several alternatives, ALD [131–135] was one of the most attractive choices. For this reason, the interest in ALD abruptly increased in the last decade [23].

2.2. Applications and earlier atomic layer deposition studies of TiO_2, ZrO_2 and HfO_2

Titanium dioxide was one of the first oxides grown by ALD [28] whereas the processes resulting in ALD of TiO_2 were investigated already in 1960-s [26,27]. High catalytic activity of TiO_2 was one of the reasons for the extensive studies of this material, especially in 1990-s [41,47,124]. However, TiO_2 was also applied in single- and multi-layer optical coatings [137–139], in chemical sensors [140,141], microelectronic [127] and spintronic [142] devices, etc. These applications additionally supported development of novel approaches for ALD of TiO_2. Several routes to ALD of this material were developed already by the middle of 1990-s [26–28,39,44,45,49,51] while in some cases, effects of process parameters on thin films properties were investigated in significant details [15,44,45,49].

The most popular precursors system used for ALD of TiO_2 in earlier works was $TiCl_4$ combined with H_2O [7,8,15,16,26–28,40–43,47,48,50–55,124]. The reactions of these precursors with porous substrates were described in studies of Prof. Aleskovskii's group [26–27] as well as by Lakomaa et al. [41] and Haukka et al. [47,124]. The crystallization processes of thin films and the effects of deposition conditions on the crystal structure and some other thin-film properties were also investigated [15,28,49,51,54,55,143,144]. In addition to the $TiCl_4$–H_2O precursor system, $TiCl_4$ combined with H_2O_2 [49] as well as titanium isopropoxide ($Ti(OC_3H_7)_4$) [39,44] and titanium ethoxide ($Ti(OC_2H_5)_4$) [45], both combined with water vapor, were employed to deposit TiO_2 films by ALD in 1990-s. By the end of 1990-s, however, these processes had not been studied as thoroughly as the $TiCl_4$-H_2O process.

In 2000 an ALD process allowing the growth of TiO_2 from TiI_4 and H_2O_2 [145] was published. Using the ALD equipment described in this thesis, this process was advanced [146–149] and a hydrogen-free process for growing TiO_2 from TiI_4 and O_2 was developed [147,149]. In these experiments, Schuisky et al. [146,149] also realized the epitaxial growth of TiO_2 on α-Al_2O_3 and MgO. In addition, the growth mechanisms and effects of process parameters on the thin film properties were studied [147,148].

Although growth mechanisms of the $TiCl_4$-H_2O ALD processes had been relatively well investigated on porous substrates [8,26–27,41,47,124] by the end of 1990-s, similar studies for planar films had been performed only in very limited cases by that time [150]. Unfortunately, the typical exposure and purge periods were markedly longer in the case of porous supports [27,41] than in the case of planar substrates [15,16,42,43]. Thus, the respective deposition mechanisms could differ significantly and there was a need in much more detail studies in the latter case. Even less information had been published on the growth mechanisms of the processes that were based on titanium ethoxide and

titanium isopropoxide. Therefore corresponding investigations were of great interest when the research described in this thesis began.

Zirconium dioxide has attracted attention as a catalyst [124], optical [151–153] and sensor [154] material as well as a dielectric with a relatively wide band gap [155–161] and high dielectric constant (permittivity) [155,162]. The main interest in ZrO_2 thin films has been related to the search for high-*k* dielectrics [130–133,157,163,164] that could replace silicon-based dielectrics in microelectronic devices. Although application of ZrO_2 in metal-oxide-semiconductor (MOS) field effect transistors has become questionable because of insufficient stability of ZrO_2 in contact with silicon [165–172], ZrO_2 can still be applied in metal-insulator-metal (MIM) capacitor structures [173], barrier layers of spin-dependent tunnel junctions [174] and nonvolatile flash memories [175,176]. As ultrathin films grown with a precise thickness control are needed in these applications, a marked interest in ALD of ZrO_2 exists.

In the earliest ALD studies, thin films of ZrO_2 were grown from $ZrCl_4$ and H_2O [73–75]. Information on the surface reactions responsible for ALD of ZrO_2 was mainly obtained from the experiments performed on porous substrates [74,75], although similar results for processes on planar substrates were even of greater interest. In addition, the number of papers describing the effect of ALD process parameters on the properties of ZrO_2 films was very limited in the beginning of 2000-s. Thus, investigations yielding information about the growth mechanisms on planar substrates and about the dependence of thin-film properties on the ALD process parameters were of significant importance. Furthermore, search for alternative ALD processes allowing deposition of thin films with reduced concentration of residues and improved dielectric properties was also of interest. An example of this kind of research was the development of the ZrI_4-based processes in studies of Kukli et al. [177–179] and Forsgren et al. [180]. These studies were carried out in parallel with those described in the original publications of the present thesis whereas the same ALD reactor and similar process parameters were used in the growth experiments.

Hafnium dioxide is a material with properties that are very similar to those of ZrO_2. The band gap values determined experimentally for HfO_2 range from 5.1–5.9 eV [181–186]. As the refractive index of HfO_2 is also relatively high [181,186–192], the material has found application in high refractive index layers of optical coatings [187,188,190,191,193] and waveguides [194–196]. However, the main interest in HfO_2 has been related to its relatively high dielectric constant reaching 19–25 at the frequency of 1 MHz [181,192] and acceptable chemical stability in contact with silicon and SiO_2 [197,198]. These properties have made HfO_2 a promising candidate for a high-*k* dielectric of next-generation microelectronic devices while application of HfO_2 as a gate dielectric of FET-s is of particular interest [199–207]. The list of FET-s, in which HfO_2 has successfully been applied, includes conventional MOS FET-s

[199–202] as well as semiconductor nanowire [203], carbon nanotube [204,205] and microtip [206] FET-s. In addition to conventional applications, this kind of FET-s can be used in scanning-probe-array type memory devices [206] and bioelectronics [207]. Another important application area of HfO_2 is capacitor structures for dynamic random access memories [136,208,209] and nanocrystal flash memory devices [210–212]. Furthermore, HfO_2 can be used in spin-dependent tunnel junctions [213] and chemical sensors [214]. Due to the high density and fast luminescence of HfO_2, scintillator applications of this material have also been discussed [215]. Finally, it should be mentioned that HfO_2 forms several crystal phases whereas one of those has been demonstrated to be potentially even harder than diamond [216]. Thus, hafnium oxide could be used in various protective coatings too.

The first paper on ALD of HfO_2 was published by Ritala et al. in 1994 [78]. The $HfCl_4$-H_2O process that was reported in this paper was the only ALD process for growing HfO_2 films, which had been published [78,79] before the research described in this thesis began. Moreover, neither experimental data on deposition mechanisms nor sufficient evidence of the influence of process parameters on properties of HfO_2 thin films had been reported by that time. During the studies that the present thesis is focussed on, several research groups proposed alternative ALD processes whereas those based on HfI_4 [217] were developed with using the same reactor, which was employed in the experiments described in this thesis.

2.3. Research objectives

The main objective of the research described in the thesis was to obtain new information on the growth mechanisms in the processes that were considered to be most promising for ALD of TiO_2, ZrO_2 and HfO_2. An important task was to get reliable data allowing one to compare different precursor systems used for deposition of a certain material. At the same time comparison of similar precursor systems used for deposition of different materials was also of great interest. Results enabling further optimization of corresponding processes were expected from these studies.

Particular attention was concentrated on crystallization processes and influence of crystallization on the growth and properties of thin films. In this connection, transitions from amorphous to crystal growth as well as formation of different crystalline phases were of interest. An effect that had not been investigated earlier was related to the influence of crystallization processes on the growth mechanism and growth rate. Although it was well known that crystallization resulted in surface roughening, the possible contribution of the changing surface structure on the mechanisms of surface reactions and correspondingly, on the growth rate of thin films in the surface-controlled ALD processes had not been investigated earlier.

Finally, the effect of structural changes on the refractive index, absorption spectra, and optical band gap, E_g, of TiO_2, ZrO_2 and HfO_2 films grown by ALD was a major task of the research. This task was chosen because there was no sufficient information on these effects when the study described in the thesis began. These thin film parameters were important not only in optical but also (directly or indirectly) in electrical applications. Indeed, E_g directly influences the band offsets between the dielectric and a metal or semiconductor in the MIM or MOS structures whereas changes in the refractive index are usually in correlation with those in the dielectric constant. Absorption spectra, in turn, are needed to determine the band gap values but they can also yield information about gap states that influence the material behavior in optical as well as electronic applications. By contrast, direct characterization of electrical properties, extensively studied by many research groups over the world, was not of primary interest in the original publications of this thesis.

3. EXPERIMENTAL METHODS

3.1. Thin film growth

The growth experiments described in this thesis were carried out with a homemade hot-wall ALD reactor [218] working at the carrier gas pressures of 0.2–1 kPa. In order to obtain sufficient purity of the reaction zone at high temperatures, inner reactor parts, which were heated and simultaneously in contact with reactive gases, were made of fused silica. An exception was a succeptor that was made of graphite. In a conventional hot-wall configuration, where only external heating was used [218,**I**], the substrate temperatures up to 750°C were obtained in the reactor. However, the reactor had also an optional succeptor with an internal infrared heater [**II**], which allowed achieving substrate temperatures up to 1000°C during the ALD growth.

Nitrogen was used as a carrier and purging gas in all growth experiments [**I–XII**]. Switching of the flow direction of the carrier gas in a metal precursor source was used to form the metal precursor pulses. In this approach, the carrier gas flowing through the precursor source carried the volatilized precursor to the reaction zone or exhaust line dependently on the flow direction chosen. The flow direction was operated with a solenoid valve that controlled the balance of the carrier gas supplied to the inlet and outlet of the metal precursor source. The flow of an oxygen precursor (H_2O, H_2O_2 or O_2) was led into the reactor through a three-way solenoid valve that switched the flow to the reactor or into the by-pass line, forming in this way the oxygen precursor pulses.

3.2. Real-time characterization of deposition process

The ALD reactor used in the experiments allowed real-time characterization of the film growth with a quartz crystal microbalance (QCM) [15,60,61,64–67,147,148,218,219, **I,III–VIII,X**]. For monitoring of the ALD processes in the real time, the films were grown on a sensor crystal of QCM and changes in the oscillation period of the crystal were recorded. In the first approximation, the increase in the oscillation period was proportional to the increase of the film mass [220]. The approach, in which the oscillation period was measured, was chosen because it had some advantages compared with the more conventional mode that was based on the recording of the oscillation frequency [221–225]. As shown by Benes et al. [220], significantly better linearity of the sensor signal versus film mass dependence was obtained in the former case than in the latter one.

In order to achieve sufficiently high sensitivity and short sampling period, quartz crystals with the oscillation frequency of around 30 MHz were used in the QCM experiments. As the most conventional AT-cut crystals were

employed, the growth temperature had to be stabilized very accurately, when the real-time studies were performed at temperatures exceeding 100–150°C. Indeed, typical values for oscillation frequency shifts were 50, 340, 1400, 3800 Hz/°C at 100, 200, 300 and 400°C, respectively. For comparison, the frequency changes corresponding to the film growth in a single ALD cycle usually did not exceed 200–300 Hz. In addition to stabilization of the sensor temperature, temperature corrections were made to the QCM data using the QCM signal recorded during relatively long purge periods before and after ALD process studies [218]. These data allowed extrapolation of the baseline to the time period, when the ALD process was recorded, and to take into account slow temperature drifts caused by the instability of heaters and room temperature. Possible routines for this kind of corrections have been described by Rahtu and Ritala [224]. It should be noted, however, that one can not separate the responses of QCM to fast temperature changes from those related to surface reactions. For this reason, the baseline corrections made in our studies were always very conservative basing mainly on the first and only in exceptional cases on the second order approximations. In the case of ALD processes described in the thesis, this kind of correction was sufficient to compensate the inaccuracy of the temperature control of the heaters and fluctuations of the room temperature.

An additional problem of the QCM measurements was the influence of the precursor pulses on the mass sensor temperature. This effect was related to temperature gradients existing in any flow-type ALD reactor and changes in the flow rate, pressure and composition of the gas phase during the precursor pulses. Corresponding temperature fluctuations occurred simultaneously with the mass changes and therefore could not be taken into account in the baseline correction routines. Nevertheless, it was possible to minimize the disturbing effects using relatively low carrier-gas pressures, low doses of precursors and well-balanced carrier-gas supply. Finally, the temperature profile was very carefully adjusted in the reaction zone. Without these measures reliable recording the mass changes was very difficult, as noticed by other authors too [226]. As a result of the efforts described here, the sensitivity ranging from 0.02 to 0.1 monolayers was realized at the sampling period of 0.5 s and temperatures up to 350°C for the materials studied in this thesis.

As ALD is a surface-sensitive process, the silver electrodes of the sensor crystals markedly influenced the results of the QCM studies in the initial stage of the film growth on the crystals. To avoid this disturbing effect, the sensor crystals were first covered with a buffer layer of the same material that was deposited in the ALD process investigated. Thus, the results obtained did not include transition effects, which might appear in the initial stage of the film growth [222]. The buffer layers used were typically 5–10 nm thick. On the other hand, the total thickness of a film deposited on a sensor crystal of QCM was

usually below 40–50 nm. For this reason, the QCM data presented in this thesis describe the thin-film growth in the thickness range of 5–50 nm.

QCM enabled monitoring of the mass changes in each reaction step (Fig. 1). Therefore it was possible to observe the character of precursor adsorption as well as the relative amount of a precursor adsorbed (mass increase Δm_1 in Fig. 1). QCM also allowed us to determine the instability of adsorbate layer formed. If the surface species decomposed or were desorbed, mass changes were observed during the purge periods (e.g. Δm_{p1} in Fig. 1). Dependently on the properties of the precursors used, exchange reaction between the film surface and oncoming precursor caused an increase (Δm_1 in Fig. 1) or decrease (Δm_2 in Fig. 1) of the film mass. Naturally, the overall growth rate, i.e. the increase of the film mass per growth cycle (Δm_0 in Fig. 1) could also be determined by QCM. However, to determine the absolute values of the mass increase per cycle, corresponding calibration of the mass sensor was needed.

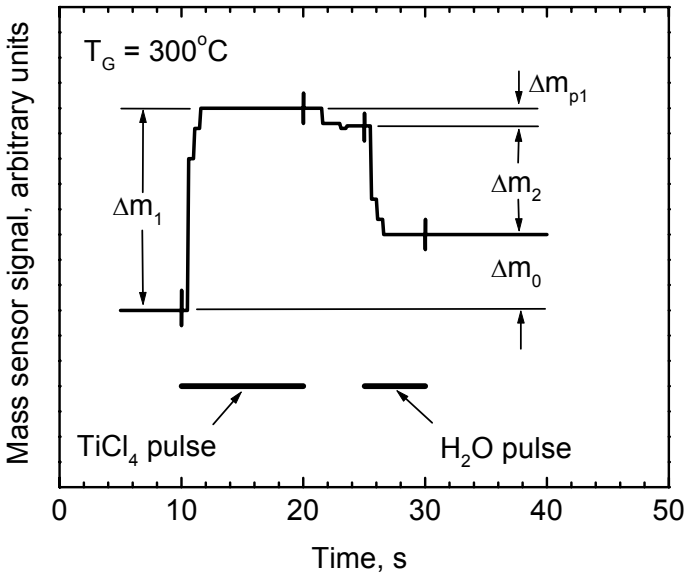

Figure 1. Mass sensor signal of QCM as a function of time in $TiCl_4$-H_2O ALD process.

Using the $\Delta m_0/\Delta m_1$ ratio, it was possible to estimate a ligand to metal ratio in an adsorbate layer formed during a metal precursor pulse [**I,III–VI,X**], provided that the film composition was known and the exchange reaction were completed. The measurement of precursor pulse delays was also possible with the QCM in the ALD reactor used [60,64,66,227] but this approach was not applied in the experiments described in this thesis.

3.3. Post-growth characterization of thin films

The films used for post-growth characterization were grown on silicon [**I–VI, VIII–XII**], fused silica [**I–X**,**XII**] and α-Al_2O_3 substrates [**IV**,**IX**]. Thin film characteristics that were determined included the growth rate, defined as a thickness (or mass) increase per ALD cycle, concentration of impurities related to the process chemistry, crystal structure, density, surface morphology and optical properties. All the parameters were determined for as-grown films.

The thickness values needed to calculate the growth rate were obtained from spectrophotometry [**I–X**,**XII**], ellipsometry [**I,II,XI**] and/or X-ray fluorescence (XRF) [**XI**] measurements. For composition characterization, the electron probe microanalysis (EPMA) [**I**,**II**,**IV**,**V**,**VII**,**VIII**,**X**], Auger electron spectroscopy (AES) [**I**,**III–V**] and time of flight elastic recoil detection analysis (TOF ERDA) [**XI**] methods were applied in the studies. In some cases, the EPMA method was also employed to measure the mass thickness, i.e. the film mass per unit area, in order to characterize the growth rate [**IV**,**VIII**].

Structural characterization was performed using the reflection high-energy electron diffraction (RHEED) [**I–VI**,**VIII–X**] and X-ray diffraction (XRD) [**I–V**,**VII–XII**] methods. The former method yielded information from a relatively thin surface layer that was typically 5–10 nm in thickness [**II,VIII**] while the latter method characterized the overall structure of a thin film. Information on the surface morphology was obtained from atomic force microscopy (AFM) studies [**V**,**VII**,**VIII**]. Cross-sectional high-resolution transmission microscopy (HRTEM) measurements enabled characterization of interface layer formation in HfO_2/Si structures [**XI**].

Refractive indices and absorption coefficients, α, were calculated from transmission spectra recorded in spectrophotometry studies of the films [**I–X**,**XII**]. From absorption spectra, optical band gaps of the materials investigated were evaluated [228,**IX**,**XII**]. In order to obtain additional data on the band gap energies and their dependence on the crystal structure, photoluminescence spectra of some ZrO_2 and HfO_2 films were also studied [215,228,**XII**].

4. RESULTS AND DISCUSSION

4.1. Titanium dioxide

4.1.1. Growth mechanisms of TiO_2

This section summarizes the ALD studies based on 4 different titanium precursors combined with H_2O and/or H_2O_2 [**III–IX**]. $TiCl_4$ and $Ti(OC_2H_5)_4$ were used in combination with H_2O [**III,V,VII–IX**] while TiI_4 and $Ti(OC_3H_7)_4$ were combined with H_2O and H_2O_2 [**IV**,**VI**].

$TiCl_4$–H_2O process. Real-time studies demonstrated that the process based on $TiCl_4$ and H_2O [**III**] most perfectly fulfilled the requirements for ALD. Adsorption of $TiCl_4$ saturated in the temperature range of 100–400°C, in which the QCM measurements were performed. The intermediate surface layer that was formed as a result of the exposure to $TiCl_4$ was stable at lower temperatures and showed only insignificant instability at 300°C (Fig. 1) and higher temperatures. Post-growth studies demonstrated that the concentration of residual chlorine was as low as 0.5 at.% in the films grown at 100°C and markedly decreased with increasing growth temperature [**III**]. Consequently, the surface reactions were complete at these temperatures.

The Cl/Ti ratio was 2.5–3.0 in the surface intermediate layer formed at 100°C during the $TiCl_4$ adsorption as estimated from the results of QCM studies [**III**]. This means that at 100°C, from 4 chlorine ligands bonded to titanium atom in $TiCl_4$, in average 1.0–1.5 ligands were removed during $TiCl_4$ adsorption. The rest of Cl ligands were adsorbed together with titanium and blocked the further adsorption of $TiCl_4$ when they formed a sufficiently abundant layer on the film surface. The removal of chlorine during $TiCl_4$ adsorption was evidently due to exchange reaction with surface OH-groups, which reacted with $TiCl_4$ and formed volatile HCl [27–28,41,42,**III**]. Thus, the abundance of surface OH-groups obviously influenced the amount of the chlorine ligands released.

With the increase of the growth temperature to 300°C the Cl/Ti ratio reached 4 in the adsorbate layer formed during $TiCl_4$ pulse [**III**]. Consequently the number of chlorine atoms released during $TiCl_4$ pulse decreased with increasing temperature and practically no chlorine was released at 300°C. These results were in good agreement with the data of Matero et al. [229] who showed that the percentage of chlorine ligands removed during TiO_2 pulse was 40–45% at 150°C and only 10–20% at 300–400°C. It is worth noting that in the latter study, QCM and quadrupole mass spectrometry (QMS) methods used gave very similar results. Although the Cl/Ti ratio in the adsorbate layer formed at 300–400°C was very close to that in $TiCl_4$, the Cl ligands did not have to stay

bonded to the Ti atom, which they were bonded to in the precursor state. As discussed by Ritala et al. [42], chemical bonds were likely rearranged in this way that some chlorine ligands belonging to a $TiCl_4$ molecule became bonded to the Ti atoms incorporated into the film in previous ALD cycles. The unsaturated Ti bonds created in this process in a precursor molecule ensured bonding of additional titanium to the surface oxygen together with the rest of chlorine ligands.

A probable reason for why no or very few chlorine ligands were removed at higher temperatures during the $TiCl_4$ pulse was the low concentration of hydroxyl groups that had been formed during the previous exposure of the surface to H_2O. It is well known that the equilibrium surface concentration of hydroxyl groups on a surface of an oxide decreases with increasing temperature [47,230] and therefore the corresponding increase of adsorbed chlorine is an expected result. An alternative possibility to explain high Cl/Ti ratio in the adsorbate layer is to assume re-adsorption of HCl released in the reaction of $TiCl_4$ with surface OH-groups [42]. Our real-time QCM studies, in which we exposed the surface of a TiO_2 film to HCl, indicated that contribution of this process to formation of the surface layer could not be significant, however [**III**].

Independently of the reasons for the increase of the Cl/Ti ratio in the intermediate surface layer, this increase leads to the decrease in the growth rate. Indeed, due to their relatively great radius, the chlorine ions coordinated to titanium adsorbed block several adsorption sites. Thus, the Cl/Ti ratio in the adsorbate layer is a factor that determines the growth rate whereas the growth per cycle decreases with increasing Cl/Ti ratio. It should be mentioned, however, that the growth rate decrease corresponds to this mechanism only when the films save their phase composition and surface microstructure with changing deposition temperature [**III**,**VII**].

An interesting result was a modest self-limited decrease of the film mass during the purge after $TiCl_4$ pulse (Fig.1). The following reaction of the surface layer with H_2O indicated that even after the decrease and saturation of the film mass on a new level, the surface layer still contained significant amounts of chlorine. Therefore the relaxation observed during the purge period was not related to the reaction of the surface with possible H_2O residues in the carrier gas. An additional important finding was that the effect was stronger at shorter $TiCl_4$ pulses. Analysis of the QCM data [**III**] indicated that the effect was unlikely caused by variation of the mass sensor temperature. More probably the effect was due to a limited loss of chlorine ligands adsorbed during the $TiCl_4$ pulse. As discussed in several papers [42,231–233], reactions between hydroxylated surface and $TiCl_4$ might lead to formation of surface species, which could be described as $Ti(OH)_xCl_{4-x}$ with $0 < x < 4$. Later the OH and Cl ligands could recombine resulting in TiO_2 formation on the surface and HCl release into the gas phase. Relatively low rate of this recombination process was a probable reason for why the mass decrease discussed was greater after shorter $TiCl_4$ pulses. In the case of longer pulses, the process obviously proceeded in a

marked extent already during the exposure to $TiCl_4$ and the removal of adsorbed ligands was compensated by additional adsorption of $TiCl_4$. The latter adsorption process took place on the surface that contained much less hydroxyl groups and thus, smaller relaxation was observed during the following purge.

During the H_2O pulse a surface reaction between the intermediate surface layer and H_2O led to an expected decrease of the film mass (Fig. 1) because heavy Cl ions were replaced with much lighter OH-groups or oxygen [**III**] whereas formation of OH-groups was more favorable at lower temperatures. As already discussed, higher concentration of OH-groups allowed more efficient adsorption of titanium precursor in the next growth cycle. Thus, sufficiently long H_2O pulses and, especially, high H_2O partial pressures were needed to achieve higher growth rates as demonstrated by Matero et al. [234] in the case of ALD of TiO_2 and several other oxides. However, if the H_2O doses exceed a certain value, then during the following purge period, the concentration of OH-groups anyway stabilizes at a level that is determined by the substrate temperature [230] rather than by preceding dose of H_2O. Of course, combining higher H_2O doses with shorter purge periods, one can achieve higher OH concentrations but in this case, mixing of the precursors in the gas phase and, correspondingly, deviations from the ALD-type growth become also more probable. In addition to the lower substrate temperature, higher H_2O dose and shorter purge period, the reduced flow rate of the carrier gas may lead to an increase in the surface concentration of OH-groups and higher growth rate [235]. Unfortunately, employing lower carrier-gas flow rates may also cause mixing of the precursors in the gas phase because of less efficient purging of the reaction zone.

TiI_4-H_2O and TiI_4-H_2O_2-H_2O processes. Although first attempts of applying TiI_4 and H_2O for ALD of TiO_2 were not successful [145], the process was later realized and studied [**IV**]. The concentration of residual iodine did not exceed 0.15 at.% in the films deposited at as low temperature as 135°C and the O/Ti ratio of all films studied by EPMA corresponded to stoichiometric TiO_2 [**IV**]. The following differences from the $TiCl_4$-H_2O process were more significant. Firstly, the ligand to Ti ratio was lower in the intermediate surface layer formed during TiI_4 pulse [**IV**] when compared with the corresponding ratio obtained under similar conditions during the $TiCl_4$ pulse [**III**]. For instance, average values of the I/Ti ratios were 2.0 ± 0.3, 2.5 ± 0.3 and 2.1 ± 0.4 at 135, 200 and 300°C [**III**] while the respective Cl/Ti values were estimated to be 3.1 ± 0.3, 3.9 ± 0.4 and 4.0 ± 0.2. Secondly, differently from the Cl/Ti ratio [**III**], the I/Ti ratio decreased with the increase of temperature from 200°C to higher values [**IV**]. Thirdly, the growth per cycle did not show complete saturation with increasing TiI_4 pulse duration [**IV**]. All these results demonstrate that the ligands were more readily released from TiI_4 than from $TiCl_4$, especially at higher temperatures, at which the concentration of OH-groups contributing to

the exchange reactions was lower than at lower temperatures [230]. This significant difference was probably related to lower thermal stability of TiI_4 compared with that of $TiCl_4$ [236]. Simple thermodynamic analysis demonstrated [**IV**] that lower stability of TiI_4 explained why ALD of TiO_2 was realized from TiI_4 and O_2 [148,149] but not from $TiCl_4$ and O_2. QCM studies of the TiI_4-O_2 process confirmed that at temperatures exceeding 200–250°C, surface hydroxyl groups were not necessary to release iodine ligands during TiI_4 adsorption [148]. The I/Ti ratios observed in the adsorbate layer after TiI_4 adsorption ranged from 1.8–2.6 at 250–350°C in the TiI_4-O_2 process [148] being very similar to those determined for the TiI_4-H_2O process at comparable growth temperatures [**IV**].

The substitution of H_2O for the H_2O_2-H_2O mixture in the TiI_4-based ALD process caused considerable changes only in the growth rate of very thin films deposited at 130–200°C provided that a commercial 35% solution of H_2O_2 was used as the oxygen precursor source [**IV**]. Somewhat higher growth rates, which were typical for the TiI_4-H_2O_2-H_2O process, were due to the higher reactivity of H_2O_2 compared to that of pure H_2O. Application of the commercial H_2O_2-H_2O solution instead of H_2O did not result, however, in marked differences in the reaction mechanism. Moreover, this substitution did not influence the growth rates of thicker films either [**IV**]. The result that the oxygen precursors differently influenced the growth rates of films with different thicknesses was related to dissimilar crystallization in the TiI_4-H_2O and TiI_4-H_2O_2-H_2O processes [**IV**]. In more detail, these effects are discussed in Section 4.1.3.

$Ti(OC_2H_5)_4$-H_2O process. In the case of the process, which was based on titanium ethoxide as the titanium precursor, the growth was not self-limited at temperatures exceeding 275–350°C [45,**V**]. At these temperatures, decomposition of titanium precursor became significant and, as $Ti(OC_2H_5)_4$ contained oxygen, TiO_2 was formed without supply any additional oxygen precursor. At lower temperatures, $Ti(OC_2H_5)_4$ could successfully be applied for ALD-type growing of TiO_2, when combined with H_2O [45,**V**,**VIII**]. QCM studies demonstrated that ligand to Ti ratio was 2.5 ± 0.3, 2.8 ± 0.4 and 3.4 ± 0.4 at 150, 200 and 250°C in the adsorbate layer formed during the $Ti(OC_2H_5)_4$ pulse [**V**]. These relatively high ratios, indicating a release of only 0.6–1.5 ligands during $Ti(OC_2H_5)_4$ adsorption, were in good agreement with the data of QMS studies of Rahtu et al. [237], who showed that at these temperatures, C_2H_5OH formed in the surface reactions was released during the H_2O pulse rather than during the $Ti(OC_2H_5)_4$ pulse. According to our QCM studies the number of ligands released during $Ti(OC_2H_5)_4$ adsorption abruptly increased with the increase of the substrate temperature from 275°C to higher temperatures. This was, however, mainly due to thermal decomposition of the precursor as the results of QMS studies confirmed [237]. Post-growth characterization of the films demonstrated that the concentration of carbon residues increased from

0.5–0.7 to 6–12 at.% with the decrease of T_G from 150 to 100°C [**V**]. Moreover, the hydrogen concentration was as high as 12.5 at.% in the films grown at 100°C [238] indicating that the surface reactions were not complete at the precursor doses used. Probably for this reason, the QCM data showed unexpected dependence of the growth mechanism on temperature at 100–150°C [**V**]. According to the QCM data, the ligand to titanium ratio established in the surface layer during the $Ti(OC_2H_5)_4$ pulse increased from 2.5 to 3.0 with the temperature decrease from 150 to 100°C [**V**]. This kind of behavior could be explained only assuming that the exchange reaction between surface OH-groups and $Ti(OC_2H_5)_4$ was not complete at lower temperatures.

$Ti(OC_3H_7)_4$-H_2O and $Ti(OC_3H_7)_4$-H_2O_2 processes. Decomposition of the titanium precursor also influenced the processes based on titanium isopropoxide. In these ALD processes, the growth rate markedly increased and the self-limited character of the surface reactions was lost at temperatures exceeding 275–300°C [44,**VI**]. At 100–275°C, self-limited ALD-type growth was observed in the $Ti(OC_3H_7)_4$-H_2O as well as $Ti(OC_3H_7)_4$-H_2O_2 process [**VI**]. Both processes resulted in the films with relatively low impurity concentrations even at the lowest growth temperature used. The carbon concentrations measured by AES were 1.3–1.6 at.% in the films grown from $Ti(OC_3H_7)_4$ and H_2O and 0.6–1.0 at.% in the films grown from $Ti(OC_3H_7)_4$ and H_2O_2 at 100°C [**VI**]. In addition to the lower impurity concentration, significantly higher growth rates were obtained at 100–150°C in the $Ti(OC_3H_7)_4$-H_2O_2 process than in the $Ti(OC_3H_7)_4$-H_2O process [**VI**]. In this connection, it is worth noting that in the $Ti(OC_3H_7)_4$-H_2O_2 process, concentrated H_2O_2 was used as the oxygen precursor while application of the commercial 35% H_2O_2-H_2O solution instead of pure H_2O did not cause marked effect.

The growth mechanism determined from the real-time QCM measurements also depended on the oxygen precursor used in the $Ti(OC_3H_7)_4$-based processes. In the $Ti(OC_3H_7)_4$-H_2O process, the ligand/Ti ratios stabilized in the adsorbate layer during the $Ti(OC_3H_7)_4$ pulse were 1.5–1.8 and 1.0–1.2 at 100–250 and 300°C, respectively [**VI**]. For comparison, Rahtu and Ritala [239] determined the values of 1.9–2.0 and 2.4 for this ratio at temperatures of 150–250 and 300°C from QCM and QMS measurements. The agreement of the results obtained in these two studies was relatively good at 150–250°C while a significant difference was observed at 300°C. A possible reason for the difference was decomposition of $Ti(OC_3H_7)_4$ that influenced the results obtained at higher temperatures and could cause marked variation of the adsorbate layer composition even at small dissimilarities in experimental conditions.

In the case of the $Ti(OC_3H_7)_4$-H_2O_2 process, the ligand/Ti ratios of 1.1–1.4, 2.3–2.8 and 1.3–1.8 were obtained at 100, 200–250 and 300°C, respectively, in the adsorbate layer formed during the $Ti(OC_3H_7)_4$ pulse [**VI**]. Hence, at lower temperatures, application of H_2O_2 instead of H_2O led to more efficient ligand

exchange during titanium precursor adsorption. Consequently, the preceding exposure to H_2O_2 had to cause more complete exchange reaction and surface hydroxylation than the exposure to H_2O did. At higher temperatures, on the contrary, the substitution of H_2O for H_2O_2 resulted in less efficient ligand exchange in the $Ti(OC_3H_7)_4$ adsorption process. Therefore under these conditions the concentration of OH-groups, which were formed during H_2O_2 pulse and took part in exchange reactions during the following $Ti(OC_3H_7)_4$ pulse, was lower than that formed during the H_2O pulse. At 150°C, contribution of surface OH-groups to the surface reactions was similar in these two processes according to QCM data [**VI**]. The growth rate was, however, 1.5 times higher in the $Ti(OC_3H_7)_4$-H_2O_2 process than in the $Ti(OC_3H_7)_4$-H_2O process [**VI**]. An explanation for this non-trivial result is that although H_2O and H_2O_2 created the same OH abundance of the TiO_2 surface, H_2O did not remove all isopropoxide ligands. These ligands reduced the number of adsorption sites during the next $Ti(OC_3H_7)_4$ pulse and in this way the growth rate as well [**VI**].

4.1.2. Influence of reaction mechanism on growth rate of TiO_2

In the case of ALD processes discussed above, the ligand to titanium ratios reached the value of 4 in the adsorbate layer formed during a titanium precursor pulse. Thus, the ligands coordinated to an adsorbed titanium atom occupied a larger surface area than that of a titanium adsorption site. Consequently, the steric hindrance influenced the growth rate in the processes described. QCM measurements performed for relatively thin (5–50 nm) films confirmed contribution of steric effects to the mass increase per cycle in the $TiCl_4$-H_2O [**III**,**VII**], TiI_4-H_2O_2-H_2O [**IV**] and $Ti(OC_3H_7)_4$-H_2O_2 [**VI**] processes. In these cases, the decrease of the ligand to titanium ratio in the adsorbate layer during the metal precursor pulse was always accompanied by an increase of the growth rate. In the $Ti(OC_2H_5)_4$-H_2O and $Ti(OC_3H_7)_4$-H_2O processes, this qualitative relationship was fulfilled only at temperatures exceeding 200–250°C. At lower temperatures, the surface exchange reactions were evidently incomplete leaving metal precursor ligands on the surface even after the oxygen precursor pulse. At the same time comparison of the growth rates and compositions of films, which were deposited in the processes employing different oxygen precursors, indicated that the latter ligands, although they reduced the growth rate, did not stay in the films. Therefore the surface layer compositions formed by the end of an ALD cycle, on one hand, and the film compositions determined in post-growth studies, on the other hand, might differ from each other. This difference was a probable reason for the disagreement between the changes in the growth rate and ligand/Ti ratio formed on the surface during the titanium precursor pulse.

Even more significant disagreement between the growth rate and ligand/Ti ratio obtained on the TiO_2 surface after a titanium precursor pulse was observed, when growth rates of thicker (80–300 nm) films were compared with each other (Table 1). In Table 1, the ligand/Ti ratios and growth rates are given for temperatures, at which the processes enabled reliable ALD-type growth and resulted in the film compositions that did not deviate significantly from the stoichiometric one. In several studies [**III–VIII,**148], growth mechanisms as well as growth rates were determined. In these cases, the ALD process parameters used for QCM measurements and growing the films for post-growth characterization were similar. Table 1 also contains some data taken from the works, in which either growth mechanisms or growth rates were determined.

Table 1. Ligand to titanium ratios determined on the surface after titanium precursor pulse and mean growth rates of TiO_2 films with thicknesses of 80–300nm

Precursors	T_G, **°C**	**Ligand/Ti**	**Growth rate, nm/cycle**	**References**
$TiCl_4$-H_2O	100	2.8 ± 0.3	0.078 ± 0.003	III,VII
	150	3.1 ± 0.3	0.048 ± 0.002	III,VII
	150	2.1–2.4	–	229
	150	–	0.04–0.06	240
	300	4.0 ± 0.2	0.072 ± 0.004	III,VII
	300	3.2–3.4	–	229
	300	–	0.05	234
	300	–	0.049–0.054	241
$Ti(OC_3H_7)_4$-H_2O_2	100	1.3 ± 0.2	0.120 ± 0.005	VI
TiI_4-H_2O	150	2.2 ± 0.3	0.075 ± 0.003	IV
	300	2.3 ± 0.4	0.11 ± 0.01	IV
TiI_4-H_2O_2-H_2O	150	2.2 ± 0.3	0.075 ± 0.003	IV
	300	2.3 ± 0.4	0.11 ± 0.01	IV
	300	1.6–2.8	–	147
TiI_4-O_2	300	2.6	0.08	148
$Ti(OC_2H_5)_4$-H_2O	150	2.5 ± 0.3	0.051 ± 0.003	V,VIII
	300	3.0 ± 0.4	0.09 ± 0.01	IV,VIII
	300	–	0.06	234

Comparing the data for the temperature range of 100–150°C, one can see an expected anti-correlation between the ligand/Ti ratios and growth rates, i.e. the higher the ligand/Ti ratio, the lower the growth rate. It should be taken into account, however, that the sizes of different ligands differ from each other, increasing in the sequence halide – ethoxide – isoprpoxide [45]. Furthermore, due to possible misfit of the sizes of absorbed species and those of adsorption sites, the closest packing of the species is not possible in the surface layer [242]. One can also see that, contrary to expectations based on the behavior of the ligand/Ti ratios in the surface layer formed during a Ti precursor pulse, comparable or even higher growth rates have been obtained at 300°C than at

100–150°C (Table 1). As shown below, this effect is related to crystallization processes.

In addition to the ALD processes represented in Table 1, the $TiCl_4$-H_2O_2 [49], $Ti(OCH_3)_4$-H_2O [243] and $Ti(OC_3H_7)_4$-O_3 [244] processes should be mentioned, although no information on the growth mechanism has been available for these three processes. Kumagai et al. [49] obtained the growth rates of 0.042 nm/cycle at 240°C and 0.065 nm/cycle at 340°C for the $TiCl_4$-H_2O_2 process [49]. These growth rates are very close to those of the $TiCl_4$-H_2O process (Table 1). For the ALD process, which was based on titanium methoxide ($Ti(OCH_3)_4$) and H_2O, Pore et al. [243] reported the growth rates of 0.042 nm/cycle at 200°C and 0.054 nm/cycle at 300°C. For the $Ti(OC_3H_7)_4$-O_3 process, Kim et al. [244] published the growth rate value of 0.054 nm/cycle for 10–100 nm thick films grown on silicon substrates at 250°C.

4.1.3. Influence of crystallization on growth and properties of TiO_2 films

Growth of amorphous and polycrystalline films. As demonstrated earlier [15,41,42,44,45,54,55,144], crystallization of TiO_2 films in the ALD processes depended on the precursors used as well as on the deposition process parameters. In the processes described above, non-epitaxial crystalline films grew at relatively low temperatures. On silicon and silica substrates, crystalline TiO_2 films were obtained at temperatures exceeding 150°C in the $TiCl_4$-H_2O process [15,**III**], 135°C in the TiI_4-H_2O process [**IV**], 166°C in the TiI_4-H_2O_2-H_2O process [**IV**] and 180°C in the $Ti(OC_2H_5)_4$-H_2O, $Ti(OC_3H_7)_4$-H_2O and $Ti(OC_3H_7)_4$-H_2O_2 processes [**V**,**VI**] provided that neither additional field nor surface pretreatment was applied. For comparison, using pretreatment of silica substrates in the flow of $TiCl_4$ at 365–530°C, Niilisk et al. [245] were able to grow crystalline TiO_2 films with anatase structure from $TiCl_4$ and H_2O even at 125°C. Moreover, in an electric field, rutile films were grown by $TiCl_4$-H_2O-based ALD on silicon substrates at room temperature, as reported by Drozd et al. [51]. In this thesis, however, crystallization of TiO_2 without additional fields on substrates without crystallization-supporting pretreatment is discussed.

The amorphous TiO_2 phase was preferentially formed in thinner films [**III,**241] and at shorter precursor pulse times [**VII**], provided that the epitaxial growth was not possible. Application of an oxygen precursor of higher reactivity, e.g. H_2O_2-H_2O mixture instead of pure H_2O [**IV**] also seemed to cause more probable growth of the amorphous phase. Obviously, the crystal growth was related to agglomeration of film material at nucleation centers in very thin films, i.e. when the film thickness was comparable to the lattice constant of a crystalline phase. In this case, crystallization led to marked surface roughening [15,**VII**,**VIII**] and increase of the surface area as well as surface

free energy. If the mean film thickness was small, the decrease in the bulk free energy accompanying formation of a more ordered structure could not compensate the increase in the surface energy. Shortening the precursor pulses evidently reduced the time left for surface migration needed for the crystal growth and, hence, expectedly resulted in more amorphous films. Similarly, application of an oxygen precursor of higher reactivity led to more complete surface reactions, reducing in this way the mean residence time of intermediate surface species and making surface migration and crystallization less probable.

The main crystalline phases that dominated in the films grown by ALD were anatase and rutile whereas rutile was usually formed in the films grown at temperatures exceeding 300–350°C. At some ALD process parameters, the high-pressure TiO_2-II phase was also formed [143,144,150,246,247]. The latter phase was observed, however, only in the films grown on the KBr substrates [246] and also on silica or silicon substrates that were close to soda-lime glass substrates during the film growth [247]. Thus, the presence of alkali metal impurities on the surface obviously contributed to the growth of the TiO_2-II phase, although post-growth AES studies did not show corresponding residues inside the films [247].

As already mentioned, crystalline phases were not always formed in the initial growth stages of non-epitaxial thin films even if the growth temperature was sufficient for formation of this phase in thicker films. For instance, up to 7 nm thick TiO_2 films grown from $TiCl_4$ and H_2O on silicon substrates at 275°C were amorphous, although the temperature of 150°C was already sufficient for the growth of the anatase phase in the films with the thicknesses exceeding 25 nm [**III**]. Similarly, at the temperatures that were sufficiently high for the rutile growth, films with the anatase structure were formed in the initial stage of deposition [247]. As a result, these films were structurally and optically inhomogeneous in the growth direction [247].

Detail studies of the TiO_2 films grown at temperatures, at which transition from amorphous to anatase growth occurred, demonstrated that nucleation started, when a certain film thickness was achieved [15,240,246,**VII**,**VIII**]. This conclusion was based on the results of SEM, AFM, RHEED and XRD [15,240,**VII**,**VIII**] as well as HRTEM [246] studies. In the initial stage of crystallization, the nucleation centers were located relatively far from each other [15,240,**VII**,**VIII**]. Growth of crystallites at these centers caused marked surface roughening observed in the $TiCl_4$-H_2O [15,240,**VII**] and $Ti(OC_2H_5)_4$-H_2O [**VIII**] ALD processes. The surface roughness increased mainly because the anatase phase grew faster than the amorphous phase did. The real-time QCM studies performed on amorphous and crystalline buffer layers [**III**] demonstrated that $TiCl_4$ was more efficiently adsorbed on the crystalline (anatase) layers. XRD investigations supported this result showing that the crystallite sizes grew faster in the growth direction than the mean thickness of films containing mixture of amorphous and anatase phases did [**VIII**].

Increasing anatase amount in the growing films resulted, therefore, in the increase of the overall growth rate. Furthermore, the increase of the surface roughness led to an increase of the surface area exposed to the precursors [**VII**,**VIII**]. For this reason the growth rate additionally increased. As a result, an abrupt increase of the growth rate was observed [**VII**,**VIII**], when the transition from amorphous to anatase growth took place with increasing T_G (Fig. 2) or film thickness (Fig. 3).

In a recent paper, Kim et al. [248] reported a very similar effect for the $Ti(OC_3H_7)_4$-H_2O process. They also observed a marked increase of the surface roughness and growth rate under the conditions, which resulted in crystallization of TiO_2 films, whereas the onset of crystallization was obtained with increasing growth temperature as well as film thickness [248]. As a similar effect occurred in three different ALD processes ($TiCl_4$-H_2O [**VII**], $Ti(OC_2H_5)_4$-H_2O [**VIII**] and $Ti(OC_3H_7)_4$-H_2O [248]), the phenomenon was evidently related to the film material (TiO_2) or oxygen precursor (H_2O) rather than to the metal precursors applied in the synthesis process.

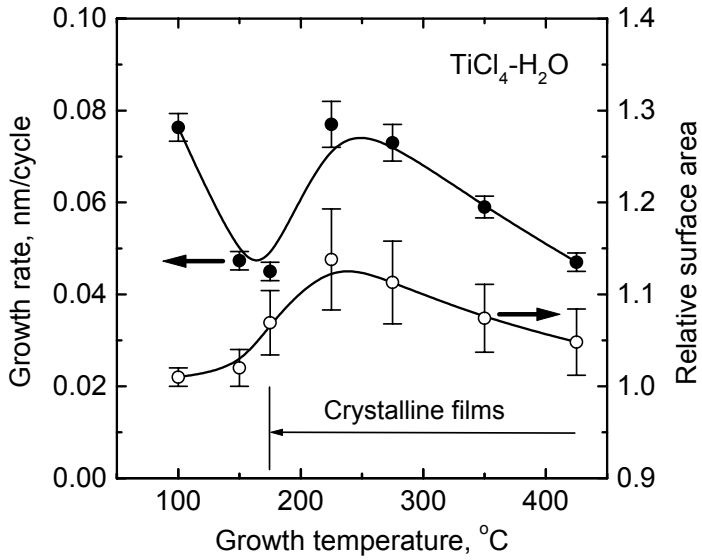

Figure 2. Comparison of growth rates and relative surface areas of TiO_2 thin films grown by ALD from $TiCl_4$ and H_2O at temperatures 100–425°C [**VII**]. All films grown at 100–150°C were amorphous while those grown at 175°C and higher temperatures contained crystalline phases [**VII**]. The films measured were 130–230 nm in thickness.

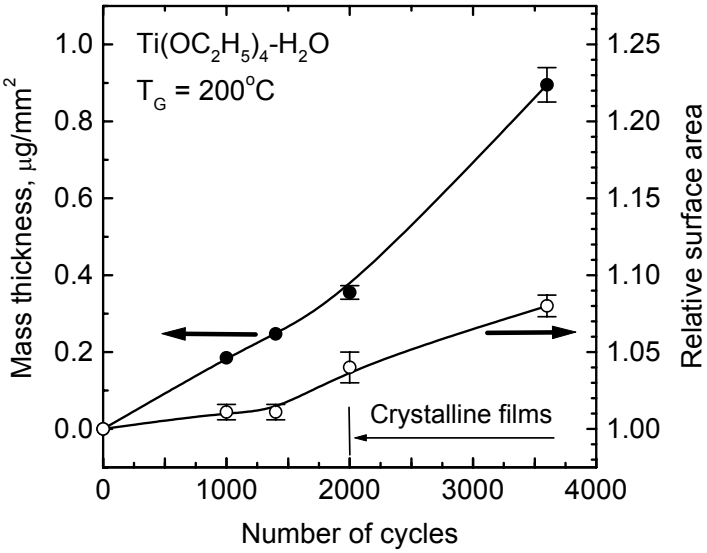

Figure 3. Mass thicknesses and relative surface areas of TiO_2 thin films grown by ALD from $Ti(OC_2H_5)_4$ and H_2O at 200°C [**VIII**]. The films grown by applying up to 1400 cycles were amorphous while those grown by applying 2000 or more cycles contained crystalline (anatase) phase [**VIII**].

Studies of the surface morphology [15,**V,VII**,**VIII**] and crystallite (grain) sizes [241,**VIII**] demonstrated that the crystallites were larger in the TiO_2 (anatase) films grown at lower temperatures. Hence, at lower temperatures, nucleation was a less probable process and an increase in the sizes of existing crystallites rather than creation of new crystallites took place.

Expectedly, no preferential in-plane orientation of anatase and rutile was observed on the silicon substrates. This was mainly because the parameters of the tetragonal unit cells of rutile and anatase differed from the parameter of the cubic unit cell of silicon too much (the difference exceeded 10%). Moreover, amorphous SiO_2 was easily formed on silicon substrates in the initial stage of TiO_2 growth [246]. Therefore the silicon substrates could not influence the in-plane crystallographic orientation of growing film. Nevertheless, preferential orientation of crystallites in the direction perpendicular to the substrate surface was observed on the crystalline silicon as well as amorphous silica substrates. For instance, anatase films grew in the ALD processes in this way that at the film surface, the (1 1 0) plane was preferentially parallel to the substrate surface [15,**IV**–**VI**,**VIII**,**IX**]. Development of this orientation with increasing film thickness [15] indicated that the preferential orientation was related to the higher growth rate of crystallites in corresponding direction. An interesting result was that the preferential orientation determined by XRD inside the TiO_2

films might markedly differ from the orientation determined by RHEED on the surface [**VIII**]. This was an additional reason for inhomogeneity that could influence the overall properties of polycrystalline thin films [247].

Epitaxial growth. Epitaxial TiO_2 films, i.e. films with the in-plane crystallographic orientation determined by single-crystal substrates, were grown by ALD on α-Al_2O_3 [146,149,**IV**,**IX**] and MgO [146,149,249,250] substrates. The first ALD process that enabled successful epitaxial growth of TiO_2 films was based on TiI_4 and H_2O_2-H_2O precursors [146]. Somewhat later the TiI_4-O_2 [149], TiI_4-H_2O [**IV**] and $TiCl_4$-H_2O [**IX**,249,250] processes were also used for the epitaxial growth of TiO_2. All the processes enabled epitaxial growth of rutile on α-Al_2O_3 and anatase on MgO.

On the substrates, which allowed epitaxial growth of a crystalline phase, this phase was formed in a wider range of substrate temperatures than on those substrates that did not allow epitaxy. On the α-Al_2O_3 substrates, for instance, films containing only the rutile phase were obtained at 350°C and higher temperatures from $TiCl_4$ and H_2O [**III**]. For comparison, no pure rutile films could be grown on silicon and silica substrates at temperatures up to 680°C [251]. In the TiI_4-H_2O_2-H_2O process, single-phase rutile films were grown on the α-Al_2O_3 substrates already at 275°C [146] while epitaxial anatase films were obtained on the MgO substrates at 200–375°C [146]. Thus, in the temperature range of 275–375°C, exactly the same process parameters led to the rutile growth on α-Al_2O_3 and anatase growth on MgO. Very similar, although somewhat weaker, phase-stabilizing role of the α-Al_2O_3 and MgO substrates appeared in the TiI_4-O_2 [149] and TiI_4-H_2O [**IV**] processes.

Comparing the growth rates of non-epitaxial and epitaxial films [148,149,**IX**], one can see that the former films tended to grow faster than the latter did. Dissimilar phase composition [149, **IX**] was one reason for this difference. However, comparison of the data published in papers of Shuisky et al. [148,149] and Mitchell et al. [250] leads to a conclusion that even at similar phase compositions, the growth rate of the polycrystalline films was higher than that of the epitaxial films. An explanation for this effect is that in non-epitaxial films, the crystallites were preferentially oriented in the direction of the fastest growth while in the epitaxial films, the substrate determined the structure orientation that could markedly differ from this direction. In addition, higher density of epitaxial films contributed to the difference in the thickness increase per cycle.

Effect of phase composition on properties of TiO_2 thin films. The results presented above demonstrate that in order to grow most homogeneous TiO_2 films, one should aim at amorphous or epitaxial growth. By contrast, polycrystalline films were inhomogeneous in a general case. The inhomogeneity and related surface roughening [15,240,**VII**,**VIII**] resulted in light scattering [46]

and increasing optical losses [15]. In the electronic applications, crystallite interfaces seemed to act as current leakage channels degrading the dielectric properties of the films [252].

Table 2. Influence of phase composition on refractive indices of TiO_2 thin films prepared by ALD.

Phase	Precursors	T_G, °C	Refractive index (at λ = 580 nm)	References
Amorphous	$TiCl_4$-H_2O	100–150	2.37–2.63	[III,VII,IX]
	$TiCl_4$-H_2O	150	2.4	[42]
	$Ti(OC_3H_7)_4$-H_2O	100	2.3	[VI]
	$Ti(OC_3H_7)_4$-H_2O	150	2.3	[44]
	$Ti(OC_2H_5)_4$-H_2O	100	2.3	[V]
	$Ti(OCH_3)_4$-H_2O	200–225	2.37–2.48	[243]
Anatase (polycrystalline)	$TiCl_4$-H_2O	175–350	2.0–2.5	[III,VII,IX]
	TiI_4-H_2O	375	2.51 ± 0.04	This work
	TiI_4-O_2	235–380	1.8–2.5	[148]
	$Ti(OC_3H_7)_4$-H_2O	225–350	2.5	[44]
	$Ti(OC_2H_5)_4$-H_2O	350	2.4–2.5	[V]
	$Ti(OCH_3)_4$-H_2O	250–400	2.43–2.53	[243]
Anatase (epitaxial)	$TiCl_4$-H_2O	275	2.65 ± 0.05	This work
Rutile (polycrystalline)	$TiCl_4$-H_2O	375	2.70	[IX]
Rutile (epitaxial)	$TiCl_4$-H_2O	425–500	2.80–2.82	[IX]

In the studies that the thesis is based on, significant efforts were concentrated on characterization of refractive indices (Table 2) of films grown in different ALD processes [**III**–**VII**,**IX**]. This was a convenient way to investigate the effect of process parameters on the thin film densities, too, because the relationship between the refractive index and density of TiO_2 was established relatively well [253,254]. The results depicted in Table 2 also include those of other authors obtained for various ALD processes [42,44,148,243]. All refractive index values depicted in Table 2 were measured at the wavelength of λ = 580 nm.

As can be seen in Table 2, the refractive indices of amorphous and polycrystalline anatase films varied in relatively wide ranges. These variations were due to differences in deposition temperatures [243,**III**,**VII**,**IX**] as well as precursors used. As a rule, the refractive index values were lower at lower temperatures, if no phase transitions took place in corresponding temperature range [243,**III**,**VII**,**IX**]. In the case of amorphous films that were obtained only at relatively low temperatures, the refractive index decrease observed with decreasing growth temperature was probably related to the increase of impurity concentrations in the films. In the case of anatase films, corresponding decrease

of refractive index was obviously due to lower packing density of crystallites in the polycrystalline films that were grown at lower temperatures. It is worth noting that due to low packing density of crystallites, the refractive indices of the latter films were sometimes even lower than those of amorphous films [243,**III**,**VII**,**IX**].

Expectedly, the refractive indices of epitaxial films were clearly higher than the refractive indices of polycrystalline films (Table 2). When comparing the refractive index of epitaxial rutile (Table 2) with the corresponding value of bulk single-crystal rutile [255], one can find no difference. It should also be mentioned that the refractive indices obtained for polycrystalline anatase and rutile were comparable to the highest refractive values of TiO_2 thin films with similar phase compositions prepared by other deposition methods. For instance, Bendavid et al. [256] reported the values of 2.56, 2.62 and 2.72 at λ = 550 nm for the amorphous, anatase and rutile films, respectively, deposited by filtered arc deposition. Using the radio-frequency magnetron sputtering method, Miao et al. [257] deposited polycrystalline anatase and rutile films with the refractive indices of 2.657 and 2.849, respectively, at the wavelength of 500 nm.

The optical band gap values that were determined for amorphous TiO_2, anatase and rutile films grown by ALD equaled to 3.40 ± 0.03, 3.35 ± 0.05 and 3.16 ± 0.05 eV, respectively [**IX**]. Corresponding values reported for films grown by other methods ranged from 3.28–3.32 eV for amorphous [258], 3.15–3.39eV for anatase [257–260] and 3.02–3.34 eV for rutile [257–260] films, when estimated assuming indirect transitions near the optical absorption edge. For comparison, the adsorption edge of anatase single crystals was located at 3.3 eV [261], while the band gap of rutile single crystals was estimated to be 3.062–3.101 eV [262] at room temperature. Therefore results obtained for different phases of TiO_2 synthesized by ALD were very similar to the data reported for single crystals and for most perfect films prepared by other deposition techniques.

4.2. Zirconium dioxide

4.2.1. Growth mechanisms of ZrO_2

$ZrCl_4$-H_2O process. According to results of QCM measurements, adsorption of $ZrCl_4$ saturated on the surface of ZrO_2, although the saturation was not complete at the exposure times up to 20 s [**X**]. At the same time the adsorbate layer formed during the $ZrCl_4$ pulse was very stable. The Cl/Zr ratio determined for the adsorbed species by QCM was 2.6 ± 0.5, 3.0 ± 0.5 and 2.8 ± 0.5 at 180, 290 and 380°C, respectively [**X**]. Thus, 1.0–1.4 chlorine atoms were removed from a $ZrCl_4$ molecule during its adsorption. Variation of this value with the growth temperature was most probably due to increasing contribution of the surface

OH-groups to the exchange reactions at lower temperatures and decreasing stability of $ZrCl_4$ at the highest temperatures used in the QCM studies. For comparison, the Cl/Zr ratios of 1.6–3.5 were determined by Kytokivi et al. [75] for the surface layer that was formed at 300°C in a similar process on porous silica and alumina supports. According to data of Rahtu and Ritala. [263], the same ratio was 2.8 at 300°C and 1.8 at 400°C, when determined from QCM measurements, and 2.4 at 300°C and 2.6 at 400°C, when determined from QMS data.

As can be seen, the data obtained from different studies overlapped within the experimental uncertainty and indicated that at 180–400°C, approximately a half or somewhat less than a half of the chlorine ligands were removed during adsorption of $ZrCl_4$. The rest of the ligands were replaced during the following H_2O pulse. Post-growth composition studies revealed that the concentration of chlorine reached 5 at.% in the films grown at 180°C [238,**X**]. Similarly the concentration of residual hydrogen was relatively high reaching 6 at.% in these films [238]. Therefore the exchange reactions were not complete at the lowest growth temperature used. With the increase of the growth temperature the concentration of impurities markedly decreased. In the films deposited at 400°C the concentration of chlorine did not exceed 0.1–0.3 at.% [238,**X**] while that of hydrogen was around 0.4 at.% [238]. In the films grown at 180–500°C, the oxygen/zirconium ratio ranged from 1.9 to 2.1 [238,264], whereas the deviations from the stoichiometric ratio never exceeded the experimental uncertainty that was ± 0.1.

$ZrCl_4$-H_2O_2-H_2O process. Substitution of H_2O for the mixture of H_2O_2-H_2O (commercial 35% solution of H_2O_2 in H_2O) did not cause marked changes in the growth mechanism. The Cl/Zr ratios established according to the QCM data [**X**] in the adsorbate layer after the $ZrCl_4$ pulse were 2.6 ± 0.5, 3.2 ± 0.5 and 2.9 ± 0.5 at 180, 290 and 380°C. Thus, the differences from the $ZrCl_4$-H_2O process were not meaningful. Similarly, the differences in the compositions of the films grown in the $ZrCl_4$-H_2O and $ZrCl_4$-H_2O_2-H_2O processes did not exceed the experimental uncertainty [**X**].

ZrI_4-H_2O_2-H_2O process. QCM studies of the ZrI_4-H_2O_2-H_2O process reported by Kukli et al. [177] demonstrated that adsorption of TiI_4 did not saturate completely and the adsorbate layer formed was not stable, probably due to decomposition of ZrI_4 and surface species formed during ZrI_4 adsorption [177]. QCM measurements performed at 300°C also indicated that the reactivity of the oxygen precursor towards these surface species might have been insufficient [177] retaining iodine on the surface even after the H_2O_2-H_2O pulse. For these reasons, no reliable data could be obtained for the I/Zr ratio in the adsorbate layer formed during the ZrI_4 pulse. Nevertheless, the ZrI_4-H_2O_2-H_2O process resulted in ZrO_2 films with relatively low concentration of residual iodine. The

iodine concentration determined from XPS studies was 1.3 at.% at 250°C. With increasing growth temperature the iodine concentration decreased and stabilized at the level of 0.7–0.8 at.% in the films grown at 300–350°C [177]. Unfortunately, the experiments performed later demonstrated that the reproducibility of the ZrI_4 process was low, making it disadvantageous compared with the $ZrCl_4$-based processes.

Other processes for ALD of ZrO_2. In 2000-s several organic compounds were investigated as zirconium precursors for ALD of ZrO_2 [265–276]. Nevertheless, only in few cases [271,274,275] the reaction mechanisms were characterized.

Hausmann et al. [272] employed zirconium alkylamide precursors ($Zr(NMe_2)_4$, $Zr(NMeEt)_4$ and $Zr(NEt_2)_4$ where Me and Et are methyl ($–CH_3$) and ethyl ($–C_2H_5$) groups, respectively) combined with H_2O for ALD of ZrO_2. Using the QCM method for real-time measurements at 200°C, they found that the data obtained were consistent with the mechanism assuming adsorption of a zirconium atom with 2 dialkylamide ligands and replacement of these ligands with 2 hydroxyls during the H_2O pulse [272].

Matero et al. [275] studied the reaction mechanisms in the ALD processes based on $Zr(dmae)_4$, $Zr(dmae)_2(O^tBu)_2$ and $Zr(dmae)_2(O^iPr)_2$ as zirconium precursors (dmae is dimethylaminoethoxide ($OC_2H_5N(CH_3)_2$), O^tBu is *tert*-butoxide ($OC(CH_3)_3$) and O^iPr is *iso*-propoxide ($OCH(CH_3)_2$ ligand). The QMS and QCM studies carried out at 190–340°C demonstrated, however, that those zirconium precursors tended to decompose thermally [275]. As a result, the growth rate did not saturate with increasing precursor doses. In addition, the films contained up to 5 at.% of carbon and 9 at.% of hydrogen impurities[275] showing that the surface reactions were not complete. Correspondingly, the contributions of the most probable decomposition and exchange reactions depended on several process parameters making impossible the determination of detailed reaction mechanisms [275].

Niinistö et al. [276] investigated surface reactions leading to the ZrO_2 growth from deuterated water and $Cp_2Zr(CH_3)_2$ where Cp is a cyclopentadienyl (C_5H_5) ligand. The gaseous reaction products observed in real-time QMS studies were CpD and CH_3D, whereas at temperatures of 210–400°C, about 90% of CH_3D was released during the $Cp_2Zr(CH_3)_2$ pulse. About 40% of the Cp ligands were released during the $Cp_2Zr(CH_3)_2$ pulse, while the following D_2O pulse removed the remaining Cp ligands from the surface. It was found that the reaction mechanism only weakly depended on the deposition temperature at 210–400°C [276]. In this context, the process was very similar to the $ZrCl_4$-H_2O and $ZrCl_4$-H_2O_2-H_2O processes, in which the effect of temperature on the reaction mechanism was also weak [263,**X**]. Thermal decomposition of $Cp_2Zr(CH_3)_2$ started to play an important role at temperatures exceeding 400°C [276].

4.2.2. Influence of reaction mechanism on growth rate of ZrO_2

Real-time QCM measurements as well as post-growth studies demonstrated a monotonic decrease of the growth rate with increasing temperature in the $ZrCl_4$-H_2O and $ZrCl_4$-H_2O_2-H_2O processes (Fig. 4). The general trend of the growth rate observed was in agreement with an expected decrease of the contribution of OH-groups to adsorption of $ZrCl_4$ at higher temperatures and corresponding, although relatively weak, increase in the Cl/Zr ratio formed in the adsorbate layer during the $ZrCl_4$ pulse [**X**]. A similar behavior of the growth rate was observed by Scarel et al. [277]. In their paper, Scarel et al. [277] reported a monotonic decrease of the growth rate from 0.14 to 0.09 nm/cyle with the increase of the deposition temperature from 160 to 350°C in the case of 17–28 nm thick films.

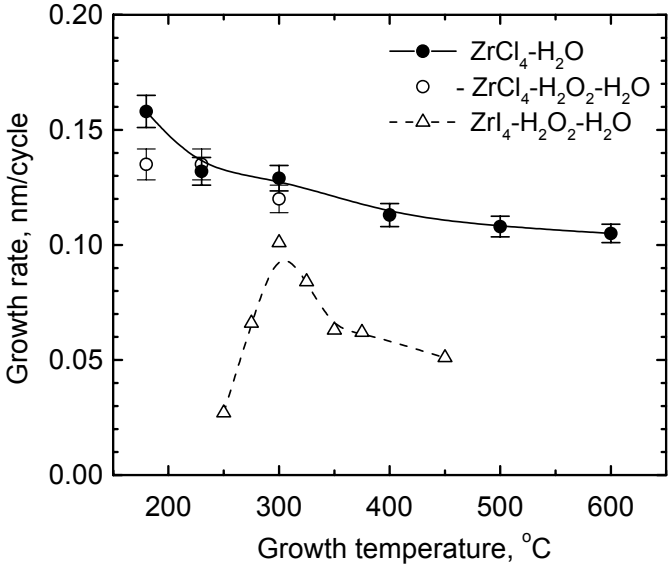

Fig. 4. Comparison of growth rates of ZrO_2 thin films determined for $ZrCl_4$-H_2O [**X**], $ZrCl_4$-H_2O_2-H_2O [**X**] and ZrI_4-H_2O_2-H_2O [177] processes at similar ALD process parameters. The thicknesses of the films grown in the ZrI_4-H_2O_2-H_2O process ranged from 27 to 125 nm while those of the films grown in the $ZrCl_4$-H_2O and $ZrCl_4$-H_2O_2-H_2O processes ranged from 180–240 nm.

Cassir et al. [162] reported a more complex temperature dependence of the growth rate in the $ZrCl_4$-H_2O process. In their experiments, the growth rate increased from 0.1 to 0.5 nm/cycle with the increase of the growth temperature from 350 to 400°C and decreased down to the level of 0.07–0.1 nm with the further increase of T_G to 425–450°C. This effect was evidently related to

crystallization processes and changes in the surface morphology [162]. Therefore the possible reasons of this anomaly are discussed in more detail in the next section.

When comparing the growth rates observed by different research groups for the $ZrCl_4$-H_2O process [73,162,234,277–280,**X**], one can see a significant scatter of results. For instance, the growth rate values ranging from 0.046 [279] to 0.13 nm/cycle [**X**] were measured for ZrO_2 films of similar thicknesses deposited at 300°C. This scatter was partly due to dissimilar precursor doses that influenced the growth rate in some extent [234] but, as demonstrated in a recent study of our group [280], the flow rate and pressure of the carrier gas had also a marked effect on the thickness increase per cycle. Obviously the purging efficiency influenced the equilibrium concentration of adsorbed species and in this way, resulted in a growth rate decrease with increasing flow rate and pressure of the carrier gas in the $ZrCl_4$-H_2O process [280].

Application of the commercial 35% solution of H_2O_2 in H_2O instead of pure H_2O in the $ZrCl_4$-based ALD process [**X**] caused neither increase in the growth rate nor significant changes in the temperature dependence of the growth rate (Fig. 4). Therefore the reactivity of H_2O was sufficient, at least at the H_2O doses and growth temperatures used in this study.

In the case of ZrI_4-H_2O_2-H_2O process, Kukli et al. [177] have recorded a decrease of the growth rate from 0.10 to 0.06 nm with the increase of growth temperature from 300 to 450°C (Fig. 4). Hence, in this temperature range, the dependence of the growth rate on temperature was similar to that observed for the $ZrCl_4$-H_2O and $ZrCl_4$-H_2O_2-H_2O processes. At the lowest growth temperature used in the ZrI_4-H_2O_2-H_2O process, i.e. at 250°C, the growth rate was, however, as low as 0.03 nm. The low growth-rate value was most probably due to insufficient reactivity of the precursors and lower concentration of crystalline phases in these films [177].

The processes based on organic zirconium precursors [265–276] have shown significant variation of the growth rate. As a rule, these precursors were of much lower stability than $ZrCl_4$ was. Correspondingly, the effect of temperature on the growth rate was very strong in the processes based on the organic zirconium precursors [265,266,270]. In addition, the precursor doses had a significant effect on the growth rate [265,269,275]. Therefore the scatter of results was large and depended on several process parameters that were not always specified. This made the meaningful comparison of the growth rate values reported by different groups problematic and, thus, the corresponding analysis was not included in the present thesis.

4.2.3. Influence of crystallization on growth and properties of ZrO_2 films

Growth of amorphous and polycrystalline films. No in-plane orientation of crystalline ZrO_2 phases was obtained on single crystal silicon substrates. An effect of single crystal MgO and α-Al_2O_3 substrates on the orientation of crystalline ZrO_2 was observed but, according to the XRD analysis, the quality of epitaxy was poor. For this reason, the problems of epitaxial growth of ZrO_2 are not discussed in this thesis. Instead, the main attention is concentrated on the growth of amorphous and polycrystalline films.

Crystallization of ZrO_2 films deposited on the single crystal silicon and amorphous silica substrates was observed in the $ZrCl_4$-H_2O and $ZrCl_4$-H_2O_2-H_2O processes already at 180°C [**X**], although the films grown at this temperature contained significant amounts of precursor ligands [238,**X**] that made the crystal growth less favorable. Thinner films grown at 180–450°C were still amorphous. The maximum thickness of films, which allowed amorphous growth at 180°C, was 50–100 nm whereas this thickness was somewhat greater for the films grown from $ZrCl_4$ and H_2O_2-H_2O than for those grown from $ZrCl_4$ and H_2O [**X**]. With the increase of growth temperature, the thickness corresponding to the transition from amorphous to crystalline phase decreased and did not exceed 1–2 nm at 450°C and higher temperatures [**X**]. These results were in good agreement with the data of Scarel et al. [277] who observed this transition at the growth temperatures of 200–250°C in the case of 21–26 nm thick films.

Cubic ZrO_2 was the first crystalline phase, which was formed at lower temperatures with the increase of the film thickness above the limits allowing stabilization of the amorphous phase [**X**]. In a pure bulk material and thick films, this phase was not stable under normal conditions but in nanocrystalline materials and sufficiently thin films, it could be stabilized due to noticeable contribution of the surface to the total free energy of the material [281]. With the further thickness increase, especially at higher temperatures, the tetragonal phase of ZrO_2 appeared in the films [**X**]. Most probably, this phase was also stabilized because of surface effects [282]. The monoclinic phase, which was the most stable one in the bulk material, was formed only in relatively thick films grown at 230°C and higher temperatures [228, **X**].

In a very similar sequence, the phases of ZrO_2 were formed in the ZrI_4-H_2O_2-H_2O process [177]. The most significant difference from the $ZrCl_4$-H_2O and $ZrCl_4$-H_2O_2-H_2O processes was that the cubic phase was more stable in the films grown from ZrI_4 and H_2O_2-H_2O. In the latter case, cubic ZrO_2 was the only crystalline phase in the films that were grown at 250–275°C and were as thick as 125 nm [177]. The halide-based precursor systems tested so far resulted in the preferential orientation of the cubic and tetragonal phases in sufficiently thick films. In these films the (001) plane of the cubic or tetragonal phase was preferentially parallel to the film surface [177,**X**]. In the films that contained

marked amounts of monoclinic ZrO_2, a preferential orientation of crystallites was also observed whereas, similarly to the (001) planes of cubic and tetragonal phases, the (001) plane of the monoclinic unit cell was parallel to the substrate surface [228,**X**]. This means that the longest edges of both tetragonal and monoclinic unit cells were preferentially oriented in the direction that was (nearly) perpendicular to the substrate surface.

Relatively little information has been published on the structure evolution in the ZrO_2 films grown by ALD in the processes based on organic precursors, although a rather great number of papers have described this kind of processes [265–276]. It seems still that a specific feature of those processes is a lower probability for formation of the cubic and tetragonal phases. For instance, Kukli et al. [265] and Putkonen and Niinistö [266] reported direct transition from the amorphous to monoclinic phase growth. Formation of cubic and tetragonal ZrO_2 was observed by Yun et al. [283], who described an ALD process where $Zr(N(C_2H_5)(CH_3))_4$ as a precursor was combined with oxygen plasma. They demonstrated that an increase of the plasma dose led to preferential formation of the cubic and/or tetragonal phases. In addition, Nam and Rhee [273] obtained cubic ZrO_2 after annealing of an initially amorphous film grown from $ZrCl_2(N(SiMe_3)_2)_2$ and H_2O. On the bases of these results, one can conclude that impurities, which probably stayed in the as-grown films from organic zirconium precursors, made the growth of the cubic and tetragonal ZrO_2 phases less favorable.

Effect of crystallization on growth rate. The growth rate of films deposited in our experiments on the silicon and silica substrates from $ZrCl_4$ and H_2O showed no marked dependence on the phase composition, which varied from the mixture of the amorphous and cubic phases to the dominating tetragonal and monoclinic phases [**X**]. It should be noted, however, that at the lowest deposition temperature used in our experiments, the growth rate was lower in the $ZrCl_4$-H_2O_2-H_2O process than in the $ZrCl_4$-H_2O one [**X**]. A possible explanation for this difference was lower crystallinity of the films deposited in the former process. Very similar effects were observed for the ZrI_4-H_2O_2-H_2O [177,178] and $Zr(OC(CH_3)_3)_4$-H_2O [265] processes. In the former case, the growth rate increased by a factor of 2.5–4 when the growth temperature was elevated from 250 to 275°C (Fig. 4) and well-crystallized films started to grow instead of poorly crystallized ones [177,178]. In the latter case Kukli et al. [265] observed transition from the amorphous to crystalline growth at 180–200°C while the growth rate increased by the factor of 1.5 with this transition. By contrast, Scarel et al [277] did not see increase of the growth rate when the crystallization processes started in their experiments. Nevertheless, this is not a surprising result because these authors studied relatively thin films (17–28 nm) where crystallization and corresponding surface roughening could not significantly contribute to the growth rate increase yet.

As already mentioned, Cassir et al. [162] observed a marked increase of the growth rate at 375–425°C on soda lime glass substrates. As demonstrated by XRD studies [162,**X**], a transition from the tetragonal to monoclinic phase growth took place at these temperatures. Simultaneously, the crystallite sizes [228] as well as the surface morphology [162] changed. These changes could well explain the growth rate increase. However, experiments performed by our group using the same deposition temperature range but fused silica and silicon substrates [228,**X**] did not show this kind of abrupt growth rate increase. Thus one could suppose that soda lime glass substrates additionally contributed to crystallization and growth rate variations in the studies of Cassir et al. [162]. This conclusion is strongly supported by the result that in the case of TiO_2 films, the soda lime glass substrates influenced the growth rate [42] as well as crystal structure [247] in a marked extent.

Influence of phase composition on properties of ZrO_2 films. Expected surface roughening related to crystallization was most clearly observed by Scarel et al [277] who studied the $ZrCl_4$-H_2O ALD process at substrate temperatures of 160–350°C. With the increase of T_G from 200 to 250°C, the growth of amorphous films was replaced with the growth of crystalline films. Simultaneously, the surface roughness increased by the factor of 2–4 in the case of films with similar thickness [277]. For comparison, the surface roughness was constant in the T_G range of 160–200°C and increased only by a factor of 1.2–1.5 with the increase of T_G from 250 to 350°C.

Cassir et al. [162] observed drastic changes in the surface morphology with appearance monoclinic phase in the films. Their AFM studies demonstrated that grain sizes markedly decreased with the transition from tetragonal to monoclinic phase. This result was in good agreement with our XRD studies showing that the crystallites with the tetragonal structure reached much larger sizes than the crystallites with the monoclinic structure did [228].

With increasing degree of crystallinity, the refractive index increased up to 2.23 in the ZrO_2 films with the tetragonal structure and up to 2.25 in the films with the monoclinic structure grown from $ZrCl_4$ and H_2O and measured at λ = 580 nm [**X**]. For comparison, refractive indices of 2.15–2.22 and 2.12–2.18 were obtained for films with cubic and tetragonal structures, respectively, grown from ZrI_4 and H_2O_2-H_2O and measured at the same wavelength [177]. Therefore these three crystalline phases showed very similar refractive index values in the thin films studied. By contrast, with increasing content of the amorphous phase, the refractive index significantly decreased. The values of 2.05 (at λ = 580 nm) were recorded for the predominantly amorphous films grown at 180°C from $ZrCl_4$ and H_2O [**X**]. The dielectric constant also weakly depended on the ratio of various crystalline phases [264] while the increasing concentration of the amorphous phase led to a decrease of this parameter too [264,277]. The values of relative dielectric constant measured at frequencies

10–100 kHz ranged from 18 to 27 in crystalline films [162,178,264,277] and from 13 to 14.5 in amorphous films [277].

Absorption spectra of ZrO_2 depended, by contrast, on the crystalline phase dominating in the films (Fig. 5). Most important changes were related to the appearance of an absorption band peaking at 5.4 eV in the spectra of monoclinic films (see the spectrum of the film grown at 600°C in Fig. 5). This absorption band was obviously the main reason for large variation of energy gap values published by different research groups. In the case of thicker films, the optical band gap was usually determined from relatively low α values ($\alpha < 10$ μm^{-1} [155,228]). Correspondingly, using the model of direct optical transitions, the band gap values of 5.16–5.28 eV [155,228] were obtained for monoclinic ZrO_2 films in good agreement with the absorption spectrum presented in Fig. 5 for a film deposited at 600°C. In the case of thinner films, these α values are not sufficiently high for reliable recording the absorption spectra. Thus, only a range of markedly stronger absorption ($\alpha > 10$ μm^{-1}) can be used to estimate energy gaps of very thin films. However, using the absorption coefficient range of 10–70 μm^{-1} much higher band gap values (E_g = 5.8 eV) have been determined for monoclinic ZrO_2 from the same model [156,228].

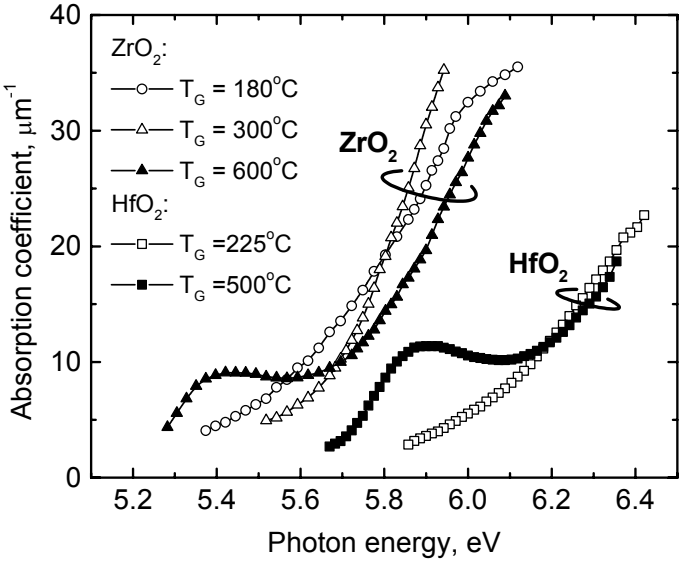

Figure 5. Room-temperature absorption spectra of ZrO_2 [228] and HfO_2 [**XII**] thin films grown on silica substrates in $ZrCl_4$-H_2O and $HfCl_4$-H_2O ALD processes, respectively. The thicknesses of the films ranged from 180 to 380 nm.

There are several reasons for the non-monotonic dependence of the absorption coefficient on the photon energy, $h\nu$. Firstly, this kind of dependence might be due to the specific band structure of this phase [156]. Secondly, quantum effects related to small sizes of crystallites with the monoclinic structure (about 20 nm in 200–230 nm thick films [228]) can cause the feature in the absorption spectra. Thirdly, exciton formation discussed by Kirm et al. [215] can explain the appearance of this feature. From these reasons, the quantum effects seem to be less probable because very similar features (Fig. 5) were observed in the absorption spectra of monoclinic HfO_2 films with the mean XRD crystallite sizes reaching 34–47 nm [**XII**]. Crystallites of these sizes were evidently too large for causing significant quantum size effects.

For the films with the dominating tetragonal phase (e.g. the film grown at 300°C in Fig. 5), the approach that was used to determine the energy gap for the direct optical transitions gave the E_g values of 5.75–5.78 eV [161,228]. For comparison, the approach assuming the indirect optical transitions gave the band-gap values of 5.22–5.26 eV [161,228]. Finally, for predominantly amorphous films that were grown at 180°C and contained inclusions of the cubic phase [**X**], the energy gap of (5.27 ± 0.07) eV was obtained for the indirect optical transitions from the absorption spectrum presented in Fig. 5. No linear part of the $(\alpha h\nu)^2$ versus $h\nu$ curve, needed to determine the energy gap for the direct optical transitions, was found in the case of these films. One should take into account, however, that relatively high concentration of impurities reaching 5–6% in those films might influence the band gap as well as the character of the optical transitions making the indirect transitions more probable.

4.3. Hafnium dioxide

4.3.1. Growth mechanisms of HfO_2

$HfCl_4$-H_2O process. According to the results of real-time QCM studies, adsorption of $HfCl_4$ was self-limited on the surface of HfO_2 and the adsorbate layer was stable in the temperature range of 180–400°C studied [**I**]. The Cl/Hf ratios established in the adsorbate layer were 2.0, 2.4, 2.6 and 3.0 at 180, 225, 300 and 400°C, respectively. The reaction of the adsorbate layer with H_2O in the next ALD step resulted in substitution of the chlorine ligands adsorbed and formation of HfO_2 with relatively low concentration of residual impurities at higher temperatures. For instance, in the films grown at 400°C and higher temperatures, the chlorine and hydrogen concentrations did not exceed 0.2 and 0.5 at.%, respectively [284,**I**]. With the decrease of T_G, the impurity concentrations increased. In the films grown at 225°C, the concentrations as high as 4.3 at.% for chlorine and 5.1 at.% for hydrogen [284, **I**] were measured.

Using the data of post-growth measurements, the self-limited character of the $HfCl_4$-H_2O process was evaluated at temperatures up to 940°C [**II**]. As demonstrated these studies, the growth rate perfectly saturated with increasing pressure of the hafnium as well as oxygen precursor [**II**]. Unfortunately, it was impossible to perform the QCM studies at temperatures exceeding 400°C. Nevertheless, the growth rate that, in agreement with the increase of the Cl/Hf ratio in the intermediate surface layer, decreased with the increase of growth temperature from 225 to 400°C continued to decrease in the temperature range of 400–750°C [280,285,**II**]. Thus, it is very probable that the Cl/Hf ratio continued its increase observed at lower temperatures. Correspondingly, taking into account the Cl/Hf ratios estimated for the adsorbate layer formed at 225–400°C, one could conclude that the ratio was close to 4 in the adsorbate layer formed at 600–940°C where the growth rate was already almost independent of T_G [**II**]. Thus, $HfCl_4$ was obviously adsorbed without exchange reactions and the chlorine ligands were removed only during the H_2O pulse at those temperatures.

HfI_4-H_2O and HfI_4-H_2O_2-H_2O processes. Our QCM studies [217] demonstrated that the amount of HfI_4 adsorbed on the surface of HfO_2 earlier exposed to H_2O or H_2O_2-H_2O mixture saturated with increasing pulse time and partial pressure of HfI_4. The saturation was, however, not complete. In addition, a decrease of the adsorbate mass, indicating decomposition of surface species, was observed during the purge that followed the HfI_4 pulse [217]. Fortunately, the effect of decomposition was not strong at the modest (up to 10 s) pulse and purge times. The I/Hf ratio, which was stabilized in the adsorbate layer during the HfI_4 pulse, was estimated to be 1.9, 2.0 and 2.3 at 220, 260 and 300°C, respectively, independently of whether H_2O or H_2O_2-H_2O mixture was the oxygen precursor. The increase of the I/Hf ratio with temperature was evidently related to the decrease of the surface OH concentration at higher temperatures. When comparing the I/Hf ratios with the corresponding Cl/Hf ratios determined for the $HfCl_4$-H_2O process, one can see that the former values were somewhat lower. Thus, HfI_4 more actively reacted with the surface during its adsorption than $HfCl_4$ did. QCM as well as post-growth composition studies demonstrated that the reaction of H_2O as well as H_2O_2-H_2O mixture with iodine ligands adsorbed together with Hf was sufficiently fast and complete. According to the X-ray photoelectron spectroscopy analysis, the films deposited at 300°C contained about 0.8 at.% of iodine while in the films grown at 400°C and higher temperatures, the iodine concentration did not exceed 0.1 at.% [217].

Other processes for ALD of HfO_2. In addition to the ALD processes described above, those based on $Hf(NO_3)_4$ [286,287] or organic compounds of hafnium [272,288–297] have been reported in 2002–2006. From these processes, only few have been studied by applying real-time methods [272] in order to

determine the reaction mechanisms. Using the QCM method, Hausmann et al. [272] investigated ALD processes based on hafnium alkylamide precursors, such as $Hf(NMe_2)_4$, $Hf(NMeEt)_4$ and $Hf(NEt_2)_4$, combined with H_2O. These authors concluded that similarly to corresponding zirconium compounds, $Hf(NMe_2)_4$, $Hf(NMeEt)_4$ and $Hf(NEt_2)_4$ were adsorbed in the exhange reactions together with 2 dialkylamide ligands at 200°C. During the following H_2O pulse these ligands were replaced by 2 hydroxyl groups [272]. In this sense, the processes described by Hausmann et al. [272] were very similar to the $HfCl_4$-H_2O and, especially, HfI_4-H_2O (HfI_4-H_2O-H_2O_2) processes.

Composition studies of the films deposited in the $Hf(NMe_2)_4$, $Hf(NMeEt)_4$ and $Hf(NEt_2)_4$-based processes revealed relatively low concentration of impurities (less than 1% of carbon and less than 0.25% of nitrogen) in the films deposited [272]. Therefore the exchange reactions were more complete in this process than in the $HfCl_4$-H_2O process performed at comparable temperatures. The decomposition of $Hf(NMe_2)_4$, $Hf(NMeEt)_4$ and $Hf(NEt_2)_4$ started to affect the ALD process markedly at 300–450°C [272]. For comparison, HfI_4 and $HfCl_4$ were successfully used for ALD growth at temperatures up to 750 [298,299,**XI**] and 940°C [300,**II**], respectively.

4.3.2. Influence of reaction mechanism on growth rate of HfO_2

Growth rate of HfO_2 decreased with increasing temperature in the $HfCl_4$-H_2O as well as HfI_4-H_2O process (Fig. 6). In both cases, the growth rate decrease observed in the temperature range of 180–400°C was in agreement with the increase of the ligand to hafnium ratio in the adsorbate layer formed during the hafnium precursor pulse [**I**]. For comparison, the growth rate was independent of the deposition temperature at 600–940°C, i.e. in the temperature range where the concentration of surface hydroxyl groups was evidently very low [**II**] and did not influence the growth rate noticeably. With the increase of growth temperature from 940 to 1000°C, the growth rate decreased down to undetectable values in the $HfCl_4$-H_2O process [**II**] that was studied at these temperatures. As no growth mechanism studies could be performed at temperatures exceeding 400°C, one can only speculate that desorption of adsorbed $HfCl_x$ species ($0 < x \leq 4$) was a probable reason for the decrease of growth rate at the highest temperatures used.

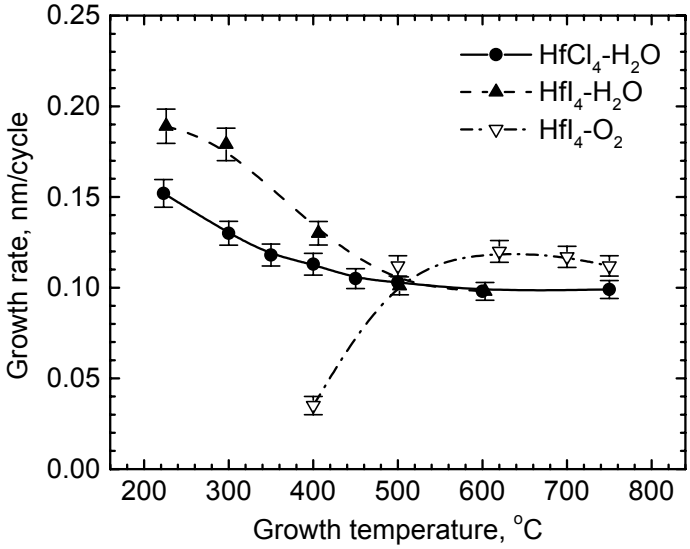

Figure 6. Effect of temperature on mean growth rate of HfO_2 films in HfI_4-O_2 [**XI**] HfI_4-H_2O, $HfCl_4$-H_2O ALD processes. Thicknesses of the films ranged from 40 to 190 nm.

At 500°C and higher temperatures, the growth rates were comparable in the $HfCl_4$-H_2O and HfI_4-H_2O processes (Fig. 6). At lower temperatures, the HfO_2 films grew with higher rate in the HfI_4-H_2O processes than in the $HfCl_4$-H_2O process. This difference was in agreement with more extensive ligand exchange during HfI_4 adsorption discussed in the previous section of this thesis.

In the case of HfI_4-O_2 process, relatively high partial pressures of O_2 were needed to achieve self-limited growth [**XI**], especially at temperatures below 600°C. Nevertheless, the growth rates obtained did not exceed 0.04 nm/cycle at 400°C [**XI**]. At 600–750°C, however, the growth rate was as high as 0.12 nm/cycle in the HfI_4-O_2 process, exceeding that obtained in the HCl_4-H_2O and HfI_4-H_2O processes in the same temperature range (Fig. 6). This difference could not be explained on the basis of the process chemistry. Consequently, dissimilar crystallization should be considered as a possible reason for that.

The most significant advantage of the HfI_4-H_2O and HfI_4-O_2 processes compared with the $HfCl_4$-H_2O process was that the former two processes allowed more uniform growth of HfO_2 films on silicon substrates at higher temperatures, especially in the initial stage of deposition [301]. There was a marked delay in the growth of HfO_2 from $HfCl_4$ and H_2O on silicon substrates at 600°C (Fig.7). The film growth was three-dimensional in its initial stage resulting in the surface with high roughness [301]. In the case of HfI_4-H_2O and HfI_4-O_2 processes, this kind of growth delay was not observed (Fig. 7). This difference was obviously due to more favorable adsorption of HfI_4 on silicon compared with that of $HfCl_4$. At 300°C and lower temperatures, no difference

was observed and the growth started without noticeable delay in the $HfCl_4$-H_2O process as well (Fig. 7).

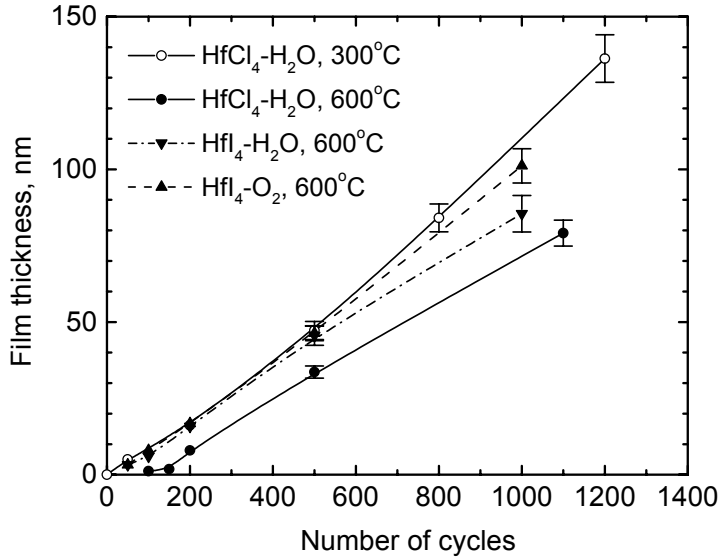

Figure 7. Dependence of HfO_2 film thickness on number of ALD cycles applied in chloride- and iodide-based processes [301].

Reasons for the growth delay in the $HfCl_4$-H_2O processes were analyzed by Alam and Green [302] and by Puurunen [303], who used data revealing this kind of effects already at 300°C. In both cases, very low growth rates observed on HF-etched silicon substrates in the initial growth stage were considered to be due low concentrations of the surface hydroxyl groups [302,303]. As a result, a limited number of nucleation cites were formed while the film started to grow three-dimensionally in the vicinity of these cites. Naturally, the surface roughness being comparable to the film thickness increased together with the thickness until the coalescence of the growth islands started. At this moment the highest growth rate was achieved. After that the surface roughness and the growth rate somewhat decreased and the deposition continued in the quasi two-dimensional mode [302,303]. Exactly this kind of behavior was observed at 600°C in the case of $HfCl_4$-H_2O process (Fig. 7). At the same substrate temperature, however, no similar effect could be seen in the case of HfI_4-H_2O and HfI_4-O_2 processes. This result confirmed different contribution of the surface hydroxyl groups to the adsorption of HfI_4 compared with that of $HfCl_4$.

Relatively large variations of the growth rates were observed in the ALD processes, in which $Hf(NO_3)_4$ [286,287] or organic compounds were used as hafnium precursors [272,288–297]. From a number of processes studied, those based on $Hf(NMeEt)_4$, $Hf(NEt_2)_4$) and $Hf(NMe_2)_4$ have shown most stable

behavior with changing precursor doses and growth temperature [288,291,295]. For instance, Kukli et al. [288] reported the growth rates decreasing from 0.1 to 0.09 nm/cycle with the increase of growth temperature from 150 to 250°C in the case of $Hf(NMeEt)_4$-H_2O process. For the $Hf(NEt_2)_4$-H_2O process, Deshpande et al. [291] obtained the growth rates that decreased from 0.16 to 0.12 nm/cycle with the increase of growth temperature from 250 to 350°C. Finally, Kukli et al. [295] recorded a decrease of the growth rate from 0.10 to 0.09 nm/cycle with the increase of temperature from 205 to 300°C in the case of $Hf(NMe_2)_4$-H_2O process [295]. These growth rate values and the dependencies of the growth rate on temperature were comparable to those recorded for the $HfCl_4$-H_2O and HfI_4-H_2O processes. With the increase of the growth temperature from 250 to 325°C in the $Hf(NMeEt)_4$-H_2O process [288] and from 300 to 400°C in the $Hf(NMe_2)_4$-H_2O process [295], the growth rate significantly increased, evidently due to decomposition of the hafnium precursors. In the case of several other hafnium precursors, the growth rates more significantly depended on the "batch" of the precursor used in the experiment [287], growth temperature [289,290,296,297] or precursor doses [289,290] making the corresponding ALD processes less reproducible.

4.3.3. Influence of crystallization on growth and properties of HfO_2 films

Phase composition. The HfO_2 films deposited on silicon and silica substrates were (quasi-) amorphous or polycrystalline dependently on the deposition process parameters. The films grown from $HfCl_4$ and H_2O or HfI_4 and H_2O at 225°C and lower temperatures were amorphous [**I,II**] or predominately amorphous with inclusions of cubic phase [285]. At higher temperatures, the amorphous phase was also formed but only in the very beginning of the deposition process. For instance, the estimated thickness of the amorphous phase formed on silicon substrates in the initial stage of the film growth was less than 30 nm at 300°C [285,301,**I**] and 10 nm at 400°C [**I**]. At 600°C, no amorphous phase was observed in the films grown from $HfCl_4$ and H_2O. By contrast, in very thin (thinner than 6–8 nm) films grown from HfI_4 and H_2O or from HfI_4 and O_2, the amorphous phase was formed even at this temperature together with the cubic phase [301].

The cubic HfO_2 phase that was stable in the pure bulk material at 2500–2900°C [304] was formed in small crystallites embedded in quasi-amorphous films at 225°C [285], in very thin films at 400–600°C [299,301] and in a surface layer of monoclinic films at 880–940°C [300,**II**]. Variation of the precursor doses demonstrated that reduced dosing of the oxygen precursors contributed to the growth of the cubic phase [299,300] in a good agreement with the results of

El-Shanshoury et al. [281] who reported formation of cubic HfO_2 in the oxidation process of hafnium films.

The monoclinic phase dominated in sufficiently thick HfO_2 films deposited at 300–940°C [**I**,**II,XI,XII**]. XRD studies of these films revealed, however, a peak that could be attributed to the metastable cubic, tetragonal or orthorhombic phase of HfO_2 [79,**I,II,XI**]. Comparison of the RHEED and XRD data allowed a conclusion that in the films grown at 300–600°C, this phase was formed at the film–substrate interface. On one hand, this result is in good agreement with the structural data of very thin films where the cubic phase was found. On the hand, there are results published [305,**I**], which indicate that the phase formed at the film–substrate interface might have been the orthorhombic rather than cubic one. If so, then the influence of intrinsic strain [306] might have caused the phase transformation from the initially cubic phase to the orthorhombic modification of HfO_2 that has otherwise been observed at high pressures [307–309]. Very recent studies demonstrated that the amount of the metastable phase formed at the interface depended also on the flow rate of the carrier gas used in the ALD process [280]. This effect as well as the phase composition of the interface layers need, however, further studies, in order to determine more reliably the mechanisms of the metastable phase formation and possible phase transitions in the interface layers.

Polycrystalline monoclinic HfO_2 films with greater thickness showed a well-developed preferential orientation (texture). In the films grown on silicon and silica substrates, the preferential orientation was developed only in the direction of the surface normal and became stronger with increasing film thickness [**II**]. This kind of behavior indicated that faster growth of crystallites in a certain direction rather than nucleation on the substrate surface was responsible for the texture formation. In the films grown on single crystal MgO substrates from HfI_4 and H_2O, by contrast, the in-plane orientation, i.e. (quasi)epitaxial growth, of monoclinic HfO_2 phase was observed [217].

Effect of crystallization on growth rate. The effect of crystallization on the growth rate of HfO_2 was weak in the case of the ALD processes studied. No direct evidence of the influence of crystallization on the growth rate versus temperature dependence was observed in the studies of halide-based ALD processes. To the best of the author's knowledge, no this kind of data have been published for other HfO_2 ALD processes either. Nevertheless, a possible reason for the growth rate increase related to the replacement of H_2O for O_2 in the HfI_4-based processes (Fig. 7) could be due to differences in crystallization. The RHEED data indicating that crystallization started in the HfI_4-O_2 process earlier than in the HfI_4-H_2O process [301] well supported this conclusion. In addition, HRTEM studies of Mitchell et al. [285] demonstrated recently that cubic inclusions of HfO_2 grew somewhat faster in quasi-amorphous films than the amorphous matrix did. The differences in the growth rates of various phases were, however, not as significant as those observed for different phases of TiO_2.

Influence of crystallization on properties of HfO_2 films. Expectedly, the surface roughness of HfO_2 films increased with the transition from the amorphous to crystalline phases. This conclusion is based on the results of optical [**XII**], HRTEM [285] and AFM [310] studies. Observed dependencies of the surface roughness on the phase composition and crystallinity were, however, weaker for HfO_2 films than for ZrO_2 and, particularly, TiO_2 films.

The refractive indices of HfO_2 films deposited in halide-based processes on silica substrates (Fig. 8) insignificantly depended on the precursor system at lower deposition temperatures (< 400°C). Stronger effect of the precursor choice on the refractive index was observed at T_G > 500°C where nucleation influenced the homogeneity of the films. At T_G < 350°C instead, a significant dependence of the refractive index on the crystallinity was observed. For amorphous films grown at 225°C, the refractive index values of 2.00 ± 0.03 were obtained at the wavelength of 500 nm. In crystalline films grown at 300°C and higher temperatures, the refractive indices were markedly higher reaching the values of 2.10–2.12 (Fig. 8) in the films with the most perfect structure formed at around 500°C [**II**]. This kind of dependence of the refractive index of HfO_2 resembled that observed for ZrO_2 [**X**] confirming the similarity of these oxides.

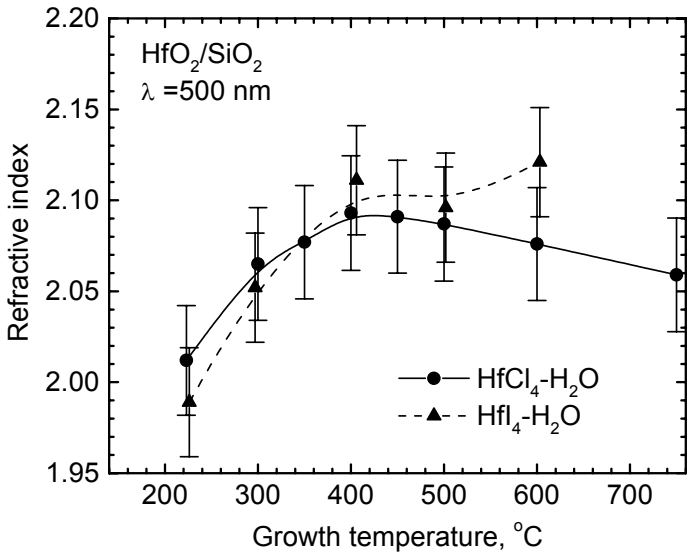

Figure 8. Effect of growth temperature on refractive indices of HfO_2 thin films grown on silica substrates in chloride- and iodide-based ALD processes. The refractive indices were determined at the wavelength of 500 nm.

The dielectric constant of HfO_2 grown in the $HfCl_4$-H_2O and HfI_4-H_2O ALD processes on silicon substrates also increased with the crystallinity of the films. In the amorphous films the relative dielectric constant ranged from 7 to 10 while in crystalline films the values of 13–18 were obtained at the frequencies of 0.5–1 MHz in our studies [217,284]. Scarel et al. [310] reported very similar dielectric constant values for amorphous and crystalline films but they used the frequency of 50 kHz in their capacitance–voltage measurements that yielded the data for calculation of the dielectric constant. In all these cases, the dielectric constant values were markedly smaller than those reported in review papers [311,312]. The reason of this difference was formation of SiO_2 [285,313,**XI**] and/or hafnium silicate [314] interface layers at the film–substrate interface. Due to their lower dielectric constants [311,312], these layers reduced the corresponding effective values of the whole insulating stack measured.

As the dielectric constant increases with crystallinity, the crystalline films could have some advantages in capacitor structures. Unfortunately, our studies [217] as well as those of other authors, e.g. Scarel et al. [310], showed that leakage currents increased with crystallinity of the HfO_2 dielectric. The leakage current increase was evidently related to fluctnations in the strength of local electric fields and contribution of grain interfaces to formation of leakage channels.

Optical absorption spectra of HfO_2 thin films [**XII**] were very similar to those of ZrO_2 films (Fig. 5). The absorption coefficient of amorphous HfO_2 (the film grown at 225°C in Fig 5) monotonically increased with the photon energy while that of monoclinic HfO_2 (the spectrum of a film grown at 500°C in Fig 5) had a local absorption maximum at 5.9 eV [**I**,**XII**]. Influence of the phase composition on formation of the feature in the absorption spectra of HfO_2 films was observed also by Cho et al. [315] and Nguyen et al. [317] who demonstrated that this peak appeared in crystalline (monoclinic) but not in amorphous HfO_2. In the study of Nguyen et al. [316], the feature was attributed to sub-band states [316]. Nevertheless, the reasons discussed in Section 4.2.3, especially the peculiarities of the band structure of monoclinic HfO_2 and excitonic absorption [215] can not be ruled out either. Comparison of our results obtained for ZrO_2 and HfO_2 allows a conclusion that the feature in the absorption spectrum was related to formation of the monoclinic structure while in the cubic and tetragonal ZrO_2 films the feature was not observed. This conclusion is in a very good agreement with the results of Schaeffer et al. [317]. In their paper published in 2003, these authors demonstrated that a similar feature peaking at 5.8 eV appeared in the spectra of imaginary dielectric constant of monoclinic HfO_2 films while the feature was not observed in the case of amorphous and tetragonal HfO_2 films [317]. Schaeffer et al. [317] explained these differences with dissimilar band structure of the monoclinic phase compared with the band structures of the amorphous and tetragonal phases.

The band gap energy of HfO_2 was estimated from the absorption spectra [**XII**]. Most reliably the band gap was determined for amorphous films. In this case, fitting the absorption spectra indicated that model assuming indirect optical transitions well described the dependence of absorption coefficient on the photon energy [**XII**]. The optical energy gap of 5.55 ± 0.03 eV was obtained from the fitting. In the case of monoclinic films, the absorption band peaking at 5.9 eV markedly influenced the results of analysis. The fitting procedure allowing determination of the indirect gap gave the values that were similar to those obtained for amorphous films. However, the absorption spectra of monoclinic films had also regions, where the absorption coefficient was well described by the model corresponding to direct optical transitions. Using this approach, energy gap of 5.7 ± 0.1 eV was obtained assuming that the 5.9 eV feature was related to the band states. When supposing that the feature was related to sub-band states [316] or excitonic absorption [215], the energy gap was estimated to be 6.12 ± 0.05 eV. The set of band-gap values obtained in this way overlapped with the data reported by other authors [181–185,315,316]. The latter values covered the energy range from 5.25 [184] to 5.9 eV [185]. Similarly to the case of ZrO_2 (Section 4.2.3), relatively large scatter of E_g values published was likely due to non-monotonic dependence of the absorption coefficient on the photon energy at the band edge and dissimilar absorption coefficient regions used for the E_g determination by different authors.

Differently from the band gap of amorphous TiO_2, the band gap of amorphous HfO_2 was narrower rather than wider compared with the band gaps of corresponding crystalline phases. This result supported very recent theoretical calculations that indicated formation of band tails in the amorphous HfO_2 and corresponding narrowing of the band gap compared with that of monoclinic HfO_2 [318]. Experimentally, the contribution of the band tails was most clearly observable in the photoluminescence exitation spectra [**XII**].

It is also worth noting that dissimilarly from some earlier data [311], E_g values, which were obtained for ZrO_2 and HfO_2 films with comparable phase compositions in identical fitting procedures, i.e. with using the same absorption coefficient ranges and the same model of optical transitions, differed markedly. The band gap of HfO_2 was by approximately 0.3 eV wider than that of ZrO_2. This difference is also rather well illustrated by the shift of the absorption spectra depicted in Fig. 5.

5. CONCLUSIONS

The research described in this thesis allowed comparison of several ALD processes for deposition of TiO_2, ZrO_2 and HfO_2. The processes that were studied included those described earlier as well as new ones ($Ti(OC_3H_7)_4$-H_2O_2, $ZrCl_4$-H_2O-H_2O_2 and HfI_4-O_2) reported in the original publications of this thesis for the first time. For the $Ti(OC_3H_7)_4$-H_2O_2 and $ZrCl_4$-H_2O-H_2O_2 processes and also for several earlier-known ALD processes the real-time characterization of the reaction mechanisms was performed for the first time. The results of the work and comparison of those with literature data demonstrated that chlorides were the most stable metal precursors from those studied so far. They could be used in wide ranges of deposition temperatures and showed high reactivity in surface reactions.

The dependence of the growth rate on the substrate temperature was demonstrated to be in agreement with the changes in the growth mechanism, when crystallization did not influence the surface roughness and adsorption of precursors. In the opposite cases, the effect of crystallization on the growth rate might even exceed the changes related to variations in the mechanisms of exchange reactions. Most significantly the crystal growth influenced ALD of TiO_2 films. TiO_2 of the anatase phase grew markedly faster than the amorphous TiO_2 phase did. This led to significant surface roughening of the TiO_2 films, which contained mixtures of amorphous and anatase phases. Faster growth of anatase and the increase of the surface area with surface roughening resulted in a dramatic growth-rate increase with the transition from the amorphous to anatase phase. This kind of crystallization-related increase of the growth rate was observed with the increase of the growth temperature as well as film thickness. Thus, a common assumption that the film thickness is proportional to the number of ALD cycles employed does not apply in the cases, when the degree of crystallinity increases and the texture becomes more developed with increasing film thickness. The development of crystallinity and texture with increasing film thickness is, however, a very usual phenomenon in ALD of polycrystalline thin films.

The growth rate of ZrO_2 and HfO_2 thin films did not depend on crystallization as strongly as the growth rate of TiO_2 did. Nevertheless, evidence of this kind of effect was found in original studies of this thesis as well as in publications of other authors. The studies performed also demonstrated that the choice of metal precursors and deposition temperature significantly influenced ALD of HfO_2 in the initial stage of the deposition on silicon substrates. A marked delay and the three-dimensional nature of the film growth was observed in the high-temperature chloride processes. Much more uniform growth without measurable delay was obtained for the iodide-based and low-temperature (300°C and lower) chloride-based ALD processes.

Crystallization of ZrO_2 and HfO_2 films in the ALD processes caused an expected increase of the optical density and dielectric constant. In the case of TiO_2, by contrast, inhomogeneous crystallization of non-epitaxial films sometimes resulted even in the decrease of the mean density compared with that of amorphous films. The optical density of epitaxial films was, however, always higher than that of the amorphous phase and reached the values of respective single crystals.

The optical band gap of amorphous TiO_2 was found to be wider than the band gaps of crystalline TiO_2 phases. On the contrary, the band gaps of amorphous phases of ZrO_2 and HfO_2 films were comparable to or even narrower than the band gaps determined for crystalline phases of corresponding oxides. Optical studies also revealed that the absorption spectra of monoclinic ZrO_2 and HfO_2 phases markedly differed from the absorption spectra of amorphous, cubic and tetragonal phases. Although similar differences between the absorption spectra of amorphous and crystalline (monoclinic) HfO_2 films have recently been observed in works of other authors, too, and explanations to these differences given, verification of the main reasons for this effect needs further studies.

ACKNOWLEDGEMENTS

The author of the thesis is thankful to all his colleagues and partners who have contributed to the studies that the present thesis is based on. Especial thanks belong to Prof. Lembit Pung for his patient supervising and to Dr. Aleks Aidla, Ms. Jelena Asari, Mr. Juhan Karlis, Mr. Aarne Kasikov, Mrs. Alma-Asta Kiisler, Dr. Kaupo Kukli, Dr. Arvo Kikas, Dr. Marco Kirm, Dr. Hugo Mändar, Dr. Ahti Niilisk, Mr. Raul Rammula, Mr. Peeter Ritslaid, Dr. Arnold Rosental, Prof. Väino Sammelselg Dr. Ilmo Sildos, Mr. Aivar Tarre and Dr. Teet Uustare, who have most directly been involved in those studies. Their contribution ranged from assistance in growth experiments and characterization of thin films to useful discussions stimulating writing of the thesis.

The author is very grateful to Prof. Markku Leskelä and Prof. Mikko Ritala for the access to the material characterization equipment available at the University of Helsinki and for the support that they offered for the ALD studies at the University of Tartu.

Successful studies were carried out jointly with Prof. Anders Hårsta, Dr. Mikael Schuisky, Dr. Katarina Forsgren and Dr. Jonas Sundqvist at the University of Tartu as well as at Uppsala University. In these studies new interesting ideas were generated and realized. In addition, this cooperation allowed an access to the characterization methods, which were available at Uppsala University but not at the University of Tartu at that time.

Efforts of Dr. Jun Lu (Uppsala University), Dr. David R.G. Mitchell (ANSTO) and Dr. Timo Sajavaara (University of Helsinki – IMEC – University of Jyväskylä) in characterization the thin films grown at the University of Tartu are highly appreciated. Thanks to their kind assistance, application of sophisticated thin-film characterization methods like high-resolution transmission electron microscopy and time-of-flight elastic recoil detection analysis became possible.

The financial support of Estonian Science Foundation and Finnish National Technology Agency to the original research described in the thesis is gratefully acknowledged.

REFERENCES

[1] V.B. Aleskovskii, V.E. Drozd, Principles of the precise synthesis of super-molecular objects: atomic layer epitaxy, molecular layering, chemical buildup, Acta Polytech. Scand. Chem. Tech. Ser. 195 (1990) 155–161.

[2] V.E. Drozd, A.A. Tulub, V. B. Aleskovskii, D.V. Korol'kov, Synthesis of oxide superalloys by ML-ALE method, Appl. Surf. Sci. 82/83 (1994) 587–590.

[3] T. Suntola, J. Antson, Method for producing compound thin films, U.S. Patent No. 4058430 (1977).

[4] M. Pessa, R. Mäkelä, T. Suntola, Characterization of surface exhange reactions used to grow compound films, Appl. Phys. Lett. 38 (1981) 131–132.

[5] M. Pessa, O. Jylhä, M. Herman, Atomic layer epitaxy of CdTe on the polar (111)A and (111)B surfaces of CdTe substrates, J. Cryst. Growth 67 (1984) 255–260.

[6] C.H.L. Goodman, M.V. Pessa, Atomic layer epitaxy, J. Appl. Phys. 60 (1986) R65–R81.

[7] T. Suntola, Atomic layer epitaxy, Mater. Sci. Rep. 4 (1989) 261–312.

[8] T. Suntola, Atomic layer epitaxy, in: Handbook of Crystal Growth 3: Thin Films and Epitaxy, Part B: Growth Mechanisms and Dynamics, Ed. D.T.J. Hurle, Elsevier, Amsterdam, 1994, pp. 601–663.

[9] L. Niinistö, M. Leskelä, Atomic layer epitaxy: chemical opportunities and challenges, Thin Solid Films 225 (1993) 130–135.

[10] J. Nishizawa, H. Abe, Molecular layer epitaxy, J. Electrochem. Soc. 132 (1985) 1197–1200.

[11] G. Oya, M. Yoshida, Y. Sawada, Growth of α-Al_2O_3 films by molecular layer epitaxy, Appl. Phys Lett. 51 (1987) 1143–1145.

[12] G. Oya, Y. Sawada, Molecular layer epitaxy of α-Al_2O_3 films, J. Cryst. Growth 99 (1990) 572–576.

[13] J. Nishizawa, T. Kurabayashi, Molecular layer epitaxy, Thin Solid Films 367 (2000) 13–24.

[14] M. Ylilammi, T. Ranta-aho, Metal fluoride thin films prepared by atomic layer deposition, J. Electrochem. Soc. 141 (1994) 1278–1284.

[15] J. Aarik, A. Aidla, T. Uustare, V. Sammelselg, Morphology and structure of TiO_2 thin films grown by atomic layer deposition, J. Cryst. Growth 148 (1995) 268–275.

[16] A. Rosental, P. Adamson, A. Gerst, A. Niilisk, Monitoring of atomic layer deposition by incremental dielectric reflection, Appl. Surf. Sci. 107 (1996) 178–183.

[17] B. Sang, M. Konagai, Growth of transparent conductive oxide ZnO films by atomic layer deposition, Jpn. J. Appl. Phys. 35 (1996) L602–L605.

[18] M. Leskelä, M. Ritala, ALD precursor chemistry: Evolution and future challenges, J. Phys. IV 9 (1999) Pr8-837–Pr8-852.

[19] M. Leskelä, M. Ritala, Atomic layer deposition (ALD): from precursors to thin film structures, Thin Solid Films 409 (2002) 138–146.

[20] M. Ritala, M. Leskelä, Atomic layer deposition, in: Handbook of Thin Film Materials, Ed. H.S. Nalwa, Vol. 1: Deposition and processing of Thin Films, Academic Press, 2002, pp. 103–159.

[21] L. Niinistö, J. Päiväsaari, J. Niinistö, M. Putkonen, M. Nieminen, Advanced electronic and optoelectronic materials by atomic layer deposition: an overview with special emphasis on recent progress in processing of high-k dielectrics and other oxide materials, Phys. Stat. Sol. (a) 201 (2004) 1443–1452.
[22] H. Kim, Atomic layer deposition of metal and nitride thin films: Current research efforts and applications for semiconductor device processing, J. Vac. Sci. Technol. B 21 (2003) 2231–2261.
[23] R. Puurunen, Surface chemistry of atomic layer deposition: A case study for the trimethylaluminum/water process, J. Appl. Phys. 97 (2005) 12301-1–52.
[24] M. Ahonen, M. Pessa, T. Suntola, A study of ZnTe films grown on glass substrates using an atomic layer evaporation method, Thin Solid Films 65 (1980) 301–307.
[25] K. Yong, J. Jeong, Application of atomic layer chemical vapor deposition for the processing of nanolaminate structures, Korean J. Chem. Eng. 19 (2002) 451–462.
[26] S.I. Kol'tsov, V.B. Aleskovskii, Reaction of titanium tetrachloride with silica gel, Zh. Prikl. Khim. 40 (1967) 907 (in Russian).
[27] S.I. Kol'tsov, G.V. Sveshnikova, V.B. Aleskovskii, Reaction of titanium tetrachloride with silicon, Izv. VUZ Khim. Khim. Tekhnol. 12 (1969) 562–564 (in Russian).
[28] G.V. Sveshnikova, S.I. Kol'tsov, V.B. Aleskovskii, Interaction of titanium tetrachloride with hydroxylated silicon surface, Zh. Prikl. Khim. 43 (1970) 430–431 (in Russian).
[29] G.V. Sveshnikova, S.I. Kol'tsov, V.B. Aleskovskii, Fabrication of a layer of silicon dioxide of a given thickness on the surface of silicon by molecular lamination, Zh. Prikl. Khim. 43 (1970) 1150–1152 (in Russian).
[30] V.B. Aleskovskii, Chemistry and technology of solid substances, Zh. Prikl. Khim. 47 (1974) 2145–2157 (in Russian).
[31] T. Suntola, A. Pakkala, S. Lindfors, Method for preparation of compound thin film and apparatus for its performing, Patent SU 1085510A (1980) (in Russian).
[32] T.S. Suntola, A.J. Pakkala, S.G. Lindfors, Apparatus for performing growth of compound thin films, U.S. Patent No. 4389973 (1981).
[33] V.-P. Tanninen, M. Oikkonen, T.O. Tuomi, X-ray diffraction study of thin electroluminescent ZnS films grown by atomic layer epitaxy, Phys. Stat. Sol. 67 (1981) 573–583.
[34] R. Törnqvist, M. Ylilammi, The decay and saturation of the emission in a.c. EL ZnS:Mn thin films, J. Lumin. 27 (1982) 285–291.
[35] M.A. Herman, M. Vulli, M. Pessa, Surface morphology of CdTe films grown on CdTe(111) substrates by atomic layer epitaxy, J. Cryst. Growth 73 (1985) 403–406.
[36] T. Yao, T. Takeda, Growth process in atomic layer epitaxy of Zn chalcogenide single crystalline films on (100) GaAs, Appl. Phys. Lett. 48 (1986) 160–162.
[37] L.A. Kolodziejski, R.L. Gunshor, Q. Fu, D. Lee, A.V. Nurmikko, J.M. Gonsalves, N. Otsuka, Excitonic trapping from atomic layer epitaxial Zn Te within ZnSe/Zn,Mn)Se heterostructures, Appl. Phys. Lett. 52 (1988) 1080 –1082.
[38] S. Dosho, Y. Takemura, M. Konagai, K. Takahashi, Atomic layer epitaxial growth of ZnSe, ZnTe, and ZnSe-ZnTe strained-layer superlattices, J. Appl. Phys. 66 (1989) 2597–2602.

[39] H. Döring, K. Hashimoto, A. Fujishima, TiO_2 thin films prepared by pulsed beam chemical vapor deposition from tiatnium tetraisopropoxide and water, Ber. Bunsenges. Phys. Chem. 96 (1992) 620–622.
[40] S.B. Desu, Ultra-thin TiO_2 films by a novel method, Mater. Sci. Engineering B13 (1992) 299–303.
[41] E.-L. Lakomaa, S. Haukka, T. Suntola, Atomic layer growth of TiO_2 on silica, Appl. Surf. Sci. 60/61 (1992) 742–748.
[42] M. Ritala, M. Leskelä, E. Nykänen, P. Soininen, L. Niinistö, Growth of titanium dioxide thin films by atomic layer epitaxy, Thin Solid Films 225 (1993) 288–295.
[43] M. Ritala, M. Leskelä, L.-S. Johansson, L. Niinistö, Atomic force microscopy study of titanium dioxide thin films grown by atomic layer epitaxy, Thin Solid Films 228 (1993) 32–35.
[44] M. Ritala, M. Leskelä, L. Niinistö, P. Haussalo, Titanium isopropoxide as a precursor in atomic layer epitaxy of titanium dioxide thin films, Chem. Mater. 5 (1993) 1174–1181.
[45] M. Ritala, M. Leskelä, E. Rauhala, Atomic layer epitaxy growth of titanium dioxide thin films from titanium ethoxide, Chem. Mater. 6 (1994) 556–561.
[46] M. Ritala, M. Leskelä, L. Niinistö, T. Prohaska, G. Friedbacher, M. Grasserbauer, Surface roughness reduction in atomic layer epitaxy growth of titanium oxide thin films, Thin Solid Films 249 (1994) 155–162.
[47] S. Haukka, E.-L. Lakomaa, T. Suntola, Surface coverage of ALE precursors on oxides, Appl. Surf. Sci. 82/83 (1994) 548–552.
[48] T. Uustare, J. Aarik, M. Elango, Oxygen depletion of crystalline (anatase) TiO_2 initiated by ionization of the K shell, Appl. Phys. Lett. 65 (1994) 2551–2552.
[49] H. Kumagai, M. Matsumoto, K. Toyoda, M. Obara, M. Suzuki, Fabrication of titanium oxide thin films by controlled growth with sequential surface chemical reactions, Thin Solid Films 263 (1995) 47–53.
[50] A. Rosental, P. Adamson, A. Gerst, H. Koppel, A. Tarre, Atomic layer deposition in travelling wave reactor: in situ diagnostics by optical reflection, Appl. Surf. Sci. 112 (1997) 82–86.
[51] V.E. Drozd, N.N. Kopilov, V.B. Aleskovski, The electrical field effect on the growth of titanium oxide layers by ML-ALE, Appl. Surf. Sci. 112 (1997) 258–263.
[52] A.A. Malkov, E.A. Sosnov, O.V. Osipenkova, A.A. Malygin, Synthesis and transformations of Ti-containing structures on the surface of silica gel, Appl. Surf. Sci. 108 (1997) 133–139.
[53] N.V. Dolgushev, A.A. Malkov, A.A. Malygin, S.A. Suvorov, A.V. Shchukarev, A.V. Beljaev, V.A. Bykov, Synthesis and characterization of nanosized titanium oxide films on the (0001) α-Al_2O_3 surface, Thin Solid Films 293 (1997) 91–95.
[54] J. Aarik, A. Aidla, A.-A. Kiisler, T. Uustare V. Sammelselg, Effect of crystal structure on optical properties of TiO_2 films grown by atomic layer deposition, Thin Solid Films 305 (1997) 270–273.
[55] V. Sammelselg, A. Rosental, A. Tarre, L. Niinistö, K. Heiskanen, K. Ilmonen, L.-S. Johansson, T. Uustare, TiO_2 thin films by atomic layer deposition: a case of uneven growth at low temperature, Appl. Surf. Sci. 134 (1998) 78–86.
[56] W. Gasser, Y. Uchida, M. Matsumura, Quasi-monolayer deposition of silicon dioxide, Thin Solid Films 250 (1994) 213–218.

[57] S.M. George, O. Sneh, A.C. Dillon, M.L. Wise, A.W. Ott, L.A. Okada, J.D. Way, Atomic layer controlled deposition of SiO_2 and Al_2O_3 using ABAB… binary reaction sequence chemistry, Appl. Surf. Sci. 82/83 (1994) 460–467.

[58] J.W. Klaus, A.W. Ott, J.M. Johnson, S.M. George, Atomic layer controlled growth of SiO_2 films using binary reaction sequence chemistry, Appl. Phys. Lett. 70 (1997) 1092–1094.

[59] H. Kattelus, M. Ylilammi, J. Saarilahti, J. Antson, S. Lindfors, Layered tantalum–aluminum oxide films deposited by atomic layer epitaxy, Thin Solid Films 225 (1993) 296–298.

[60] J. Aarik, A. Aidla, K. Kukli, In situ characterization of ALE- growth by reagent pulse delay times in a flow-type reactor, Appl. Surface Sci. 75 (1994) 180–184.

[61] J. Aarik, A. Aidla, K. Kukli, T. Uustare, Deposition and etching of tantalum oxide films in atomic layer epitaxy process, J. Cryst. Growth 144 (1994) 116–119.

[62] K. Kukli, J. Aarik, A. Aidla, O. Kohan, T. Uustare, V. Sammelselg, Properties of tantalum oxide thin films grown by atomic layer deposition, Thin Solid Films 260 (1995) 135–142.

[63] K. Kukli, M. Ritala, M. Leskelä, Atomic layer epitaxy growth of tantalum oxide thin films from $Ta(OC_2H_5)_5$ and H_2O, J. Electrochem. Soc. 142 (1995) 1670–1675.

[64] H. Siimon, J. Aarik, Reactivities of $TaCl_5$ and H_2O as precursors for atomic layer deposition, J. Phys. IV C5, 5 (1995) 277–282.

[65] J. Aarik, K. Kukli, A. Aidla and L. Pung, Mechanism of suboxide growth and etching in atomic layer epitaxy of tantalum oxide from $TaCl_5$ and H_2O, Appl. Surf. Sci. 103 (1996) 331–341.

[66] K. Kukli, J. Aarik, A. Aidla, H. Siimon, M. Ritala, M. Leskelä, In situ study of atomic layer epitaxy growth of tantalum oxide thin films from $Ta(OC_2H_5)_5$ and H_2O, Appl. Surf. Sci. 112 (1997) 236–242.

[67] J.Aarik, A.Aidla, A.Jaek, A-A.Kiisler, A.-A.Tammik, Properties of amorphous Al_2O_3 films grown by ALE, Acta Polytech. Scand. 195 (1990) 201–208.

[68] L. Hiltunen, H. Kattelus, M. Leskelä, M. Mäkelä, L. Niinistö, E. Nykänen, P. Soininen, M. Tiitta, Growth and characterization of aluminum oxide thin films deposited from various source materials by atomic layer epitaxy and chemical vapor deposition processes, Mater. Chem. Phys. 28 (1991) 379–388.

[69] J.F. Fan, K. Toyoda, Growth-temperature dependence of the quality of Al_2O_3 prepared by sequential surface chemical reaction of trimethylaluminium and H_2O_2, Jpn. J. Appl. Phys. 32 (1993) L1349–L1351.

[70] V.E. Drozd, A.P. Baraban, I.O. Nikiforova, Electrical properties of Si–Al_2O_3 structures grown by ML-ALE method, Appl. Surf. Sci. 82/83 (1994) 583–586.

[71] E.-L. Lakomaa, A. Root, T. Suntola, Surface reactions in Al_2O_3 growth from trimethylaluminium and water by atomic layer epitaxy, Appl. Surf. Sci. 107 (1996) 107–115.

[72] K. Kukli, M. Ritala, M. Leskelä, J. Jokinen, Atomic layer epitaxy growth of aluminum oxide thin films from a novel $Al(CH_3)_2Cl$ precursor and H_2O, J. Vac. Sci. Technol. A 15 (1997) 2214–2218.

[73] M. Ritala, M. Leskelä, Zirconium dioxide thin films deposited by ALE using zirconium tetrachloride as precursor, Appl. Surf. Sci. 75 (1994) 333–340.

[74] A. Kytökivi, E.-L. Lakomaa, A. Root, Controlled formation of ZrO_2 in the reaction of $ZrCl_4$ vapor with porous silica and γ-alumina surfaces, Langmuir 12 (1996) 4395–4403.
[75] A. Kytökivi, E.-L. Lakomaa, A. Root, H. Österholm, J.-P. Jacobs, H. Brongersma, Sequential saturating reactions of $ZrCl_4$ and H_2O vapors in the modification of silica and γ-alumina with ZrO_2, Langmuir 13 (1997) 2717–2725.
[76] K. Kukli, J. Ihannus, M. Ritala, M. Leskelä, Properties of Ta_2O_5-based dielecric naolaminates deposited by atomic layer epitaxy, J. Electrochem. Soc. 144 (1997) 300–306.
[77] K. Kukli, M. Ritala, M. Leskelä, Properties of $(Nb_{1-x}Ta_x)_2O_5$ solid solutions and $(Nb_{1-x}Ta_x)_2O_5$–ZrO_2 nanolaminates grown by atomic layer epitaxy, NanoStructured Mater. 8 (1997) 785–793.
[78] M. Ritala, M. Leskelä, L. Niinistö, T. Prohaska, G. Friedbacher, M. Grasserbauer, Development of crystallinity and morphology in hafnium dioxide thin films grown by atomic layer epitaxy, Thin Solid Films 250 (1994) 72–80.
[79] K. Kukli, J. Ihannus, M. Ritala, M. Leskelä, Tailoring the dielectric properties of HfO_2–Ta_2O_5 nanolaminates, Appl. Phys. Lett. 68 (1996) 3737–3739.
[80] H. Viirola, L. Niinistö, Controlled growth of tin dioxide thin films by atomic layer epitaxy, Thin Solid Films 249 (1994) 144–149.
[81] H. Viirola, L. Niinistö, Controlled growth of antimony-doped tin dioxide thin films by atomic layer epitaxy, Thin Solid Films 251 (1994) 127–135.
[82] M. Utriainen, S. Lehto, L. Niinistö, C. Dücso, N.Q. Khanh, Z.E. Horváth, I. Bársony, B. Pécz, Porous silicon host matrix for deposition by atomic layer epitaxy, Thin Solid Films 297 (1997) 39–42.
[83] T. Asikainen, M. Ritala, M. Leskelä, Growth of In_2O_3 thin films by atomic layer epitaxy, J. Electrochem. Soc. 141 1994) 3210–3213.
[84] M. Ritala, T. Asikainen, M. Leskelä, Enhanced growth rate in atomic layer epitaxy of indium oxide and indium-tin oxide thin films, Electrochem. Solid State Lett. 1 (1998) 156–157.
[85] B. Sang, A. Yamada, M. Konagai, Textured ZnO thin films for solar cells grown by a two-step process with the atomic layer deposition technique, Jpn. J. Appl. Phys. 37 (1998) L206–L208.
[86] M. Nieminen, L. Niinistö, E. Rauhala, Growth of gallium oxide thin films from gallium acetylacetonate by atomic layer epitaxy, J. Mater. Chem. 6 1996) 27–31.
[87] S. Haukka, M. Lindblad, T. Suntola, Growth mechanisms of mixed oxides on alumina, Appl. Surf. Sci. 112 (1997) 23–29.
[88] S.M. Bedair, M.A. Tischler, T. Katsuyama, N.A. El-Masry, Atomic layer epitaxy of III–V binary compounds, Appl. Phys. Lett. 47 (1985) 51–53.
[89] M.A. Tischler, N.G. Anderson, S.M. Bedair, Ultrathin InAs/GaAs single quantum well structures grown by atomic layer epitaxy, Apll. Phys. Lett. 49 (1986) 1199–1200.
[90] S.M. Bedair, B.T. McDermott, Y. Ide, N.H. Karam, H. Hashemi, M.A. Tischler, M. Timmons, J.C.L. Tarn, N. El-Masry, Recent development in atomic layer epitaxy of III–V compounds, J. Cryst. Growth 93 (1988) 182–189.
[91] J.R. Gong, D. Jung, N.A. El-Masry, S.M. Bedair, Atomic layer epitaxy of AlGaAs, Appl. Phys. Lett. 57 (1990) 400–402.

[92] M. Hashemi, J. Ramdani, B.T. McDermott, K. Reid, S.M. Bedair, Atomic layer epitaxy of planar-doped structures for nonalloyed contacts and field-effect transistor, Appl. Phys. Lett. 56 (1990) 964–966.
[93] S.P. DenBaars, C.A. Beyler, A. Hariz, P.D. Dapkus, GaAs/AlGaAs quantum well lasers with active regions grown by atomic layer epitaxy, Appl. Phys. Lett. 51 (1987) 1530–1532.
[94] S.P. DenBaars, P.D. Dapkus, C.A. Beyler, A. Hariz, K.M. Dzurko, Atomic layer epitaxy for the growth of heterostructure devices, J. Cryst. Growth 93 (1988) 195–200.
[95] S.P. DenBaars, P.D. Dapkus, Atomic layer epitaxy of compound semiconductors with metalorganic precursors, J. Cryst. Growth 98 (1989) 195–208.
[96] M. Ozeki, K. Mochizuki, N. Ohtsuka, K. Kodama, New approach to the atomic layer epitaxy of GaAs using a fast gas stream, Appl. Phys. Lett. 53 (1988) 1509–1511.
[97] K. Mochizuki, M. Ozeki, K. Kodama, N. Ohtsuka, Carbon incorporation in GaAs layer grown by atomic layer epitaxy, J. Cryst. Growth 93 (1988) 557–561.
[98] H. Ohno, S. Ohtsuka, H. Ishii, Y. Matsubara, H. Hasegawa, Atomic layer epitaxy of GaAs using triethylgallium and arsine, Appl. Phys. Lett. 54 (1989) 2000–2002.
[99] E. Colas, R. Bhat, B.J. Skromme, G.C. Nihous, Atomic layer epitaxy of device quality GaAs, Appl. Phys. Lett. 55 (1989) 2769–2671.
[100] K. Mori, M. Yoshida, A. Usui, H. Terao, GaAs growth by atomic layer epitaxy using diethylgalliumchloride, Appl. Phys. Lett. 52 (1988) 27–29.
[101] A. Koukitu, H. Nakai, A. Saegusa, T. Suzuki, O. Nomura, H. Seki, Solid composition of In_{1-x} Ga_xAs grown by the halogen transport atomic layer epitaxy, Jpn. J. Appl. Phys. 27 (1988) L744–L746.
[102] A. Koukitu, N. Takahashi, Y. Miura, H. Seki, Determination of surface chemical species in GaAs atomic layer epitaxy by in situ gravimetric monitoring, Jpn. J. Appl. Phys. 33 (1994) L613–L616.
[103] H.P. Kattelus, J. Ahopelto, I. Suni, Growth of GaAs and InAs by atomic layer epitaxy using Ga and In chlorides and AsH_3, Acta Polytech. Scand. Electric. Engin. Ser. 64 (1989) 155–164.
[104] J. Ahopelto, H.P Kattelus, J. Saarilehti, I. Suni, Atomic layer epitaxy of III–V compounds in a hydride vapor phase system, J. Cryst. Growth 99 (1990) 550–555.
[105] Y. Jin, R. Kobayashi, K. Fujii, F. Hasegawa, Atomic layer epitaxy of GaAs using $GaCl_3$ and AsH_3, Jpn. J. Appl. Phys. 29 (1990) L1350–L1352.
[106] R. Kobayashi, S. Narahara, K. Ishikawa, F. Hasegawa, In situ observation of atomic layer epitaxy of GaAs using $GaCl_3$ by surface photo-absorption method, Jpn. J. Appl. Phys. 32 (1993) L164–L166.
[107] M. A. Khan, R.A. Skogman, J.M. Van Hove, D.T. Olson, J.N. Kznia, Atomic layer epitaxy of GaN over sapphire using switched metalorganic chemical vapor deposition, Appl. Phys. Lett. 60 (1992) 1366–1368.
[108] A. Ludviksson, D.W. Robinson, J. W. Rodgers, The interaction of dimethylaminealane and ammonia on clean oxidized Al(111): atomic layer growth of aluminum nitride, Thin Solid Films 289 (1996) 6–13.

[109] Y.F. Nicolau, J.C. Menard, Solution growth of ZnS, CdS and $Zn_{1-x}Cd_xS$ thin films by the successive ionic-layer adsorption and reaction process: growth mechanism, J. Cryst. Growth 92 (1988) 128–142.
[110] Y.F. Nicolau, J.C. Menard, Procedure for solution growth of ZnS, CdS and $Zn_{1-x}Cd_xS$ thin films by the successive ionic-layer adsorptions and reactions, J. Appl. Electrochem. 20 (1990) 1063–1066.
[111] R. Resch, T. Prohaska, G. Friedbacher, M. Grasserbauer, T. Kanniainen, S. Lindroos, M. Leskelä, L. Niinistö, J.A.C. Broekaert, In-situ investigation of ZnS deposition on mica by successive ionic layer adsorption and reaction method as studied with atomic force microscopy, Fresenius J. Anal. Chem. 353 (1995) 772–777.
[112] D.W. Suggs, I. Villegas, B.W. Gregory, J.L.Stikney, Formation of compound semiconductors by electrochemical atomic layer epitaxy, J. Vac. Sci. Technol. A 10 (1992) 886–891.
[113] J. Nishizawa, K. Aoki, S. Suzuki, K. Kikuchi, Molecular layer epitaxy of silicon, J. Cryst. Growth 99 (1990) 502–505.
[114] E. Hasunuma, S. Sugahara, S. Hoshino, S. Imai, K. Ikeda, M. Matsumura, Gas-phase-reaction-controlled atomic-layer-epitaxy of silicon, J. Vac. Sci. Technol. A 16 (1998) 679–684.
[115] P. Mårtensson, J.-O. Carlsson, Atomic layer epitaxy of copper on tantalum, Chem. Vapor Deposition 3 (1997) 45–50.
[116] T. Aaltonen, A. Rahtu, M.Ritala; M. Leskelä, Reaction mechanism studies on Atomic layer deposition of ruthenium and platinum, Electrochem. Solid State Lett. 6 (2003) C130–C133.
[117] T. Aaltonen, M. Ritala, Y.-L. Tung, Y. Chi, K. Arstila, K. Meinander, M. Leskelä, Atomic layer deposition of noble metals: exploration of the low limit of the deposition temperature, J. Mater. Res. 19 (2004) 3353–3358.
[118] J.W. Elam, C.E. Nelson, R.K. Grubbs, S.M. George, Kinetics of the WF_6 and Si_2H_6 surface reactions during tungsten atomic layer deposition, Surf. Sci. 479 (2001) 121–135.
[119] Y. Suda, Migration-assisted Si subatomic-layer epitaxy from Si_2H_6, J. Vac. Sci. Technol. A 15 (1997) 2463–2468.
[120] H. Akazakawa, Y. Utsumi, T. Urisu, M. Nagase, Si crystal growth mediated by synchrotron-radiation-stimulated hydrogen desorption, Phys. Rev. B 47 (1993) 15946–15949.
[121] H. Akazagawa, Temperature effects on synchrotron-radiation-exited Si atomic layer epitaxy using disilane, Appl. Surf. Sci. 82/83 (1994) 394–399.
[122] O. Nilsen, H. Fjellvåg, A. Kjekshus, Growth of calcium carbonate by the atomic layer chemical vapour deposition technique, Thin Solid Films 450 (2004) 240–247.
[123] A. Kytökivi, J.-P. Jacobs, A. Hakuli, J. Meriläinen, H.H. Brongersma, Surface Characteristics and activity of chromia/alumina catalysts prepared by atomic layer epitaxy, J. Catal. 162 (1996) 190–197.
[124] S. Haukka, E.-L. Lakomaa, T. Suntola, Adsorption controlled preparation of heterogeneous catalysts, in: A. Dabrowski (ed), Studies in Surface Science and Catalysis, Vol. 120A, Adsorption and its Applications in Industry and Environmental Protection, Elsevier, Amsterdam, 1999, pp. 715–750.

[125] S. Tang, R.M. Wallace, A. Seabaugh, D. King-Smith, Evaluating the minimum thickness of gate oxide on silicon using first-principles method, Appl. Surf. Sci. 135 (1998) 137–142.
[126] J. Cai, C.-T. Sah, Gate tunneling currents in ultrathin oxide metal-oxide-silicon transistors, J. Appl. Phys. 89 (2001) 2272–2285.
[127] S.A. Campbell, D.C. Gilmer, X. Wang, M. Hsieh, H.-S. Kim, W.L. Gladfelter, J. Yan, MOSFET transistors fabricated with high permittivity TiO_2 dielectrics, IEEE Trans. Electron. Devices 44 (1997) 104–109.
[128] H. Jung, K. Im, H. Hwang, D. Yang, Electrical characteristics of an ultrathin (1.6 nm) TaO_xN_y gate dielectric, Appl. Phys. Lett. 76 (2000) 3630–3631.
[129] G.D. Wilk, R.M. Wallace, J.M. Anthony, Hafnium and zirconium silicates for advanced gate dielectrics, J. Appl. Phys. 87 (2000) 484–492.
[130] T. Ngai, J. Qi, R. Sharma, J. Fretwell, X. Chen, J.C. Lee, S. Banerjee, Electrical properties of ZrO_2 gate dielectric on SiGe, Appl. Phys. Lett. 76 (2000) 502–504.
[131] M. Houssa, V.V. Afanas'ev, A. Stesmans, Variation in the fixed charge density of SiO_x/ZrO_2 gate dielectric stacks during postdeposition oxidation, Appl. Phys. Lett. 77 (2000) 1885–1887.
[132] C.M. Perkins, B.B. Triplett, P. McIntyre, K.C. Saraswat, S. Haukka, M. Tuominen, Electrical and material properties of ZrO_2 gate dielectrics grown by atomic layer deposition, Appl. Phys. Lett. 78 (2001) 2357–2359.
[133] M.A. Gribelyuk, A. Callegari, E.P. Gusev, M. Copel, D.A. Buchanan, Interface reactions in ZrO_2 based gate dielectrics, J. Appl. Phys. 92 (2002) 1232–1237.
[134] H. Zhang, R. Solanki, Atomic layer deposition of high dielectric constant nanolaminates, J. Electrochem. Soc. 148 (2001) F63–F66.
[135] O. Sneh, R.B. Clark-Phelps, A.R. Londergan, J. Winkler, T.E. Seidel, Thin film atomic layer depsoition equipment for semiconductor processing, Thin Solid Films 402 (2002) 248–261.
[136] H. Hu, C. Zhu, Y.F. Lu, M.F. Li, B.J. Cho, W.K. Choi, A high performance MIM capacitor using HfO_2 dielectrics, IEEE Electron. Device Lett. 23 (2002) 514–516.
[137] T. Honda, K. Yanashima, J. Yoshino, H. Kukimoto, F. Koyama, K. Iga, Fabrication of a ZnSe-based vertical Fabry-Perot cavity using SiO_2/TiO_2 multilayer reflectors and resonant emission characteristics, Jpn. J. Appl. Phys. 33 (1994) 3960–3961.
[138] H. Kumagai, K. Toyoda, K. Kobayashi, M. Obara, and Y. Iimura, Titanium oxide/aluminum oxide multilayer reflectors for "water-window" wavelengths, Appl. Phys. Lett. 70 (1995) 2338–2340.
[139] K. Tappura, J. Aarik, M. Pessa, High-power GaInP-AlGaInP quantum-well lasers grown by solid source molecular beam epitaxy, IEEE Photon. Technol. Lett. 8 (1996) 319–321.
[140] A. Bearzotti, A. Bianco, G. Montesperelli, E. Traversa, Humidity sensitivity of sputtered TiO_2 thin films, Sensors and Actuators B 18–19 (1994) 525–528.
[141] H. Tang, K. Prasad, R. Sanjinés, F Lévy, TiO_2 anatase thin films as gas sensors, Sensors and Actuators B 26–27 (1995) 71–75.
[142] M. Bibes, M. Bowen, A. Barthélémy, A. Anane, K. Bouzehouane, C. Carrétéro, E. Jacquet, J.P. Contour, O. Durand, Growth and characterization of TiO_2 as a barrier for spin-polarized tunneling, Appl. Phys. Lett. 82 (2003) 3269–3271.

[143] J. Aarik, A. Aidla, T. Uustare, Atomic layer growth of TiO_2-II thin films, Phil. Mag. Lett. 73 (1996) 115–119.
[144] J. Aarik, A. Aidla, V. Sammelselg, T. Uustare, Effect of growth conditions on formation of TiO_2-II thin films in atomic layer deposition process, J. Cryst. Growth 181 (1997) 259–264.
[145] K. Kukli, M. Ritala, M. Shuisky, M. Leskelä, T. Sajavaara, J. Keinonen, T. Uustare, A. Hårsta, Atomic layer deposition of titanium oxide from TiI_4 and H_2O_2, Chem. Vapor. Deposition 6 (2000) 303–310.
[146] M. Schuisky, A. Hårsta, A. Aidla, K. Kukli, A.-A. Kiisler, J. Aarik, Atomic layer chemical vapor deposition of TiO_2: low temperature epitaxy of rutile and anatase, J. Electrochem. Soc. 147 (2000) 3319–3325.
[147] K. Kukli, A. Aidla, J. Aarik, M. Shuisky, A. Hårsta, M. Ritala, M. Leskelä, Real-time monitoring in atomic layer deposition of TiO_2 from TiI_4 and H_2O–H_2O_2, Langmuir 16 (2000) 8122–8128.
[148] M. Schuisky, J. Aarik, K. Kukli, A. Aidla, A. Hårsta, Atomic layer deposition of thin films using O_2 as oxygen source, Langmuir 17 (2001) 5508—5512.
[149] M. Schuisky, K. Kukli, J. Aarik, J. Lu, A. Hårsta, Epitaxial growth of TiO_2 films in a hydroxyl-free ALD process, J. Cryst. Growth 235 (2002) 293–299.
[150] J. Aarik, A. Aidla, V. Sammelselg, H. Siimon, T. Uustare, Control of thin film structure by reactant pressure in atomic layer deposition of TiO_2, J. Cryst. Growth 169 (1996) 496–502.
[151] S. M. Edlou, A. Smajkiewicz, G. A. Al-Jumaily, Optical properties and environmental stability of oxide coatings deposited by reactive sputtering, Appl. Opt. 32 (1993) 5601–5605.
[152] C. Urlacher, C. Maco de Lucas, E. Bernstein, B. Jacquier, J. Mugnier, Study of erbium doped ZrO_2 waveguide elaborated by sol-gel process, Opt. Mater. 12 (1999) 19–25.
[153] D. Lo, L. Shi, J. Wang, G.-X. Zang, X. Zhu, Zirconia and zirconia-organically modified silicate distributed feedback waveguide lasers tunable in the visible, Appl. Phys. Lett. 81 (2002) 2707–2709.
[154] R.S. Niranjan, S.D. Sathaye, I.S. Mulla, Bilayered tin oxide:zirconia thin film as a humidity sensor, Sens. Actuators B 81 (2001) 64–67.
[155] M. Balog, M. Schieber, M. Michman, S. Patai, The chemical vapor deposition and characterization of ZrO_2 films from organometallic compounds, Thin Solid Films 47 (1977) 109–120.
[156] R.H. French, S.J. Glass, F.S. Ohuchi, Y.-N. Xu, W.Y. Ching, Experimental and theoretical determination of the electronic structure and optical properties of three phases of ZrO_2, Phys. Rev. B 49 (1994) 5133–5142.
[157] M. Houssa, M. Tuominen, M. Naili, V. Afanas'ev, A. Stesmans, S. Haukka, M.M. Heyns, Trap-assisted tunneling in high permittivity gate dielectric stacks, J. Appl. Phys. 87 (2000) 8615–8620.
[158] S. Miyazaki, M. Narasaki, M. Ogasawara, M. Hirose, Characterization of ultrathin zirconium oxide films on silicon using photoelectron spectroscopy, Microelectron. Eng. 59 (2001) 373–378.
[159] H. Nohira, W Tsai, W. Besling, E. Besling, E. Young, J. Petry, T. Conard, W. Vandervorst, S. De Gendt, M. Heyns, J. Maes, M. Tuominen, Characterization of ALCVD-Al_2O_3 and ZrO_2 layer using X-ray photoelectron spectroscopy, J. Non-Crystalline Solids 303 (2002) 83–87.

[160] Z.W. Zhao, B.K. Tay, G.Q. Yu, S.P. Lau, Optical properties of filtered cathodic vacuum arc-deposited zirconium oxide thin films, J. Phys.: Condensed Matter 15 (2003) 7707–7715.
[161] C.R. Aita, E.E. Hoppe, R.S. Sorbello, Fundamental optical absorption edge of undoped tetragonal zirconium dioxide, Appl. Phys. Lett. 85 (2003) 677–679.
[162] M. Cassir, F. Goubin, C. Bernay, P. Vernoux, D. Lincot, Synthesis of ZrO_2 thin films by atomic layer deposition: growth kinetics, structural and electrical properties, Appl. Surf. Sci. 193 (2002) 120–128.
[163] W.-J. Qi, R. Nieh, B.H. Lee, L. Kang, Y. Jeon, J.C. Lee, Electrical and reliability characteristics of ZrO_2 deposited directly on Si for gate dielectric application, Appl. Phys. Lett. 77 (2000) 3269–3271.
[164] T. Ngai, W.J. Qi, R. Sharma, J. Fretwell, X. Chen, J.C. Lee, S. Banerjee, Transconductance improvement in surface-channel SiGe p-metal-oxide-silicon field-effect transistors using a ZrO_2 gate dielectric, Appl. Phys. Lett. 78 (2001) 3085–3087.
[165] T.S. Jeon, J.M. White, D.L. Kwong, Thermal stability of ultrathin ZrO_2 films prepared by chemical vapor deposition on Si(100), Appl. Phys. Lett. 78 (2001) 368–370.
[166] J.P. Chang, Y.-S. Lin, Thermal stability of stacked high-k dielectrics on silicon, Appl. Phys. Lett. 79 (2001) 3824–3826.
[167] S. Stemmer, Z. Chen, R. Keding, J.P. Maria, D. Wicaksana, A.I. Kingon, Stability of ZrO_2 layers on Si(001) during high-temperature anneals under reduced oxygen partial pressures, J. Appl. Phys. 92 (2002) 82–86.
[168] N.L. Zhang, Z.T. Song, Q. Wan, Q.W. Shen, C.L. Lin, Interfacial and micro-structural properties of zirconium oxide thin films prepared directly on silicon, Appl. Surf. Sci. 202 (2002) 126–130.
[169] H. Watanabe, N. Ikarashi, Thermal decomposition of ZrO_2/SiO_2 bilayer on Si(001) caused by void nucleation and its lateral growth, Appl. Phys. Lett. 80 (2002) 559–561.
[170] K. Muraoka, Reaction steps of silicidation in $ZrO_2/SiO_2/Si$ layered structure, Appl. Phys. Lett. 80 (2002) 4516–4518.
[171] J.M. Howard, V. Craciun, C. Essary, R.K. Singh, Interfacial layer formation during high-temperature annealing of ZrO_2 thin films on Si, Appl. Phys. Lett. 81 (2002) 3431–3433.
[172] S.K. Dey, C.G. Wang, D. Tang, M.J. Kim, W. Carpenter, C. Werkhoven, E. Shero, Atomic layer chemical vapor deposition of ZrO_2-based dielectric films: nanostructure and nanochemistry, J. Appl. Phys. 93 (2003) 4144–4157.
[173] J.P. Chang, Y.-S. Lin, Highly conformal ZrO_2 deposition for dynamic random access memory application, J. Appl. Phys. 90 (2001) 2964–2969.
[174] J. Wang, P.P. Freitas, E. Snoeck, P. Wei, J.C. Soares, Spin-dependent tunnel junctions with ZrO_2 barries, Appl. Phys. Lett. 79 (2001) 4387–4389.
[175] D.-W. Kim, F.E. Prins, T. Kim, S. Hwang, C.H. Lee, D.-L. Kwong, S.K. Banerjee, Reduction of charge-transport characteristics of SiGe dot floating gate memory device with ZrO_2 tunneling oxide, IEEE Trans. Electron. Devices 50 (2003) 510–513.
[176] V.A. Gritsenko, K.A. Nasyrov, Yu.N. Novikov, A.L. Aseev, S.Y. Yoon, J.-W. Lee, E.-H. Lee, C.W. Kim, A new low voltage fast SONOS memory with high-k dielectric, Solid-State Electron. 47 (2003) 1651–1656.

[177] K. Kukli, K. Forsgren, J. Aarik, T. Uustare, A. Aidla, A. Niskanen, M. Ritala, M. Leskelä, A. Hårsta, Atomic layer deposition of zirconium oxide from zirconium tetraiodide, water and hydrogen peroxide, J. Cryst. Growth 231 (2001) 262–272.
[178] K. Kukli, K. Forsgren, M. Ritala, M. Leskelä, J. Aarik, A. Hårsta, Dielectrivc properties of zirconium oxide grown by atomic layer deposition from iodide precursor, J. Electrochem. Soc. 148 (2001) F227–F232.
[179] K. Kukli, M. Ritala, T. Uustare, J. Aarik, K. Forsgren, T. Sajavaara, M. Leskelä, A. Hårsta, Influence of thickness and growth temperature on the properties of zirconium oxide films grown by atomic layer deposition on silicon, Thin Solid Films 410 (2002) 53–60.
[180] K. Forsgren, J. Westlinder, J. Lu, J. Olsson, Iodide-based atomic layer deposition of ZrO_2: aspects of phase stability and dielectric properties, Chem. Vapor Deposition 8 (2002) 105–109.
[181] M. Balog, M. Schieber, M. Mitchman, S. Patai, Chemical vapor deposition and characterization of HfO_2 films from organo-hafnium compounds, Thin Solid Films 41 (1977) 247–259.
[182] S.-G. Lim, S. Kriventsov, T.N. Jackson, J.H. Haeni, D.G. Schlom, A.M. Balbashov, R. Uecker, P. Reiche, J.L. Freeouf, G. Luckovsky, Dielectric functions and optical bandgaps of high-K dielectrics for metal-oxide-semiconductor field-effect transistors by far ultraviolet spectroscopic ellipsometry, J. Appl. Phys. 91 (2002) 4500–4505.
[183] H. Kato, T. Nango, T. Miyagawa, T. Katagiri, K.S. Seol, Y. Ohki, Plasma-enhanced chemical vapor deposition and characterization of high-permittivity hafnium and zirconium silicate layers, J. Appl. Phys. 92 (2002) 1106–1111.
[184] H.Y. Yu, M.F. Li, B.J. Cho, C.C. Yeo, M.S. Joo, D.-L. Kwong, J.S. Pan; C.H. Ang, J.Z. Zheng, S. Ramanathan, Energy gap and band alignment for $(HfO_2)_x(Al_2O_3)_{1-x}$ on (100)Si, Appl. Phys. Lett. 81 (2002) 376–378.
[185] V.V. Afanas'ev, A. Stesmans, F. Chen, X. Shi, S.A. Campbell, Internal photoemission of electrons and holes from (100)Si into HfO_2, Appl. Phys. Lett. 81 (2002) 1053–1055.
[186] T. Nishide, S. Honda, M. Matsuura, M. Ide, Surface, structural and optical properties of sol-gel derived HfO_2 films, Thin Solid Films 371 (2000) 61–65.
[187] A.J. Waldorf, J.A. Dobrowolski, B.T. Sullivan, L.M. Plante, Optical coatings deposited by reactive ion plating, Appl. Opt. 32 (1993) 5583–5593.
[188] M. Gilo, N. Croitoru, Study of HfO_2 films prepared by ion-assisted deposition using a gridless end-hall ion source, Thin Solid Films 350 (1999) 203–208.
[189] M. Alvisi, S. Scaglione, S. Martelli, A. Rizzo, L. Vasanelli, Structural and optical modification in hafnium oxide thin films related to the momentum parameter transferred by ion assistance, Thin Solid Films 354 (1999) 19–23.
[190] M. Alvisi, M. Di Giulio, S.G. Marrone, M.R. Perrone, M.L. Protopapa, A. Valentini, L. Vasanelli, HfO_2 films with high laser damage threshold, Thin Solid Films 358 (2000) 250–258.
[191] M. Alvisi, F. De Tomasi, M.R. Perrone, M.L. Protopapa, A. Rizzo, F. Sarto, S. Scaglione, Laser damage dependence on structural and optical properties of ion-assisted HfO_2 thin films, Thin Solid Films 396 (2001) 44–52.
[192] Z.J. Yan, R. Xu, Y.Y. Wang, S. Chen, Y.L. Fan, Z.M. Jiang, Thin HfO_2 films grown on Si(100) by atomic oxygen assisted molecular beam epitaxy, Appl. Phys. Lett. 85 (2004) 85–87.

[193] Y. Zhao, T. Wang, D. Zhang, J. Shao, Z. Fan, Laser conditioning and multi-shot laser damage accumulation effects of HfO_2/SiO_2 antireflective coatings, Appl. Surf. Sci. 245 (2005) 335–339.
[194] S.J.L. Ribeiro, Y. Messadeq, R.R. Gonçalves, M. Ferrari, M. Montagna, M.A. Aegerter, Low optical loss planar waveguides prepared in an organic-inorganic hybrid system, Appl. Phys. Lett. 77 (2000) 3502–3504.
[195] R. Gonçalves, G. Carturan, L. Zampedri, M. Ferrari, M. Montagna, A. Chiasera, G.C. Righini, S. Pelli, S.J.L. Ribeiro, Y. Messadeq, Sol-gel Er-doped SiO_2–HfO_2 planar waveguides: a viable system for 1.5 μm application, Appl. Phys. Lett. 81 (2002) 28–30.
[196] R. Gonçalves, G. Carturan, M. Montagna, M. Ferrari, L. Zampedri, S. Pelli, G.C. Righini, S.J.L. Ribeiro, Y. Messadeq, Erbium-activated HfO_2-based waveguides for photonics, Opt. Mater. 25 (2004) 131–139.
[197] M. Gutowski, J.E. Jaffe, C.-L. Liu, M. Stoker, R.I. Hedge, R.S. Rai, P.J. Tobin, Thermodynamic stability of high-K dielectric metal oxides ZrO_2 and HfO_2 in contact with Si and SiO_2, Appl. Phys. Lett. 80 (2002) 1897–1899.
[198] Y.-S. Lin, R. Puthenkovilakam, P.J. Chang, Electric property and thermal stability of HfO_2 on silicon, Appl. Phys. Lett. 81 (2002) 2041–2043.
[199] P.D. Ye, G.D. Wilk, B. Yang, J. Kwo, S.N.G. Chu, S. Nakahara, H.-J.L. Gossmann, J.P. Mannaerts, M. Hong, K.K. Ng, J. Bude, GaAs metal–oxide–semiconductor field-effect transistor with nanometer-thin dielectric grown by atomic layer deposition, Appl. Phys. Lett. 83 (2003) 180–182.
[200] D. Wu, J. Lu, H. Radamson, P.-E. Hellström, S.-L. Zhang, M. Östling, E. Vainonen-Ahlgren, E. Tois, M. Tuominen, Influence of surface treatment prior to ALD high-k dielectrics on the performance of SiGe surface-channel pMOSFETs, IEEE Electron Device Lett. 25 (2004) 289–291.
[201] P.S. Lysaght, B. Foran, G. Bersuker, J.J. Peterson, C.D. Young, P. Majhi, B.-H. Lee, H.R. Huff, Physical comparison of HfO_2 transistors with polycrystalline silicon and TiN electrodes, Appl. Phys. Lett. 87 (2005) 082903-1–3.
[202] R. Mitsuhashi, K. Yamamoto, S, Hayashi, A. Rothschild, S. Kubicek, A. Veloso, S. Van Elshocht, M. Jurczak, S. De Gendt, S. Biesemans, M. Niwa, 45 nm LSTP FET with FUSI Gate on PVD-HfO_2 with excellent drivability by advanced PDA treatment, Microelectron. Engin. 80 (2005) 7–10.
[203] D. Wang, Q. Wang, A. Javey, R. Tu, H. Dai, H. Kim, P. McIntyre, T. Krishnamohan, K.C. Saraswat, Germanium nanowire field-effect transistors with SiO_2 and high-k HfO_2 gate dielectrics, Appl. Phys. Lett. 83 (2003) 2432–2434.
[204] A. Javey, J. Guo, D.B. Farmer, Q. Wang, D. Wang, R.G. Gordon, M. Lundstrom, H. Dai, Carbon nanotube field-effect transistors with integrated ohmic contacts and high-k gate dielectrics, Nano Lett. 4 (2004) 447–450.
[205] A. Javey, J. Guo, D.B. Farmer, Q. Wang, E. Yenilmez, R.G. Gordon, M. Lundstrom, H. Dai, Self-aligned ballistic molecular transistors and electrically parallel nanotube arrays, Nano Lett. 4 (2004) 1319–1322.
[206] K.-M. Kim, B.J. Choi, S.K. Kim, C.S. Hwang, Fabrication of a metal-oxide-semiconductor-type capacitive microtip array using SiO_2 or HfO_2 gate insulators, Appl. Phys. Lett. 85 (2004) 5412–5414.
[207] F. Wallrapp, P. Fromherz, TiO_2 and HfO_2 in electrolyte-oxide-silicon configuration for application in bioelectronics, J. Appl. Phys. 99 (2006) 114103-1–10.

[208] X. Yu, C. Chu, H. Hu, A. Chin, M.F. Li, B.J. Cho, D.-L. Kwong, P.D. Foo, M.B. Yu, A high-density MIM capacitor (13 fF/μm^2) using ALD HfO_2 dielectrics, IEEE Electron Device Lett. 24 (2003) 63–65.
[209] S.J. Kim, B.J. Cho, M.-F. Li, C. Zhu, A. Chin, D.-L. Kwong, Lanthanide (Tb)-doped HfO_2 for high-density MIM capacitors, IEEE Electron Device Lett. 24 (2003) 442–444.
[210] J.J. Lee, X. Wang, W. Bai, N. Lu, D.-L. Kwong, Theoretical and experimental investigation of Si nanocrystal memory device with HfO_2 high-k tunneling dielectric, IEEE Trans. Electron Devices 50 (2003) 2067–2072.
[211] T.H. Ng, V. Ho, L.W. Teo, M.S. Tay, B.H. Koh, W.K. Chim, W.K. Choi, A.Y. Du, C.H. Tung, Fabrication and characterization of a trilayer germanium nanocrystal memory device with hafnium dioxide as the tunnel dielectric, Thin Solid Films 462–463 (2004) 46–50.
[212] Z. Tan, S.K. Samanta, W.J. Yoo, S. Lee, Self-assembly of Ni nanocrystals on HfO_2 and N-assisted Ni confinement for nonvolatile memory application, Appl. Phys. Lett. 86 (2005) 013107-1–3.
[213] C.L. Platt, B. Dieny, A.E. Berkowitz, Spin-dependent tunneling in HfO_2 tunnel junctions, Appl. Phys. Lett. 69 (1996) 2291–2293.
[214] S. Capone, G. Leo, R. Rella, P. Siciliano, L. Vasanelli, M. Alvisi, L. Mirenghi, A. Rizzo, Physical characterization of hafnium oxide thin films and their application as gas sensing devices, J. Vac. Sci. Technol. A 16 (1998) 3564–3568.
[215] M. Kirm, J. Aarik, M. Jürgens, I. Sildos, Thin Films of HfO_2 and ZrO_2 as potential scintillators, Nucl. Instrum. Meth. Phys. Res. A 537 (2005) 251–255.
[216] J.M. Léger, J. Haines, B. Blanzat, Materials potentially harder than diamond: quenchable high-pressure phases of transition metal dioxides, J. Mater. Sci. Lett. 13 (1994) 1688–1690.
[217] K. Forsgren, A. Hårsta, J. Aarik, A. Aidla, J. Westlinder, J. Olsson, Deposition of HfO_2 thin films in HfI_4-based processes, J. Electrochem. Soc. 149 (2002) F139-F144.
[218] J. Aarik, A. Aidla, A. Jaek, M. Leskelä, L. Niinistö, In situ study of a strontium β-diketonate precursor for thin-film growth by atomic layer epitaxy, J. Mater. Chem. 4 (1994) 1239–1244.
[219] J. Aarik, A. Aidla, A. Jaek, M. Leskelä, L. Niinistö, Precursor properties of calcium β-diketonate in vapor phase atomic layer epitaxy, Appl. Surf. Sci. 75 (1994) 33–38.
[220] E. Benes, M. Gröschl, W. Burger, M. Schmid, Sensors based on piezoelectric resonators, Sensors and Actuators A48 (1995) 1–21.
[221] A.I. Romanychev, V.E. Drozd, V.B. Aleskovskii, Growth of zinc and cadmium sulfide films with the aid of ellipsometry and a quartz resonance balance, J. Appl. Chem. USSR 62 (1989) 11.
[222] E.B. Yousfi, J. Fouache, D. Lincot, Study of atomic layer epitaxy of zinc oxide by in-situ quartz crystal microgravimetry, Appl. Surf. Sci. 153 (2000) 223–234.
[223] A. Rahtu, T. Alaranta, M. Ritala, In situ quartz crystal microbalance and quadrupole mass spectrometry studies of atomic layer deposition of aluminum oxide from trimethylaluminum and water, Langmuir 17 (2001) 6506–6509.
[224] A. Rahtu, M. Ritala, Compensation of temperature effects in quartz crystal microbalance measurements, Appl. Phys. Lett. 80 (2002) 521–523.

[225] J.W. Elam, M.J. Pellin, $GaPO_4$ sensors for gravimetric monitoring during atomic layer deposition at high temperatures, Anal. Chem. 77 (2005) 3531–3535.
[226] M.N. Rocklein, S.M. George, Temperature-induced apparent mass changes observed during quartz crystal microbalance measurements of atomic layer deposition, Anal. Chem. 75 (2003) 4975–4982.
[227] J. Aarik, H. Siimon, Characterization of adsorption in flow type atomic layer epitaxy reactor, Appl. Surf. Sci. 81 (1994) 281–287.
[228] J. Aarik, H. Mändar, M. Kirm, Spectroscopic characterization of ZrO_2 thin films grown by atomic layer deposition, Proc. Estonian Acad. Sci. Phys. Math. 52 (2003) 289–298.
[229] R. Matero, A. Rahtu, M. Ritala, In situ quadrupole mass spectrometry and quartz crystal microbalance studies on the atomic layer deposition of titanium dioxide from titanium tetrachloride and water, Chem. Mater. 13 (2001) 4506–4511.
[230] S. Bourgeois, F. Jomard, M. Perdereau, Use of isotopic labelling in a SIMS study of the hydroxylation of TiO_2(100) surfaces, Surf. Sci. 279 (1992) 349–354.
[231] S. Haukka, E.-L. Lakomaa, A. Root, An IR and NMR study of the chemisorption of $TiCl_4$ on silica, J. Phys. Chem. 97 (1993) 5085–5094.
[232] W. Gu, C.P. Tripp, Role of water in the atomic layer deposition of TiO_2 on SiO_2, Langmuir 21 (2005) 211–216.
[233] R.L. Puurunen, Formation of metal oxide particles in atomic layer deposition during the chemisorption of metal chlorides: A review, Chem. Vap. Deposition 11 (2005) 79–90.
[234] R. Matero, A. Rahtu, M. Ritala, M. Leskelä, T. Sajavaara, Effect of water dose on the atomic layer deposition rate of oxide thin films, Thin Solid Films 368 (2000) 1–7.
[235] J. Aarik, A. Aidla, A. Kasikov, H. Mändar, R. Rammula, V. Sammelselg, Influence of carrier gas pressure and flow rate on atomic layer deposition of HfO_2 and ZrO_2 thin films, Appl. Surf. Sci. 252 (2006) 5723–5734.
[236] J.E. Huheey, E.A. Keitler, R.L. Keitler, Inorganic Chemistry. Principles of Structure and Bonding, Harper Collins College Publishers, New York (1993), pp. A21–A34.
[237] A. Rahtu, K. Kukli, , M. Ritala, In situ mass spectrometry study on atomic layer deposition from metal (Ti, Ta and Nb) ethoxides and water, Chem. Mater. 13 (2001) 817–823.
[238] V. Sammelselg, E. Rauhala, K. Arstila, A. Zakharov, J. Aarik, A. Kikas, J. Karlis, A. Tarre, A. Seppälä, J. Asari, I. Martinson, Study of thin oxide films by electron ion and synchrotron radiation beams, Mikrochim. Acta 139 (2002) 165–169.
[239] A. Rahtu, M. Ritala, Reaction mechanism studies on titanium isopropoxide–water atomic layer deposition process, Chem Vap. Deposition 8 (2002) 21–28.
[240] V. Sammelselg, A. Rosental, A. Tarre, L. Niinistö, K. Heiskanen, K. Ilmonen, L.-S. Johansson, T. Uustare, TiO_2 thin films by atomic layer deposition: a case of uneven growth at low temperature, Appl. Surf. Sci. 134 (1998) 78–86.
[241] D.R.G. Mitchell, D.J. Attard, G. Triani, Transmission electron microscopy studies of atomic layer deposition TiO_2 films grown on silicon, Thin Solid Films 441 (2003) 85–95.
[242] M. Ylilammi, Monolayer thickness in atomic layer deposition, Thin Solid Films, 279 (1996) 124–130.

[243] V. Pore, A. Rahtu, M. Leskelä, M. Ritala, T. Sajavaara, J. Keinonen, Atomic layer deposition of photocatalytic TiO_2 thin films from titanium tetramethoxide and water, Chem. Vap. Deposition 10 (2004) 143–148.
[244] S.K. Kim, W.-D. Kim, K.-M. Kim, C.S. Hwang, J. Jeong, High dielectric constant TiO_2 thin films on a Ru electrode grown at 250°C by atomic layer deposition, Appl. Phys. Lett. 85 (2004) 4112–4114.
[245] A. Niilisk, A. Rosental, T. Uustare, A. Kasikov, A. Tarre, Chloride atomic-layer chemical vapor deposition of TiO_2 with a chloride pretreatment of substrates, J. Phys. IV 11 (2001) Pr11-103–Pr11-107.
[246] D.R.G. Mitchell, G. Triani, D.J. Attard, K.S. Finnie, P.J. Evans, C.J. Parbé, J.R. Barlett, Atomic layer deposition of TiO_2 and Al_2O_3 thin films and nanolaminates, Smart Mater. Struct. 15 (2006) S57–S64.
[247] A. Kasikov, J. Aarik, H. Mändar, M. Moppel, M. Pärs, T. Uustare, Refractive index gradients in TiO_2 thin films grown by atomic layer deposition, J. Phys. D: Appl. Phys. 39 (2006) 54–60.
[248] W.D. Kim, G.W. Hwang, O.S. Kwon, S.K. Kim, M. Cho, D.S. Jeong, S.W. Lee, M.H. Seo, C.S. Hwang, Y.-S. Min, Y.J. Cho, Growth characteristics of atomic layer deposited TiO_2 thin films on Ru and Si electrodes for memory capacitor applications, J. Electrochem. Soc. 152 (2005) C552–C559.
[249] V. Kiisk, I. Sildos, J. Aarik, The influence of a waveguiding structure on the excitonic luminescence of anatase thin films, Opt. Mater. 27 (2004) 115–118.
[250] D.R.G. Mitchell, D.J. Attard, G. Triani, Characterization of epitaxial TiO_2 thin films grown on MgO(0 0 1) using atomic layer deposition, J. Cryst. Growth 285 (2005) 208–214.
[251] A. Niilisk, M. Moppel, M. Pärs, I. Sildos, T. Jantson, T. Avarmaa, R. Jaaniso, J. Aarik, Structural study of TiO_2 thin films by micro-raman spectroscopy, Central Eur. J. Phys. 4 (2006) 105–116.
[252] I. Jõgi, J. Aarik, M. Laan, J. Lu, K. Kukli, H. Käämbre, T. Sajavaara, T. Uustare, Effect of preparation conditions on properties of atomic layer deposited TiO_2 thin films in Mo-TiO_2-Al stacks, Thin Solid Films 510 (2006) 39–47.
[253] C.R. Ottermann, K. Bange, Correlation between the density of TiO_2 films and their properties, Thin Solid Films 286 (1996) 32–34.
[254] D. Mergel, Modeling thin TiO_2 films of various densities as an effective optical medium, Thin Solid Films 397 (2001) 216–222.
[255] M. Cardona, G. Harbeke, Optical properties and band structure of wurtzite-type crystals and rutile, Phys. Rev. 137 (1965) A1467–A1476.
[256] A. Bendavid, P.J. Martin, H. Takikawa, Deposition and modification of titanium dioxide thin films by filtered arc deposition, Thin Solid Films 360 (2000) 241–249.
[257] L. Miao, P. Jin, K. Kaneko, A. Terai, N. Nabatova-Gabain, S. Tanemura, Preparation and characterization of polycrystalline anatase and rutile TiO_2 thin films by rf magnetron sputtering, Appl. Surf. Sci. 212–213 (2003) 255–263.
[258] A. Bendavid, P.J. Martin, Å. Jamting, H. Takikawa, Structural and optical properties of titanium dioxide thin films by filtered arc deposition, Thin Solid Films 355–356 (1999) 6–11.
[259] H. Tang, K. Prasad, R. Sanjinès, P.E. Schmid, F. Lévy, Electrical and optical properties of TiO_2 anatase thin films, J. Appl. Phys. 75 (1994) 2024–2047.

[260] T. Sumita, T. Yamaki, S. Yamamoto, A. Miyashita, Photo-induced surface charge separation of highly oriented TiO_2 anatase and rutile thin films, Appl. Surf. Sci. 200 (2002) 21–26.
[261] T. Sekiya, K. Ichimura, M. Igarashi, S. Kurita, Absorption spectra of anatase TiO_2 single crystals heat-treated under oxygen atmosphere, J. Phys. Chem. Solids 61 (2000) 1237–1242.
[262] J. Pascual, J. Camassel, H. Mathieu, Fine structure in the intrinsic absorption edge of TiO_2, Phys. Rev. B 18 (1978) 5606–5614.
[263] A. Rahtu, M. Ritala, Reaction mechanism studies on the zirconium chloride–water atomic layer deposition process, J. Mater. Chem. 12 (2002) 1484–1489.
[264] K. Kukli, M. Ritala, J. Aarik, T. Uustare, M. Leskelä, Influence of growth temperature on properties of zirconium dioxide films grown by atomic layer deposition, J. Appl. Phys. 92 (2002) 1833–1840.
[265] K. Kukli, M. Ritala, M. Leskelä, Low-temperature deposition of zirconium oxide-based nanocrystalline films by alternate supply of $Zr(OC(CH_3)_3)_4$ and H_2O, Chem. Vap. Deposition 6 (2000) 297–302.
[266] M. Putkonen, L. Niinistö, Zirconia thin films by atomic layer epitaxy. A comparative study on the use of novel precursors with ozone, J. Mater. Chem. 11 (2001) 3141–3147.
[267] A. Nakajima, T. Kidera, H. Ishii, S. Yokoyama, Atomic layer deposition of ZrO_2 with a Si nitride barrier layer, Appl. Phys. Lett. 81 (2002) 2824–2826.
[268] Y. Kim, J. Koo, J. Han, S. Choi, H. Jeon, C.G. Park, Characteristics of ZrO_2 gate dielectric deposited using Zr t-butoxide and $Zr(NEt_2)_4$ precursors by plasma enhanced atomic layer deposition method, J. Appl. Phys. 92 (2002) 5443–5447.
[269] R. Matero, M. Ritala, M. Leskelä, A.C. Jones, P.A. Williams, J. F. Bickley, A. Steiner, T.J. Leedham, H.O. Davies, Atomic layer deposition of ZrO_2 thin films using a new alkoxide precursor, J. Non-Cryst. Solids 303 (2002) 24–28.
[270] M. Putkonen, J. Niinistö, K. Kukli, T. Sajavaara, M. Karppinen, H. Yamauchi, L. Niinistö, ZrO_2 thin films grown on silicon substrates by atomic layer deposition with $Cp_2Zr(CH_3)_2$ and water as precursors, Chem. Vap. Deposition 9 (2003) 207–212.
[271] J. Niinistö, M. Putkonen, L. Niinistö, K. Kukli, M. Ritala, M. Leskelä, Structural and dielectric properties of thin ZrO_2 films on silicon grown by atomic layer deposition from cyclopentadienyl precursor, J. Appl. Phys. 95 (2004) 84–91.
[272] D.M. Hausmann, E. Kim, R.G. Gordon, Atomic layer deposition of hafnium and zirconium oxides using metal amide precursors, Chem. Mater. 14 (2002) 4350–4358.
[273] W.-H. Nam, S.-W. Rhee, Atomic layer deposition of ZrO_2 thin films using dicholobis[bis-(trimethylsilyl)amido]zirconium and water, Chem. Vap. Deposition 10 (2004) 201–205.
[274] S.X. Lao, R.M. Martin, J.P. Chang, Plasma enhanced atomic layer deposition of HfO_2 and ZrO_2 high-k thin films, J. Vac. Sci. Technol. A 23 (2005) 488–496.
[275] R. Matero, M. Ritala, M. Leskelä, T. Sajavaara, A.C. Jones, J.L. Roberts, Evaluation of new aminoalkoxide precursors for atomic layer deposition. Growth of zirconium dioxide thin films and reaction mechanism studies, Chem. Mater. 16 (2004) 5630–5636.

[276] J. Niinistö, A. Rahtu, M. Putkonen, M. Ritala, M. Leskelä, L. Niinistö, In situ quadrupole mass spectrometry study of atomic-layer deposition of ZrO_2 using $Cp_2Zr(CH_3)_2$ and water, Langmuir 21 (2005) 7321–7325.
[277] G. Scarel, S. Ferrari, S. Spiga, C. Wiemer, G. Tallarida, M. Fanciulli, Effects of growth temperature on the properties of atomic layer deposition grown ZrO_2 films, J. Vac. Sci. Technol. A 21 (2003) 1–7.
[278] E. Bonera, G. Scarel, M. Fanciulli, Structure evolution of atomic layer deposition grown ZrO_2 films by deep-ultra-violet Raman and far-infrared spectroscopies, J. Non-Cryst. Solids 322 (2003) 105–110.
[279] A.K. Jonsson, G.A. Niklasson, M. Ritala, M. Leskelä, K. Kukli, Dielectric permittivity and intercalation parameters of Li ion intercalated atomic layer deposited ZrO_2, J. Electrochem. Soc. 151 (2004) F54–F58.
[280] J. Aarik, A. Aidla, A. Kasikov, H. Mändar, R. Rammula, V. Sammelselg, Influence of carrier gas pressure and flow rate on atomic layer deposition of HfO_2 and ZrO_2 thin films, Appl. Surf. Sci. 252 (2006) 5723–5734.
[281] I.A. El-Shanshoury, V.A. Rudenko, I.A. Ibrahim, Polymorphic behavior of thin evaporated films zirconium and hafnium oxides, J. Amer. Ceram. Soc. 53 (1970) 264–268.
[282] R.C. Garvie, Stabilization of the tetragonal structure in zirconia microcrystals, J. Phys. Chem. 82 (1978) 218–224.
[283] S.J. Yun, J.W.Lim, J.H. Lee, Effect of plasma on characteristics of zirconium oxide films deposited by plasma-enhanced atomic layer deposition, Electrochem. Solid-State Lett. 8 (2005) F47–F50.
[284] K. Kukli, J. Aarik, M. Ritala, T. Uustare, T. Sajavaara, J. Lu, J. Sundqvist, A. Aidla, L. Pung, A. Hårsta, M. Leskelä, Effect of selected atomic layer deposition parameters on the structure and dielectric properties of hafnium oxide films, J. Appl. Phys. 96 (2004) 5298–5307.
[285] D.R.G. Mitchell, A. Aidla, J. Aarik, Transmission electron microscopy studies of HfO_2 thin films grown by chloride-based atomic layer deposition, Appl. Surf. Sci. 253 (2006) 606–617.
[286] J.F. Conley, Y. Ono, W. Zhuang, D.J. Tweet, W. Gao, S.K. Mohammed, R. Solanki, Atomic layer deposition of hafnium oxide using anhydrous hafnium nitrate, Electrochem. Solid State Lett. 5 (2002) C57–C59.
[287] J.F. Conley, Y. Ono, R. Solanki, G. Stecker, W. Zhuang, Electrical properties of HfO_2 deposited via atomic layer deposition using $Hf(NO_3)_4$ and H_2O, Appl. Phys. Lett. 82 (2003) 3508–3510.
[288] K. Kukli, M. Ritala, T. Sajavaara, J. Keinonen, M. Leskelä, Atomic layer deposition of hafnium dioxide films from hafnium tetrakis(ethylmethylamide) and water, Chem. Vap. Deposition 8 (2002) 199–204.
[289] K. Kukli, M. Ritala, M. Leskelä, T. Sajavaara, J. Keinonen, A.C. Jones, J.L. Roberts, Atomic layer deposition of hafnium dioxide films from 1-methoxy-2-methyl-2-propanolate complex of hafnium, Chem. Mater. 13 (2003) 1722–1727.
[290] K. Kukli, M. Ritala, M. Leskelä, T. Sajavaara, J. Keinonen, A.C. Jones, N.L. Tobin, Atomic layer deposition of hafnium dioxide films from hafnium hydroxylamide and water, Chem Vap. Deposition 10 (2004) 91–96.
[291] A. Deshpande, R. Inman, G. Jursich, C. Takoudis, Atomic layer deposition and characterization of hafnium oxide grown on silicon from tetrakis(diethylamino)-hafnium and water vapor, J. Vac Sci. Technol. A22 (2004) 2035–2040.

[292] R. Chen, H. Kim, P.C. McIntyre, D.W. Porter, S.F. Bent, Achieving area-selective atomic layer deposition on patterned substrates by selective surface modification, Appl. Phys. Lett. 86 (2005) 191910-1–3.
[293] D. Triyoso, R.I. Hedge, B.E. White, P.J. Tobin, Physical and electrical characteristics of atomic-layer-deposited hafnium dioxide formed using hafnium tetrachloride and tetrakis(ethylmethylaminohafnium), J. Appl. Phys. 97 (2005) 124107-1–9.
[294] D.B. Farmer, R.G. Gordon, ALD of high-k dielectrics on suspended functionalized SWNTs, Electrochem. Solid State Lett. 8 (2005) G89–G91.
[295] K.Kukli, T. Pilvi, M. Ritala, T. Sajavaara, J. Lu, M. Leskelä, Atomic layer deposition of hafnium dioxide thin films from hafnium tetrakis(dimethylamide) and water, Thin Solid Films 491 (2005) 328–338.
[296] J. Niinistö, M. Putkonen, L. Niinistö, S.L. Stoll, K. Kukli, T. Sajavaara, M. Ritala, M. Leskelä, Controlled growth of HfO_2 thin films by atomic layer deposition from cyclopentadienyl-type precursor and water, J. Mater. Chem. 15 (2005) 2271–2275.
[297] J. Niinistö, M. Putkonen, L. Niinistö, K. Arstila, T. Sajavaara, J.Lu, K. Kukli, M. Ritala, M. Leskelä, HfO_2 films grown by ALD using cyclopentadienyl-type precursors and H_2O or O_3 as oxygen source, J. Electrochem. Soc. 153 (2006) F39–F45.
[298] K. Kukli, M. Ritala, J. Sundqvist, J. Aarik, J. Lu, T. Sajavaara, M. Leskelä, A. Hårsta, Properties of hafnium oxide films grown by atomic layer deposition from hafnium tetraiodide and oxygen, J. Appl. Phys. 92 (2002) 5698–5703.
[299] J. Sundqvist, A. Hårsta, J. Aarik, K. Kukli, A. Aidla, Atomic layer deposition of polycrystalline HfO_2 films by the HfI_4-O_2 precursor combination, Thin Solid Films 427 (2003) 147–151.
[300] J. Aarik, A. Aidla, H. Mändar, T. Uustare, K. Kukli, M. Schuisky, Phase transformations in hafnium dioxide thin films grown by atomic layer deposition at high temperatures, Appl. Surf. Sci. 173 (2001) 15–21.
[301] J. Aarik, A. Aidla, A. Kikas, T. Käämbre, R. Rammula, P. Ritslaid, T. Uustare, V. Sammelselg, Effects of precursors on nucleation in atomic layer deposition of HfO_2, Appl. Surf. Sci. 230 (2004) 292–300.
[302] M.A. Alam, M.L. Green, Mathematical desciption of atomic layer deposition and its application to the nucleation and growth of HfO_2 gate dielectric layers, J. Appl. Phys. 94 (2003) 3403–3413.
[303] R.L. Puurunen, Analysis of hydroxyl group controlled atomic layer deposition of hafnium dioxide from hafnium tetrachloride and water, J. Appl. Phys. 95 (2004) 4777–4786.
[304] J. Wang, H.P. Li, R. Stevens, Hafnia and hafnia-toughened ceramics, J. Mater. Sci. 27 (1992) 5397–5430.
[305] C. Wiemer, S. Ferrari, M. Fanciulli, G. Pavia, L. Lutterotti, Combining grazing incidence X-ray diffraction and X-ray reflectivity for the evaluation of the structural evolution of HfO_2 thin films with annealing, Thin Solid Films 450 (2004) 134–137.
[306] R.C. Cammarata, Surface and interface stress effects on interfacial and nanostructured materials, Mater. Sci. Engineering A 237 (1997) 180–184.

[307] J.M. Leger, A. Atouf, P.E. Tomaszewski, A.S. Pereira, Pressure-induced phase transitions and volume changes in HfO_2 up to 50 GPa, Phys. Rev. B 48 (1993) 93–98.
[308] A. Jayaraman, S.Y. Wang, S.K. Sharma, L.C. Ming, Pressure-induced phase transformations in HfO_2 to 50 GPa studied by Raman spectroscopy, Phys. Rev. B 48 (1993) 9205–9211.
[309] O. Ohtaka, H. Fukui, K. Funakoshi, W. Utsumi, T. Irifune, T. Kikegawa, Phase relations and EOS of ZrO_2 and HfO_2 under high temperature and high pressure, High Pressure Res. 22 (2002) 221–226.
[310] G. Scarel, S. Spiga, C. Wiemer, G. Tallarida, S. Ferrari, M. Fanciulli, Trends of structural and electrical properties in atomic layer deposited HfO_2 films, Mater. Sci. Engineering B109 (2004) 11–16.
[311] P.W. Peacock, J. Robertson, Band offsets and Shottky barrier heigths of high dielectric constant oxides, J. Appl. Phys. 92 (2002) 4712–4721.
[312] J.Y. Lee, B.C. Lai, The electrical properties of high-dielectric-constant and ferroelectric thin films for very large scale integration cicuits, in: Handbook of Thin Film Materials, Ed. H.S. Nalwa, Vol. 3: Ferroelectric and Dielectric Thin Films, Academic Press, 2002, pp. 1–98.
[313] J. Lu, J. Aarik, J. Sundqvist, K. Kukli, A. Hårsta, J.-O. Carlsson, Analytical TEM characterization of the interfacial layer between ALD HfO_2 film and silicon substrate, J. Cryst. Growth 273 (2005) 510–514.
[314] K. Kukli, J. Aarik, T. Uustare, J. Lu, M. Ritala, A. Aidla, L. Pung, A. Hårsta, M. Leskelä, A. Kikas, V. Sammelselg, Engineering structure and properties of hafnium oxide films by atomic layer deposition temperature, Thin Solid Films 479 (2005) 1–11.
[315] Y.J. Cho, N.V. Nguyen, C.A. Richter, J.R. Ehrstein, B.H. Lee, J.C. Lee, Spectroscopic ellipsometry characterization of high-*k* dielectric HfO_2 thin films and the high-temperature annealing effects on their optical structure, Appl. Phys. Lett. 80 (2002) 1249–1251.
[316] N.V. Nguyen, A.V. Davydov, d. Chandler-Horowitz, M.M. Frank, Sub-bandgap defect states in polycrystalline hafnium oxide and their supression by admixture of silicon, Appl. Phys. Lett. 87 (2005) 192903-1–3.
[317] J. Schaeffer, N.V. Edwards, R. Liu, D. Roan, B. Hradsky, R. Gregory, J. Kulik, E. Duda, L. Contreras, J. Christiansen, S. Zollner, P. Tobin, B.-Y. Nguyen, R. Nieh, M. Ramon, R. Rao, R. Hedge, R. Rai, J. Baker, S. Voight, HfO_2 gate dielectrics deposited via tetrakis diethylamido hafnium, J. Electrochem. Soc. 150 (2003) F67–F74.
[318] J.L. Gavartin, D. Munos-Ramo, A.L Shluger, G. Bersuker, Polaron trapping in oxygen deficient and disordered HfO_2: theoretical insight, ECS Transactions 3 (2006) 277–290.

SUMMARY IN ESTONIA

TITAAN-, TSIRKOONIUM- JA HAFNIUMDIOKSIIDIDE AATOMKIHTSADESTAMINE: KASVUMEHHANISMID JA ÕHUKESTE KILEDE OMADUSED

Väitekirjas kirjeldatud uuringutes võrreldi omavahel mitmeid titaandioksiidi (TiO_2), tsirkooniumdioksiidi (ZrO_2) ja hafniumdioksiidi (HfO_2) aatomkihtsadestamiseks sobivaid tehnoloogilisi protsesse. Nende hulgas oli varemtuntuid, aga ka selliseid, mida väitekirja originaalpublikatsioonides kirjeldati esmakordselt. Esmakordselt uuriti uute ning mitmete varemkirjeldatud protsesside reaktsioonimehhanisme, kasutades selleks reaalajalisi meetodeid. Saadud tulemused ja nende võrdlus kirjanduse andmetega näitasid, et seni kasutatud metallilähteainetest olid stabiilseimad kloriidid. Neid võis kasutada laias temperatuuride vahemikus ja nad olid piisavalt aktiivsed pinnareaktsioonides.

Selgitati välja, et kilede kasvukiiruse sõltuvus kasvualuse temperatuurist oli kooskõlas muutustega kilede kasvul toimuvates pinnareaktsioonides juhul, kui kristallisatsioon ei mõjutanud pinnakaredust ja adsorptsioonivõimet. Vastasel juhul võisid kristallisatsiooniprotsessidest tingitud kasvukiiruse muutused isegi ületada neid, mis olid põhjustatud muutustest pinnal toimunud asendusreaktsioonides. Kõige enam mõjutasid kristallisatsiooniprotsessid TiO_2 kilede kasvu. Nimelt kasvas kristalliline, anataasi struktuuriga TiO_2 märksa kiiremini kui amorfne TiO_2. Seetõttu suurenes tunduvalt selliste TiO_2 kilede pinnakaredus, mis sisaldasid nii amorfset kui ka anataasi faasi. Anataasi faasi kiirem kasv ja pinna karenemisega seonduv kile efektiivse pindala suurenemine põhjustasid kile kasvu järsu kiirenemise juhul, kui toimus üleminek amorfsest faasist anataasi faasi. Selline, kristalliseerumisest tingitud kasvukiiruse suurenemine oli jälgitav nii kasvutemperatuuri tõusul kui ka kile paksuse suurenemisel. Seega tavaliselt kasutatav eeldus, et kile paksus on võrdeline rakendatud aatomkihtsadestamise tsüklite arvuga, s.t. materjali sünteesiks kasutatud reaktsiooniastmete arvuga, ei pea paika juhtudel, kui kilede kristallilisuse ja/või kristalliitide eelisorientatsiooni aste suureneb koos kile paksuse suurenemisega. Kilede kristallstruktuuri ja kristalliitide eelisorientatsiooni väljakujunemine kile kasvu käigus on aga väga sageli esinev nähtus polükristalliliste kilede kasvul.

ZrO_2 ja HfO_2 kilede kasvukiirus ei sõltunud kilede kristalliseerumisest nii tugevalt kui TiO_2 kasvukiirus. Sellegipoolest leiti nii käesoleva dissertatsiooni originaalpublikatsioonides kui ka teiste autorite töödes tõendeid selle kohta, et ka ZrO_2 ja HfO_2 kilede puhul esineb seda laadi sõltuvus. Tehti ka kindlaks, et kasvutemperatuuri ja lähteainete valik mõjutas oluliselt HfO_2 kilede kasvu algfaasi ränialustel. Märgatav kasvu alguse viivis ja järgnev kolmemõõtmeline kasv olid jälgitavad kloriidil põhinevates kõrge-temperatuurilistes protsessides.

Palju ühtlasemalt ja ilma olulise viiviseta kasvas HfO_2 jodiidipõhistes ja madalatemperatuurilistes (kuni 300°C) aatomkihtsadestamise protsessides.

ZrO_2 ja HfO_2 kilede kristalliseerumine aatomkihtsadestamise protsessides põhjustas optilise tiheduse ja dielektrilise konstandi ootuspärase suurenemise. TiO_2 kilede puhul viis mitte-epitaksiaalsete kilede ebaühtlane kristalliseerumine mõnikord ka kilede keskmise optilise tiheduse vähenemiseni. Epitaksiaalsetel kiledel oli optiline tihedus siiski alati palju suurem kui amorfsetel kiledel, ulatudes monokristallide vastavate väärtusteni.

Amorfsete TiO_2 kilede optiline keelutsoon osutus märgatavalt laiemaks kristalliliste faaside keelutsoonist. Amorfsete ZrO_2 ja HfO_2 kilede keelutsooni laiused olid aga võrreldavad või isegi väiksemad kui vastavate oksiidide kristalliliste faaside keelutsooni laiused. Optilised mõõtmised näitasid sedagi, et monokliinse struktuuriga HfO_2 ja ZrO_2 kilede neeldumisspektrid erinesid oluliselt amorfsete ning kuubilise ja tetragonaalse struktuuriga kilede neeldumisspektritest. Kuigi seda efekti on hiljem jälgitud ja põhjendatud ka teiste autorite poolt, nõuab nähtuse põhjuste lõplik väljaselgitamine siiski täiendavaid eksperimentaalseid ja teoreetilisi uuringuid.

ORIGINAL PUBLICATIONS

J. Aarik, A. Aidla, A.-A. Kiisler, T. Uustare, V. Sammelselg, Influence of substrate temperature on atomic layer growth and properties of HfO_2 thin films, Thin Solid Films 340 (1999) 110–116.

J. Aarik, A. Aidla, H. Mändar, V. Sammelselg, T. Uustare, Texture development in nanocrystalline hafnium dioxide thin films grown by atomic layer deposition, J. Cryst. Growth 220 (2000) 105–113.

J. Aarik, A. Aidla, H. Mändar, T. Uustare, Atomic layer deposition of titanium dioxide from $TiCl_4$ and H_2O: investigation of growth mechanism, Appl. Surf. Sci. 172 (2001) 148–158.

J. Aarik, A. Aidla, T. Uustare, K. Kukli, V. Sammelselg, M. Ritala, M. Leskelä, Atomic layer deposition of TiO_2 thin films from TiI_4 and H_2O, Appl. Surf. Sci. 193 (2002) 277–286.

J. Aarik, A. Aidla, V. Sammelselg, T. Uustare, M. Ritala, M. Leskelä, Characterization of titanium dioxide atomic layer growth from titanium ethoxide and water, Thin Solid Films 370 (2000) 163–172.

J. Aarik, A. Aidla, T. Uustare, M. Ritala, M. Leskelä, Titanium isopropoxide as a precursor for atomic layer deposition: Characterization of titanium dioxide growth process, Appl. Surf. Sci. 161 (2000) 385–395.

J. Aarik, A. Aidla, H. Mändar, V. Sammelselg, Anomalous effect of temperature on atomic layer deposition of titanium dioxide, J. Cryst. Growth 220 (2000) 531–537.

J. Aarik, J. Karlis, H. Mändar, T. Uustare, V. Sammelselg, Influence of structure development on atomic layer deposition of TiO_2 thin films, Appl. Surf. Sci. 181 (2001) 339–348.

J. Aarik, A. Aidla, H. Mändar, T. Uustare, M. Schuisky, A. Hårsta, Atomic layer growth of epitaxial TiO_2 thin films from $TiCl_4$ and H_2O on α-Al_2O_3 substrates, J. Cryst. Growth 242 (2002) 189–198.

J. Aarik, A. Aidla, H. Mändar, T. Uustare, V. Sammelselg, Growth kinetics and structure formation of ZrO_2 thin films in chloride-based atomic layer deposition process, Thin Solid Films 408 (2002) 97–103.

J. Aarik, J. Sundqvist, A. Aidla, J. Lu, T. Sajavaara, K. Kukli, A. Hårsta, Hafnium tetraiodide and oxygen as precursors for atomic layer deposition of hafnium oxide thin films, Thin Solid Films 418 (2002) 69–72.

J. Aarik, H. Mändar, M. Kirm, L. Pung, Optical characterization of HfO_2 thin films grown by atomic layer deposition, Thin Solid Films 466 (2004) 41–47.

CURRICULUM VITAE

Name:	Jaan Aarik
Date and place of birth:	January 1, 1951, Lääne-Virumaa, Estonia
Citizenship:	Estonian
Current employment:	Institute of Physics, University of Tartu (researcher)
Address:	Institute of Physics, University of Tartu, Tähe 4, 51010 Tartu, Estonia
Telephone:	+ 372 7375 877
E-mail:	jaan.aarik@ut.ee

Education:

The 1st Secondary School of Rakvere, 1969
Tartu State University, 1974, diploma in physics (*cum laude*)
University of Tartu, 1994, MSc. (in physics)

Research and professional experience:

1971–1974: Tartu State University (research assistant)
1974–1986: Institute of Physics, Academy of Sciences of Estonian SSR (researcher)
1986 – present time: University of Tartu (engineer, head of division, researcher)
1990–1992: Institute of Physics, Estonian Academy of Sciences (researcher)
1994–1995, 1996–1997: Tampere University of Technology (researcher)
1997–1999: Coherent Tutcore Ltd. (consultant)

Main research areas: thin-film technology, solid-state physics

Publications: 141 scientific articles

Awards:

State Prize of Estonian SSR in Science and Technology, 1982
Prize of Estonian Physical Society, 2005

ELULUGU

Nimi: Jaan Aarik
Sünniaeg ja -koht: 01.01.1951, Lääne-Virumaa
Kodakondsus: Eesti
Praegune töökoht (amet): Tartu Ülikooli Füüsika Instituut (teadur)
Aadress: Tartu Ülikooli Füüsika Instituut, Tähe 4, 51010 Tartu
Telefon: 7375 877
E-post: jaan.aarik@ut.ee

Haridus:

Rakvere I Keskkool, 1969
Tartu Riiklik Ülikool, 1974, füüsika (*cum laude*)
Tartu Ülikool, 1994, MSc (füüsika)

Töökogemus:

1971–1974: Tartu Riiklik Ülikool (laborant)
1974–1986: ENSV TA Füüsika Instituut (nooremteadur, vanemteadur)
1986 – käesoleva ajani: Tartu Ülikool (juhtivinsener, vanemteadur, sektorijuhataja, teadur)
1990–1992: Eesti TA Füüsika Instituut (vanemteadur)
1994–1995, 1996–1997: Tampere Tehnika Ülikool (teadur)
1997–1999: Coherent Tutcore Ltd. (konsultant)

Peamised uurimisvaldkonnad: tahkisekilede tehnoloogia, tahkisefüüsika

Publikatsioonid: 141 teaduslikku artiklit

Saadud autasud:

Eesti NSV riiklik preemia teaduse ja tehnika alal, 1982
Eesti Füüsika Seltsi aastapreemia, 2005